WINTER 2025



JOURNAL OF MANAGEMENT

ENGINEERING INTEGRATION

AIEMS VOL18 NO2

ISSN: 1939-7984(Print) 3065-1433 (Online)

JOURNAL OF MANAGEMENT AND ENGINEERING INTEGRATION

Editor-in-Chief

Edwin Sawan, Ph.D., P.E.

Professor Emeritus

Wichita State University

Edwin.sawan@wichita.edu

AIEMS President

Gamal Weheba, Ph.D.

Professor and ASQ Fellow

Wichita State University

gamal.weheba@wichita.edu

Scope: The Journal of Management and Engineering Integration (JMEI) is a double-blind refereed journal dedicated to exploring the nexus of management and engineering issues of the day. JMEI publishes two issues per year, one in the Summer and another in Winter. The Journal's scope is to provide a forum where engineering and management professionals can share and exchange their ideas for the collaboration and integration of Management and Engineering research and publications. The journal will aim on targeting publications and research that emphasizes the integrative nature of business, management, computers and engineering within a global context.

EDITORIAL REVIEW BOARD

Sue Abdinnour Ph.D. Wichita State University, USA sue.abdinnour@wichita.edu

Gordon Arbogast, Ph.D. Jacksonville University, USA garboga@ju.edu

Deborah Carstens, Ph.D. Florida Institute of Technology, USA <u>carstens@fit.edu</u>

Martí Casadesús, Ph.D. University of Girona, Spain marti.casadesus@udg.edu

Hossein Cheraghi, Ph.D. West New England University, USA cheraghi@wne.edu

Mohammed Darwish, Ph.D. Kuwait University, Kuwait m.darwish@ku.edu.kw

Pedro Domingues, Ph.D. University of Minho, Portugal Pedrodomin1@sapo.pt

Aneta Kucinska-Landwojtowicz, Ph.D. Opole University of Technology, Poland Prorwsp@po.edu.pl

Pradeep Kumar, Ph.D. Indian Institute of Technology, India pradeep.kumar@me.iitr.ac.in

Luiz Carlos de Cesaro Cavaler, Ph.D. Federal University of Rio Grande do Sul, Brazil luiz.cavaler@satc.edu.br Mohammad Kanan, Ph.D. University of Business & Technology, KSA m.kanan@ubt.edu.sa

Tamer Mohamed, Ph.D. The British University in Egypt, Egypt tamer.mohamed@bue.edu.eg

Bilal Obeidat, Ph.D. Queen Rania Teacher Academy, Jordan b.obeidat@grta.edu.jo

Nabin Sapkota, Ph.D. Northwestern State University, USA sapkotan@nsula.edu

Joseph E. Sawan, Ph.D. University of Ottawa, Canada jsawan@uottawa.ca

Scott D. Swain, Ph.D. Clemson University, USA sdswain@clemson.edu

Alexandra Schönning, Ph.D. University of North Florida, USA aschonni@unf.edu

John Wang, Ph.D. Montclair State University, USA wangi@montclair.edu

Gamal Weheba, Ph.D. Wichita State University, USA gamal.weheba@wichita.edu

Wei Zhan, D.Sc., PE Texas A&M University, USA wei.zhan@tamu.edu

REVIEWERS

The Journal Editorial Team would like to thank the reviewers for their time and effort. The comments that we received were very constructive and detailed. They have been very helpful in our effort to continue to produce a top-quality journal. Your participation and timely response are very important for providing a distinguished outlet for original articles. In this issue, articles are assigned digital object identification (DOI) numbers to make sure readers and researchers can reliably find your work and to help track the ways your work is cited by others.

Edwin Sawan, Ph.D., P.E. Editor-in-Chief

Sue Abdinnour

Sura Al-Qudah Tony Lewis

Abdelhakim Al Turk Adam Lynch

Saleh Ateiwi Roger Merriman

Arpita Jadav

Deborah S. Carstens Hamzah Mousa

Leonidah Chepkoech Paul D Nugent

Elizabeth Cudney Ewa Rudnicka

Pedro Cupertino Scott Swain

Tristan Davison John Wang

Ahmad Elshennawy Gamal Weheba

Cody Farlow Brooke Wheeler

Andrzej Gapinski Fujian Yan

Scott Hall Bayram Yildirim

Abdelnasser Hussein

TABLE OF CONTENTS

Natasha Spivak, Ethan Boyes and Abdelhakim A. Al Turk	
BRIDGING THEORY AND PRACTICE: 3D PRINTING AS A HANDS-ON TOOL FOR	6
STEM HIGHER EDUCATION	U
Yutaka Shirai, Yukio Maruyama and Hiroyuki Ono	
EXAMINING MODAL SHIFT IN JAPAN'S LOGISTICS	18
Pedro Cordeiro Povoa Cupertino and Adam Carlton Lynch	
CONCEPTS FOR A NEW CYBER-PHYSICAL SYSTEM: ADDRESSING NATIONAL DEFENSE CHALLENGES IN UAV OPERATIONS	35
Isabella Laurynn DeLoach, Sara Bergamini, Dowon Choi, Vivek Sharma and Brooke E. Wheeler The Effect Of Pilot Mental Health On Passenger Willingness To Fly	45
Tony Lewis and Joshua Shackman	
AUTHENTIC CRISIS LEADERSHIP & EMPLOYEE MOTIVATION: COMPARING DIVERGENT COVID-ERA EXECUTIVE COMPENSATION STRATEGIES IN THE CRUISE LINE INDUSTRY	58
Mehrnoosh Saeyan, Ahmad Elshennawy and Elizabeth A. Cudney	
IMPLEMENTATION OF THE KANO MODEL IN HEALTHCARE SETTINGS: A NARRATIVE REVIEW	73
Yimesker Yihun, Yi Sheng Tan, Safeh Clinton Mawah, Amanuel Tereda and Hongsheng He REAL-TIME GRASPING FORCE ESTIMATION AND STABILITY IN INDUSTRIAL ROBOTIC GRIPPER	86
Ashlynn Clark, Ridge Towner and Adam Carlton Lynch	
APPLYING LEAN ASSESSMENTS TO OPTIMIZE MACHINE EFFICIENCY AND MINIMIZE WASTE	96
Saleh Ateiwi, Hamzah Mousa and Gamal Weheba	
Analysis Of Wildlife Strikes Using Control Charts	106
Saurabh Sanjay Singh and Deepak Gupta	
A SOFT ACTOR-CRITIC APPROACH FOR ENERGY-CONSCIOUS FLEXIBLE JOB SHOP SCHEDULING INCORPORATING MACHINE USAGE CONSTRAINTS AND JOB RELEASE TIMES	116
Abdelhakim A. Al Turk and Gamal Weheba	
Innovations In Powder Materials For Binder Jetting	127
Isaac M. Silver and Brooke E. Wheeler	
ELECTRIC AIRCRAFT: INFRASTRUCTURE CHALLENGES FOR AIRPORTS	139

BRIDGING THEORY AND PRACTICE: 3D PRINTING AS A HANDS-ON TOOL FOR STEM HIGHER EDUCATION

Natasha Spivak ¹
Ethan Boyes ¹
Abdelhakim A. Al Turk ¹
¹ Kent State University
Aalturk3@kent.edu

Abstract

Oftentimes, STEM students struggle to connect concepts in the classroom without the help of physical representations. By implementing additive manufacturing processes in higher-level education, professors can better convey concepts to their students. This study was done at Kent State University's College of Aeronautics and Engineering to evaluate the implementation of 3D printing in STEM classes. Surveys and 3D models were sent to students to assess their satisfaction with the implementation. Results showed increased engagement and improved comprehension of difficult course material. This suggests that 3D printing can serve as an effective instructional tool in supporting student learning and retention.

Keywords: Additive Manufacturing, 3D Printing, Higher Education, STEM, Student Understanding.

1. Introduction

At universities worldwide that teach STEM (Science, Technology, Engineering, and Mathematics), students encounter many complex concepts, from learning Computer-Aided Design (CAD) to understanding how airplanes fly. These topics can be difficult to grasp at first, and often the class moves forward before every student has mastered the material. To support learning, 3D-printed models can be used as teaching aids. In this study, students were first surveyed on whether they believed 3D models could help them better understand concepts. Models were then distributed during coursework to reinforce the current topic. A post-survey measured whether the models improved comprehension and overall student satisfaction. Because learning challenging material is a universal struggle, incorporating 3D-printed models into higher education could provide a valuable way to enhance understanding and engagement.

This paper will begin by reviewing prior research relevant to the use of 3D printing in education. The next section will outline the study's methodology, followed by a discussion of the applications of 3D models in STEM higher education. The subsequent section will present and analyze survey results in detail. Attention will then turn to the challenges and benefits of incorporating 3D models to support learning. Finally, the paper will conclude with future directions and closing remarks, based on the study conducted at Kent State University's College of Aeronautics and Engineering.

2. Literature Review

Ford et al. (2018) focused on the idea that 3D printing in education can be applied in various environments for various levels of education, ranging from elementary to secondary education.

Submitted: April 28, 2025 Revised: August 26, 2025 These environments include public spaces such as libraries, maker spaces, classrooms, and special education. 3D printed objects were provided to K-12 students, with K-4 students benefiting most from its "visualization" benefits and its "show, touch and tell" type technology." Improved mathematical understanding and introduction to spatial knowledge have also been seen in younger students, especially those relating to geometric concepts. In universities, 3D printing has increased test models for experimentation and capstone research projects. Major takeaways from this were cost, extended printing times, and unequal technology experience, especially seen in older students. After implantation, students were more confident, and in a class of 180 undergraduate students, 72% of students claimed the 3D model aided in their understanding of the concept. Regardless of the audience, introducing 3D printing to the classroom benefited understanding, creativity, and engagement with the curriculum material.

Sun and Li (2018) primarily addressed the effects of 3D printing exhibited in STEM education, focusing on the challenge to "combine theory with practice". Application of this technology can help aid in understanding mathematical equations such as the Klein Bottle used in MATLAB software. When this concept was introduced to students, it was difficult for them to conceptualize the shape based solely on mathematical equations and 2D images. Following the use of 3D printing, students could gain a better understanding of the shape's complexity. This technology amplifies the established benefits of STEM, such as critical thinking and design skills. This has become increasingly important in all levels of education, including K-12 and secondary. 3D printing has been tested in various subjects, such as art design and geometry. What makes the integration of 3D printing helpful to students is the capability to visualize abstract concepts presented by the teacher. The study distinguished 3D printing as a tool that harmoniously integrates technology with education.

3D printing has many benefits. However, something that is often overlooked is the ability to educate students better. Assante et al. (2020) conducted a research study on the application of 3D printing in European Education and discussed how 3D printing is a powerful tool in education and how programs must be created to advance students' and teachers' knowledge on the subject. A survey was conducted to test this. With more than 160 replies to the survey from VET centers, educators, 3D printing suppliers, and manufacturing centers for FabLab. 52% of the 160 responses were from various types of educators. The survey asked some fundamental questions regarding the benefits of using 3D printing in education. These questions showed that people believed that 3D printing would help improve coursework comprehension and increase active learning. Many people thought that engineering and industrial technology education would be highly assisted by 3D printing technology.

To test the theory that 3D printing could assist education, Bicer et al. (2017) conducted a free-to-all summer camp with 95 students of varying ages. The study began with a survey asking the students two Likert scale questions asking if they agreed or disagreed: "I believe STEM courses and careers require a lot of creativity" and "I believe STEM courses and careers often involve solving problems that require artistic solutions." After this survey was given to the students, they were given a project to design a 3D model with three constraints. The first constraint is that students must create their object entirely. Second, students must be able to explain this object. Finally, the student must ensure this object fits the printer being used. After this project was completed, another survey was conducted. This project changed the students' views on what is important in STEM careers. The score had increased from before the project to after by 61%. Then, when students were asked if their perceptions had changed about the need for problem-solving in STEM fields, there was a significant increase of 66%.

3. Problem Statement and Methodology

Many students struggle through the coursework of many different STEM courses, and students who do not understand the topics feel left behind, wanting a deeper explanation, and a 3D printed model could fill that void. To test the implementation of 3D printed models to improve comprehension of STEM coursework.

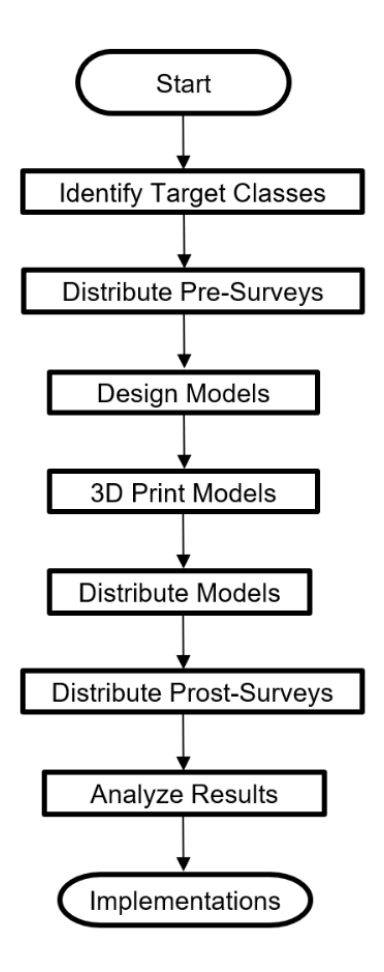


Figure 1: Research Methodology

As indicated in the flow chart in Figure 1, the first step in this research is to identify the classes that are targeted in this implementation. In the second step, a pre-survey was sent out asking questions assessing whether the student feels that implementation of 3D models could assist in their learning and if the models could better represent physically a topic they are struggling with mentally. The survey was conducted using the Likert Scale format, except for the personal information section, and there were 185 responses. Then, a consultation with the professors of these courses was held to find models from which they felt students could benefit. The models were printed on open-source Creality Ender Cr10s-Pro refurbished printers given to the College of Engineering. After being fully printed and assembled, the models were brought into the classroom for students to use. The models were used to demonstrate different ways to design CAD software and to demonstrate complex concepts in higher-level coursework. Then, a post-survey was conducted to see if the models were helpful in learning about new topics. Then after looking at data provided by the post survey the possibilities of new implementation for future work and method of incorporating 3D printed models in the classroom.

4. Pre-Survey

A pre-survey was conducted in four STEM courses to better understand student perspectives on integrating 3D printing into STEM courses: Computer Aided Design I and II, Additive Manufacturing, and Dynamics. This first survey was a preliminary survey analyzing whether students believe they will benefit from 3D-printed parts to assist in understanding concepts during lectures. This survey includes the following nine questions listed in Table 1.

Table 1. Pre-Survey Question

Question Number	Questions	Disagree	Neutral	Agree
1	What course are you filling this out for?	N/A	N/A	N/A
2	Are you familiar with 3D printing technology?	31%	N/A	69%
3	Have you ever taken a course that has incorporated 3D printed models?	67.4%	N/A	32.6%
4	How often do you struggle with connecting concepts during lectures?	58.3%	30.3%	11.3%
5	Would having access to a 3D printed model related to the current topic being explained help you better understand the concept?	6.5%	31.9%	61.7%
6	Would you be more interested in registering for a course that incorporated 3D printed models?	5.4%	22.7%	71.9%
7	Would you be more engaged during class if 3D printed models were offered?	4.9%	15.7%	79.5%
8	Do you believe that access to 3D printed models would improve your grade?	12.5%	36.2%	51.3%
9	Would you be willing to pay a small fee to cover the cost of 3D printing material?	47.5%	25.9%	11.9%

Question 5 stated "Would having access to a 3D printed model related to the current topic being explained help you better understand the concept". Only 12 of 185 people selected that access to a 3D model would not be beneficial. This shows the desire for models in these STEM courses. Question 7, "Would you be more engaged during class if 3D printed models were offered," with lectures lasting up to an hour and thirty minutes, students can feel drained and gradually become less attentive. Implementing 3D models can keep students engaged, as 176 of 185 testified models will help improve engagement.

Survey results showed that 71.9% of students expressed increased interest in registering for courses that incorporated 3D printed models. Additionally, 79.5% of students indicated they would be more engaged during class if 3D printed models were offered, highlighting the strong positive impact of hands-on learning tools on student interest and engagement.

5. Applications in STEM Education

At Kent State University's College of Aeronautics and Engineering, classes that could benefit from 3D models were targeted. After this first survey was sent out, the professors met to learn about the courses they teach and what 3D-printed models they found could be most helpful in conveying concepts incorporated into their curriculum. After these meetings, parts were designed and printed using Inventor and open-source Creality Ender Cr10s-Pro refurbished printers. These finished parts were brought to the professors to present to their students.

CAD I (ENGR 13586) and CAD II (ENGR 23585) are introductory courses in computer-aided design followed by an advanced course. Students use software such as Autodesk Inventor to explore the creation of different shapes. The physical parts were handed out to students while the professor explained the modeling steps, helping them better understand the design features and geometry being discussed. Figure 2 represents Blocks used in CAD courses.



Figure 2. Blocks for CAD Courses

Dynamics (ENGR 25400) explores kinematics and kinetics acting on rigid bodies in 3D motion. Students analyze these variables with calculations and schematics. The model shown in Figure 3 represents a block and crank mechanism. It was designed specifically to give students a hands-on way to visualize how motion transfers through rotating parts. As the professor explained the theory and calculations, students could interact with the physical model, reinforcing their understanding through both visual and tactile learning.



Figure 3. Block & Crank

Additive Manufacturing (ENGR 42710) discusses topics related to AM, such as design, post-processing, and applications in the real world. This course requires knowledge from CAD I and is paired with a lab section to apply these concepts in practice. Printed parts were offered to this course, and feedback was collected after the parts were introduced. Figures 4 and 5 represent some of the models provided for students. Figure 4 depicts a stylized hand model with lattice structures integrated into the design. This piece exemplifies the capabilities of multi-material and multi-color printing, as well as lightweight design strategies enabled by AM. Figure 5 shows a highly detailed anatomical heart model, which was used to demonstrate biomedical applications of AM, including surgical planning and prosthetic development.



Figure 4. Stylized Hand Model

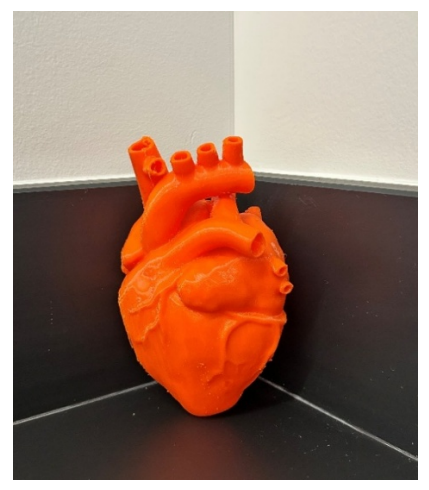


Figure 5. 3D Printed Heart

6. Post Survey

Following this administration, students received a post-survey regarding their experience with the 3D-printed parts used during the lecture. More specifically, the survey assessed the students' satisfaction by evaluating the effectiveness of the 3D-printed models in enhancing their learning experience. This survey included the following questions shown in Table 2. Question number 2 asked "Did this integration help you better understand and connect the concepts you were struggling with

at the beginning of this study". With an agreeing position of 55.2% of the participants, the integration of 3D printed models majorly improves the understanding of concepts in the classroom. Only 13% of respondents thought that the 3D printed models were not useful in the coursework. In terms of engagement in the classroom question 4" Did you find yourself more engaged with the material when 3D printed models were offered?", shows that 57.6% of students felt more engaged in the classroom. Being engaged in class plays a huge part in daily learning for students. In addition to that, a total of 71.6% of students indicated increased interest in registering for courses that incorporate 3D printed models, suggesting strong student enthusiasm for integrating hands-on learning tools into STEM education.

Table 2. Post-Survey Results

Question Number	Question	Disagree	Neutral	Agree
1	What course are you filling this out for?	N/A	N/A	N/A
2	Did this integration help you better understand and connect the concepts you were struggling with at the beginning of the study?	13%	31.8%	55.2%
3	Would you be more interested in registering for a course that incorporates 3D printed models?	3.8%	24.5%	71.6%
4	Did you find yourself more engaged with the material when 3D printed models were offered?	12.5%	30.3%	57.6%
5	Interacting with the 3D-printed models improved your ability to visualize abstract STEM concepts?	14.2%	26%	59.7%
6	Compared to traditional learning methods (e.g., textbooks, lectures), how would you rate the usefulness of 3D-printed models?	5.8%	23.4%	70.8%
7	Would you be willing to pay a small fee to cover cost of 3D printing material?	39%	28.6%	32.5%
8	Did implementation of 3D printed models improve your grade since the last survey?	68.6%	N/A	31.4%

7. Benefits of 3D Printing in STEM Education

The following section outlines the key benefits of integrating 3D printing into STEM education, as identified through the outcomes of the conducted project at Kent State University and some similar projects conducted at other Colleges. These findings are based on direct observations, student feedback, and the measurable impact of hands-on activities during the project. 3D printed models provided students with physical representations that enhanced their understanding and interaction with STEM concepts. The main benefits observed include enhanced engagement, development of visual orientation skills, support for interdisciplinary learning, and improved accessibility.

As students progress in their education, topics become increasingly complex and harder to explain using 2D models such as diagrams or schematics. 3D-printed models can enhance STEM learning by sparking curiosity, improving problem-solving and critical thinking, and building confidence. Before introducing this technology, an assessment should be made to identify student needs, learning styles, and the potential benefits of the models. Since many STEM concepts involve movement or force, these models can illustrate how processes interact within a system. Because they are tangible, students can explore orientations that are not achievable with 2D. Even in virtual settings, Mandal (2020) found that demonstrations of 3D-printed models during online classes improved student understanding. Regardless of format or learning style, 3D-printed models can be customized to support engagement, comprehension, and interest in STEM subjects.

Especially while working with complex math ideas, introducing 3D printed objects into higher-level education classrooms has helped students understand these concepts through the relation of sight and touch by bringing them into a 3D space. To fully understand 3D mathematical concepts, students need to know the proper mathematical language and understand what they mean. Introducing 3D models into the classroom can help students bridge this gap. This exceptional understanding is crucial to the learning process because it helps students practically reason through problems and describes what is happening with the mathematical language they are learning. An experiment done over the course of four years conducted by Herrera et al. (2019) involved two groups, one control, who learned special mathematical skills. Results showed that the experimental group's final grades on a 0-100 scale were 15 points more than the control group.

As reported by Kuzmenko et al. (2020), as students excel further in higher education, the complexity of concepts increases. This makes it crucial for teachers to use aids during lectures to ensure their students grasp the entirety of the concept. Varying from lecture alone to lecture, 3D technologies and practical examples are used to describe concepts. The data in table 3, clearly shows that the implementation of 3D technologies significantly affected the percentage of information retained over three different lengths of time. Although the percentage decreases over time, there is still an increase in retained information and consistency of knowledge with 3D technologies.

Storing information in memory over a certain Methods of teaching (training) material presenting in technical period of time institutions of higher education 5 hours 5 days 1 year Lecture-story 65 11 4 Lecture + innovative ICT 74 27 15 Lecture (distinguishing the components 83 63 31 of Stem-education) Lecture + 3D technologies + STEM-97 95 74 education elements (practical examples)

Table 3. Efficiency of Application of Innovative 3D Technologies, (Kuzmenko et al. (2020))

8. Challenges and Considerations

When integrating this technology into classrooms and communities, there are a few challenges to keep in mind. The initial cost of these machines and materials is quite high. In addition to this, there will be issues of designing and printing the models if the professors do not have prior experience in this craft. A solution to this problem would be training courses which could cost more money. Some curriculums and subjects may blend better with this sort of teaching technique than others. The following sections outline some of the key obstacles currently faced by educators and institutions as they seek to incorporate 3D printing into their teaching strategies.

Not all schools have equal access to 3D printing technology, leading to disparities in learning opportunities among students across different regions or socioeconomic backgrounds. Gallup & Pearce (2020) tested the economic standpoint of schools using 3D printers to create learning models for students of varying age groups. Models of varying complexity were created to form a frame that displays the Pythagorean Theorem to combustion engine models. The models were downloaded from MyMiniFacotry and are completely free. In a set of 38 models, the average amount each was downloaded was 1500 times, and the average annual savings per model was 11,822 USD. Only 38 learning aids in an average of 3.42 years have saved the international educational community 1.7 million USD. 3D printers capable of printing these aids cost 500-1000 USD, with each roll of material costing 20 USD. The educational community would be saving a large amount of money by printing aids rather than ordering them from Amazon.

Üçgül and Altiok (2023) investigated the methods used to instruct teachers to use 3D printing technology. To instruct teachers, they were placed into a design course, where they learned how to design objects for 3D printing. At the end of this course, the teachers designed their own 3D models to be printed and assembled to implement in their classrooms. The coursework is out there to instruct teachers on classroom implementation; however, they must take the time to learn these skills. This becomes a challenge when teachers already face demanding schedules and limited professional development opportunities. Without dedicated time and support, adoption of 3D printing in classrooms may be inconsistent or superficial.

There are many courses in STEM education where 3D models would not be of assistance. For example, an introduction to MATLAB would be a course where models would be useless. MATLAB is a coding software that allows complex manipulation of matrices and the creation of 3D graphics for 3D graphs. 3D models would be useless when attempting to learn a programming language. They

would also not facilitate learning in courses involving quality engineering, engineering ethics, and project management. This highlights the importance of aligning instructional tools with course objectives. Not all STEM subjects benefit equally from hands-on physical modeling.

9. Implementations

The result from the post survey indicates that there can be many possible implementations of 3D printed models in the classroom. This study only encompassed a small number of courses in STEM higher educational coursework. With more classes involved in 3D printing models to convey topics, there would be a greater understanding of concepts across all coursework. There would be an increase in passing grades in courses, and students would feel more confident in their abilities. In addition to that, a request will be made to faculty members across STEM disciplines to consider integrating 3D printing into their syllabi. By incorporating 3D printed models into course curricula, instructors can provide students with a more interactive and tangible approach to learning.

As an additional type of implementation, it is being considered to incorporate this project into reverse engineering exercises. For instance, in CAD courses, 3D printed models could be provided to students along with precision measuring tools such as calipers. Students would then be tasked with generating corresponding CAD files based on the physical models. This approach would reinforce technical drawing and modeling competencies and promote the development of critical thinking and problem-solving skills.

As a next step, outreach will be made to the School of Architecture at Kent State University to explore the possibility of implementing a version of this study within their curriculum. Given the design-oriented and hands-on nature of architectural education, the integration of 3D printing is expected to align well with their teaching approach. Future studies should aim to include a broader range of disciplines and academic levels, and longitudinal data should be gathered to assess the sustained impact of 3D printed learning tools across diverse educational contexts.

10. Conclusion

Recognizing the challenges STEM students face in connecting abstract concepts, this study investigated the use of Additive Manufacturing and 3D Printing to enhance learning in higher education. Conducted at Kent State University's College of Aeronautics and Engineering, the project used surveys and 3D printed models to assess student satisfaction, revealing increased engagement and improved comprehension.

Post-survey results demonstrated that the integration of 3D printed models improved students' understanding (55.2%), enhanced classroom engagement (57.6%), and increased interest in registering for courses utilizing such tools (71.6%), highlighting the strong positive impact of handson learning aids in STEM education. 3D printing is very effective in helping students learn in the classroom. The models created through this method benefited many colleges students' learning at Kent State University. Through the post-survey results, students showed improvement in learning difficult concepts they were struggling with. There was also increased student engagement and interest in future course incorporation. By translating abstract concepts into tangible models, students were able to grasp ideas more quickly and retain information better. This hands-on approach also encouraged collaborative learning and peer-to-peer discussion.

3D models cannot be used to convey concepts in all courses, and professors and students alike will need to learn the software before accessing this technology. While 3D printed models can be assistive in some courses, there are somewhere that do not affect students learning. On the other

hand, this technology can be used in many courses and subjects. It is beneficial in providing students with a visual and physical representation of the concept being taught, which increases student engagement towards the coursework during lectures. Therefore, selecting appropriate courses for implementation is critical to maximizing the benefits of 3D printing. Understanding both the limitations and opportunities of technology ensures its effective integration into the curriculum. Future studies should investigate a broader range of disciplines and course levels to assess the full impact of 3D learning tools. Longitudinal data could also help evaluate sustained benefits over time and across various educational contexts.

11. Disclaimer Statements

Funding: None

Conflict of Interest: None

12. References

- Assante, D., Cennamo, G. M., & Placidi, L. (2020, April). 3D printing in Education: an European perspective. In 2020 IEEE global engineering education conference (EDUCON) (pp. 1133-1138). IEEE. https://doi.org/10.1109/EDUCON45650.2020.9125311
- Bicer, A., Nite, S. B., Capraro, R. M., Barroso, L. R., Capraro, M. M., & Lee, Y. (2017, October). Moving from STEM to STEAM: The effects of informal STEM learning on students' creativity and problem-solving skills with 3D printing. In 2017 IEEE frontiers in education conference (FIE) (pp. 1-6). IEEE. https://doi.org/10.1109/FIE.2017.8190545
- Ford, S., & Minshall, T. (2019). Invited review article: Where and how 3D printing is used in teaching and education. Additive manufacturing, 25, 131-150. http://dx.doi.org/10.1016/j.addma.2018.10.028
- Gallup, N., & Pearce, J. M. (2020). The economics of classroom 3-D printing of open-source digital designs of learning aids. Designs, 4(4), 50. http://dx.doi.org/10.3390/designs4040050
- Herrera, L.M., Perez, J.C., & Ordonez, S.L. (2019). Developing spatial mathematical skills through 3D tools: augmented reality, virtual environments and 3D printing. International Journal on Interactive Design and Manufacturing, 13, 1385-1399. https://link.springer.com/article/10.1007/s12008-019-00595-2
- Kuzmenko, O., Dembitska, S., & Radul, S. (2020). Implementation of STEM-Education Elements in the Process of Teaching Professional Subjects in Technical Institutions of Higher Education. Modern approaches to knowledge management development: collective monograph, 85-95 http://dx.doi.org/10.31649/2524-1079-2021-6-1-021-026
- Mandal, N., (2021). 3D printed models to enhance engineering student engagement and learning. Global Journal of Engineering Education, 23, 176-184. http://www.wiete.com.au/journals/GJEE/Publish/TOCVol23No3.html
- Ramirez, M.V. & Gordy, C.L. (2020). STEM Build: An Online Community to Decrease Barriers to Implementation of Inclusive Tactile Teaching Tools. Journal of Microbilogy & Biology Education, 21(1), 1-7. http://dx.doi.org/10.1128/jmbe.v21i1.1963
- Sun, Y., & Li, Q. (2018, April). The application of 3D printing in STEM education. In 2018 IEEE international conference on applied system invention (ICASI) (pp. 1115-1118). IEEE http://dx.doi.org/10.1109/ICASI.2018.8394476
- Üçgül, M., & Altıok, S. (2023). The perceptions of prospective ICT teachers towards the integration of 3D printing into education and their views on the 3D modeling and printing course. Education and Information Technologies, 28(8), 10151-10181. http://dx.doi.org/10.1007/s10639-023-11593-z

The Journal of Management and Engineering Integration (JMEI) © 2025 by AIEMS Inc., is licensed under CC BY 4.0. To view a copy of this license, visit https://creativecommons.org/licenses/by/4.0/

2025DOI: 10.62704/10057/31191

EXAMINING MODAL SHIFT IN JAPAN'S LOGISTICS

Yutaka Shirai ¹
Yukio Maruyama ¹
Hiroyuki Ono ¹

¹ Chiba Institute of Technology, Japan

yutaka.shirai@p.chibakoudai.jp

Abstract

The current Japanese distribution industry is confronting difficulties that can be divided broadly into three categories. The first include those related to the shortage of truck drivers (labor shortages). The second category includes difficulties related to the CO2 emissions of trucks (environmental load). The last are difficulties related to a rapid increase in home-delivery services caused by the growth of e-commerce markets. In response to all of these difficulties, a modal shift from trunk cargo transportation that uses trucks to railroad or maritime transportation is important. Therefore, a comparative analysis of the characteristics of intercity truck, rail and vessel transportation in the total cargo volume of Japan conducted for this study is performed from the perspective of three factors including distance, time required and fares, with discussion of effective modes of transportation (modal shift).

Keywords: Logistics; Modal Shift; Truck Transportation; Rail Transportation; Vessel Transportation

1. Introduction

Effective April 2024, the maximum limit of 960 hours (hr) per year was placed on overtime work in Japan pursuant to the Act on the Arrangement of Related Acts to Promote Work Style Reform. Coinciding with this, the standard for improving working hours of car drivers, in which the portal-to-portal time of truck drivers was specified by the Ministry of Health, Labor and Welfare (MHLW), was revised to ensure compliance with the portal-to-portal time. The possibility that these two factors will cause distribution in Japan to be stagnant has been indicated. Without specific measures taken, approximately 34% of transportation capacity is estimated to become insufficient by 2030, suggesting a need to raise distribution efficiency.

The Japanese distribution industry today is confronting difficulties that can be broadly divided into three categories. The first are difficulties related to the shortage of truck drivers (labor shortages) (Tsuchiya and Kurokawa, 2022). The number of young truck drivers is on a declining trend because of long working hours and low wages. The second category includes environmental difficulties related to the CO2 emissions of trucks (Shirai, Furihata and Ono, 2016; Siskos and Moysoglou, 2019; Velázquez-Martínez, Fransoo, Blanco and Valenzuela-Ocaña, 2016). Reduction of the environmental load imposed by the logistics industry is strongly demanded because of the global trend of reducing greenhouse gas emissions as a measure against global warming. Trucks impose the most burdensome environmental load among the modes of transportation for domestic distribution, including trucks, railroads and vessels (Sohoni, Thomas and Rao, 2017; Wang, Nozick, Xu and Gearhart, 2018). The last category comprises difficulties related to a rapid increase in homedelivery services because of the growth of e-commerce markets (Sheth, 2020). In e-commerce

Submitted: April 28, 2025 Revised: September 3, 2025 markets, the volume of distribution is rising steeply in line with remarkable growth in the usage rate of e-commerce websites as a result of changes in the lifestyles of many people through the popularization of the internet and smartphones, increased telecommuting and demands for communicable disease prevention.

In response to these challenges, the use of a modal shift to convert truck-line cargo transportation from trucks to railroads or vessels is important (Sohoni, Thomas and Rao, 2017; Wang, Nozick, Xu and Gearhart, 2018). Modal shift is the replacement of truck transportation with modes of transportation imposing less environmental loading such as rail or vessel transportation. Modal shift is attracting attention as an important means to achieve sustainable distribution. Although many companies engage in vessel transportation in Japan, only one company operates a nationwide network of rail transportation in Japan: the Japan Freight Railway Company (Japan Freight Railway Company, 2024). Rail and vessel transportation is characterized by low-cost and efficient (large-quantity) transportation with a high on-time performance rate (stability) for the longest route section, which is achieved by combining container cargo and truck transportation. Additionally, it supports the daily life of many people as an environmentally friendly mode of transportation (environmental friendliness). Determining the optimum mode of transportation for each condition by identifying the benefits and shortcomings of truck, rail and vessel transportation based on their characteristics is necessary for modal shift promotion.

This study is based on a comparative analysis of the characteristics of intercity truck, rail and vessel transportation in the total cargo volume of Japan with emphasis on three factors, including distance, time required and fares. Based on those findings, discussion is undertaken of the effective modes of transportation (modal shift).

2. Factor Calculation Analysis

Three-factor calculation analysis is conducted to identify the current statuses of necessary factors for the three modes of transportation, i.e., trucks, railroads and vessels. The necessary factors are distance, time required and fares in transportation sections. Having defined these three concepts as three factors, we designate the derivation of the three factors of each mode of transportation the three-factor calculation. Information related to the three factors of truck, rail and vessel transportation for each intercity route section is not publicly available. Therefore, three-factor data must be derived and compared for the three factors calculated for route sections that are selected in advance. The cargo volume transferred between cities must be identified to perform analyses particularly addressing intercity routes, which can reveal paths the streamlining and optimization of logistics through the promotion of modal shift.

The areas to be studied are the routes between Tokyo and each of the 13 cities in Eastern Japan and those between Tokyo and each of the 13 cities in Western Japan, as presented below. Figure 1 shows the positional relations of the areas to be studied in Eastern Japan. Figure 2 depicts those of the areas to be studied in Western Japan.

Eastern Japan (13 cities)

Hokkaido: Kitami, Asahikawa, Kushiro, Obihiro, Sapporo Muroran and Hakodate.

Tohoku: Aomori, Iwate, Akita, Miyagi, Yamagata and Fukushima.

Western Japan (13 cities)

Chugoku, Kansai and Chubu: Shizuoka, Aichi, Kyoto, Osaka, Okayama and Hiroshima.

Kyushu: Fukuoka, Saga, Nagasaki, Kumamoto, Miyazaki and Kagoshima.

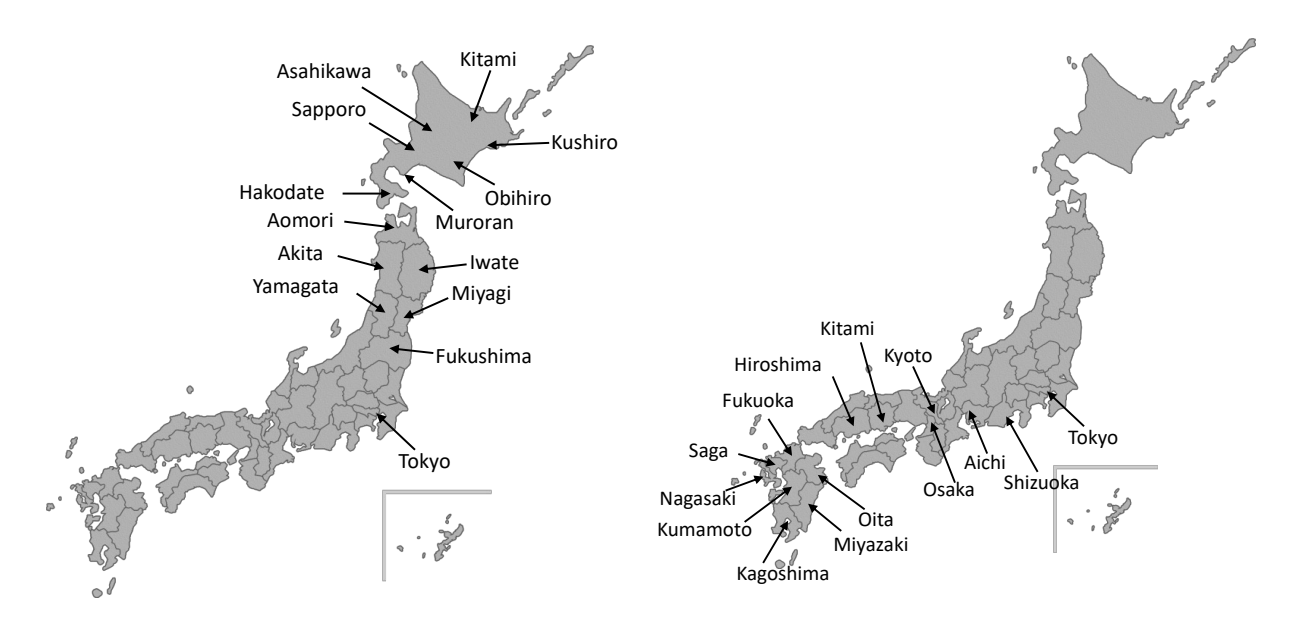


Figure 1. Positional Relations of The Areas in This Study in Eastern Japan

Figure 2. Positional Relations of The Areas in This Study in Western Japan

2.1 Calculation of Three Factors Affecting Truck Transportation

The following are the formulas for the calculation of the three factors of truck transportation.

Distance of truck transportation TD

$$TD = da + db + dc + dd$$
 (Eastern Japan) (1)

$$TD = db + dc + dd$$
 (Western Japan) (2)

da: Transportation distance of trucks traveling on highways in Hokkaido route sections (only Eastern Japan).

db: Transportation distance of trucks traveling on highways in Honshu route sections (Western Japan and Kyushu route sections).

dc: Distance of truck transportation from shippers to interchanges (goods collection distance).

dd: Distance of truck transportation from interchanges to shippers (delivery distance).

Time required for truck transportation TT

$$TT = ta + tb + tc + td$$
 (Eastern Japan) (3)

$$TT = tb + tc + td$$
 (Western Japan) (4)

ta: Duration of transportation by trucks traveling on highways in Hokkaido route sections (only Eastern Japan).

tb: Duration of transportation by trucks traveling on highways in Honshu route sections (Western Japan and Kyushu route sections).

tc: Duration of truck transportation from shippers to interchanges (goods collection time).

td: Duration of truck transportation from interchanges to shippers (time required for delivery).

Fares for truck transportation TF

$$TF = fa + fb + fc + fd$$
 (Eastern Japan) (5)

$$TF = fb + fd$$
 (Western Japan) (6)

fa: fares for truck transportation in Hokkaido route sections (only Eastern Japan).

fb: fares for truck transportation in Honshu route sections (Western Japan and Kyushu route sections).

fc: Highway tolls for Hokkaido route sections and Tsugaru Kaikyo Ferry fares (only Eastern Japan).

fd: Highway tolls for Honshu route sections (Western Japan and Kyushu route sections).

Goods collection distances and delivery distances are specified as 20 km based on the average calculated from the survey report of the Ministry of Land, Infrastructure Transport and Tourism (MLIT) (MLIT, 2024). The time necessary for goods collection and delivery is specified as 1.25 hr (1 hr 15 min) by calculating the time required for a general car to travel 20 km. Fares for Hokkaido and Honshu route sections (including Kyushu) and goods collection and delivery are found by calculating from the "standard fares" in the distance-based fares specified by the MLIT (MLIT, 2024). Truck transportation uses trucks with a maximum load of 14,200 kg (14.2 tons).

Table 1 presents the results of three-factor calculation for truck transportation from each city to Tokyo (data from 2023).

2.2 Three-Factor Calculation for Rail Transportation

The following are formulas used for the calculation of the three factors of rail transportation.

Distance of rail transportation RD

$$RD = de + df + dg (7)$$

de: Distance of intercity rail transportation.

df: Distance of truck transportation from shippers to goods stations (goods collection distance).

dq: Distance of truck transportation from goods stations to shippers (delivery distance).

Time required for rail transportation RT

$$RT = te + tf + tg (8)$$

te: Duration of intercity rail transportation.

tf: Duration of truck transportation from shippers to goods stations (time required for goods collection).

tg: Duration of truck transportation from goods stations to shippers (time required for delivery).

Fares for rail transportation RF

$$RF = fe + ff + fg + fh$$
 (Eastern Japan) (9)

$$RF = fe + ff + fg$$
 (Western Japan) (10)

fe: Fares for intercity rail transportation.

ff: Fares for truck transportation from shippers to goods stations (fares for goods collection).

fg: Fares for truck transportation from goods stations to shippers (delivery charges).

fh: Special fees for Seikan Tunnel added to rail transportation between Honshu and Hokkaido (only Eastern Japan).

Rail transportation uses 12-foot containers (5 tons). Table 2 presents the results of three-factor calculations for rail transportation from each city to Tokyo (data from 2023).

Table 1. Results of Three-Factor Calculation for Truck Transportation from Each City to Tokyo

	Dep	Departure				Breakdown (k	ո (km)				Breakdown (hour)	(hour)					Brea	Breakdown (JPY)	
	Area	City	Arrival	Distance (km)	Distance on highways of Hokkaido (da)	Distance on highways of Honshu (db)	Distance of goods collection (dc)	Distance of delivery (dd)	Time necessary (Duration on highways of Hokkaido (ta)	Duration on highways of Honshu (tb)	Duration of goods collection (tc)	Duration of delivery (td)	Fares per truck (14.2 tons) (JPY)	Fares per ton (JPY)	Fares in Hokkaido per truck (fa)	Fares in Honshu per truck	Highway tolls and ferry fares for Hokkaido per truck (fc)	Highway tolls for Honshu per truck (fd)
		Kitami		1,351	581	731	20	20	19.25	8.50	8.25	1.25	1.25	466,690	32,865	158,640	193,860	88,760	25,430
		Asahikawa		1,233	463	731	20	20	17.50	6.75	8.25	1.25	1.25	436,470	30,737	130,460	193,860	86,720	25,430
		Kushiro		1,324	554	731	20	20	18.75	8.00	8.25	1.25	1.25	464,580	32,717	158,640	193,860	86,650	25,430
(:	Hokkaido	Obihiro		1,210	440	731	20	20	17.25	6.50	8.25	1.25	1.25	424,960	29,927	121,060	193,860	84,610	25,430
seitie		Sapporo		1,089	319	731	20	20	15.75	5.00	8.25	1.25	1.25	392,810	27,663	92,860	193,860	80,660	25,430
(13 प		Muroran		896	198	731	20	20	14.00	3.25	8.25	1.25	1.25	361,000	25,423	64,660	193,860	77,050	25,430
ued		Hakodate	Tokyo	788	18	731	20	20	11.75	1.00	8.25	1.25	1.25	311,040	21,904	21,080	193,860	70,670	25,430
rn Ja		Aomori		713	-	673	20	20	10.00	-	7.50	1.25	1.25	240,390	16,929	-	216,460		086'87
ətse		lwate		594		554	20	20	8.50	,	00'9	1.25	1.25	197,210	13,888	'	176,980	•	20,230
3		Akita		641	-	601	20	20	10.00	-	7.50	1.25	1.25	212,370	14,956	-	190,140	-	22,230
	LONOKU	Miyagi		414	,	374	20	20	7.00		4.50	1.25	1.25	144,250	10,158	1	129,620		14,630
		Yamagata		426	-	386	20	20	7.25	-	4.75	1.25	1.25	149,550	10,532		134,880	-	14,670
		Fukushima		300	-	260	20	20	5.75	-	3.25	1.25	1.25	114,400	8,056	-	103,320	-	11,080
		Shizuoka		221	-	181	20	20	5.25	•	2.75	1.25	1.25	086'96	6,830	-	88,670	•	8,310
		Aichi		392	ı	352	20	20	6.50		4.00	1.25	1.25	148,920	10,487	,	133,870	•	15,050
	Chugoku,	Kyoto		200		460	20	20	7.50		5.00	1.25	1.25	194,450	13,694	,	176,250		18,200
(s	Chubu	Osaka		591		551	20	20	8.50	,	6.00	1.25	1.25	209,580	14,759	,	190,380	•	19,200
eitie		Okayama		695		655	20	20	9.75		7.25	1.25	1.25	235,380	16,576	ı	210,780	•	24,600
(۲3		Hiroshima		847	,	807	20	20	11.75		9.25	1.25	1.25	281,820	19,846	1	251,640		30,180
uede		Fukuoka	Tokyo	1,123	,	1,083	20	20	15.00		12.50	1.25	1.25	367,140	25,855	,	327,250	•	39,890
st u J		Saga		1,149	,	1,109	20	20	15.25		12.75	1.25	1.25	366,260	25,793	,	327,250	•	39,010
Veste		Nagasaki		1,268	,	1,228	20	20	16.50		14.00	1.25	1.25	410,100	28,880	,	367,390	•	42,710
٨	Kyushu	Kumamoto		1,223	,	1,183	20	20	16.00	•	13.50	1.25	1.25	395,320	27,839	1	354,010	•	41,310
		Oita		1,176	1	1,136	20	20	15.75		13.25	1.25	1.25	381,370	26,857	1	340,630	ı	40,740
		Miyazaki		1,284	1	1,244	20	20	17.25		14.75	1.25	1.25	409,630	28,847	1	367,390	•	42,240
		Kagoshima		1,395	,	1,355	20	20	18.25		15.75	1.25	1.25	441,860	31,117		394,150		47,710

Table 2. Results Of Three-Factor Calculation for Rail Transportation from Each City to Tokyo

	Dep	Departure			B	Breakdown (km)	h)		Bre	Breakdown (hour)	ur)				Brea	Breakdown (JPY)	
				Distance	Dictance	Distance of	Distance		noitering	Duration	Duration	Fares per 12- foot container	Fares per	Fares for rail	Fares for goods	Fares for delivery	Seikan Tunnel
	Area	City	Arrival			goods collection	delivery (<i>dg</i>)	necessary (hour)		of goods collection	of delivery (tg)	(5 tons) (JPY)	ton (JPY)	container (5 tons)	foot container (5 tons)	container (5 tons)	12-foot container (5 tons)
						(6)				(6)				(<i>fe</i>)	(<i>ff</i>)	(fg)	(<i>fh</i>)
		Kitami	_	1,581	1,541	20	20	49.00	46.50	1.25	1.25	101,280	20,256	89,500	5,540	5,540	700
		Asahikawa	_	1,403	1,363	20	20	45.75	43.25	1.25	1.25	91,780	18,356	80,000	5,540	5,540	200
		Kushiro	_	1,545	1,505	20	20	52.75	50.25	1.25	1.25	101,280	20,256	89,500	5,540	5,540	700
(Hokkaido	Obihiro	_	1,419	1,379	20	20	45.75	43.25	1.25	1.25	91,780	18,356	80,000	5,540	5,540	700
səiti:		Sapporo	_	1,287	1,247	20	20	23.75	21.25	1.25	1.25	86,780	17,356	75,000	5,540	5,540	700
१३ व		Muroran	_	1,167	1,127	20	20	41.25	38.75	1.25	1.25	81,780	16,356	70,000	5,540	5,540	700
ued		Hakodate	Tokyo	981	941	20	20	20.75	18.25	1.25	1.25	69,780	13,956	58,000	5,540	5,540	700
rn Ja		Aomori	_	729	689	20	20	32.50	30.00	1.25	1.25	56,580	11,316	45,500	5,540	5,540	1
ətse		lwate	_	613	573	20	20	18.00	15.50	1.25	1.25	51,580	10,316	40,500	5,540	5,540	1
3		Akita	_	089	640	20	20	23.75	21.25	1.25	1.25	54,080	10,816	43,000	5,540	5,540	
	Lonoku	Miyagi	_	390	350	20	20	10.50	8.00	1.25	1.25	38,580	7,716	27,500	5,540	5,540	1
		Yamagata	_	501	461	20	20	18.00	15.50	1.25	1.25	45,080	9,016	34,000	5,540	5,540	
		Fukushima		310	270	20	20	15.50	13.00	1.25	1.25	34,580	6,916	23,500	5,540	5,540	
		Shizuoka		214	174	20	20	6.25	3.75	1.25	1.25	29,580	5,916	18,500	5,540	5,540	
		Aichi	_	415	375	20	20	12.50	10.00	1.25	1.25	40,080	8,016	29,000	5,540	5,540	
	Chugoku,	Kyoto	_	552	512	20	20	12.25	9.75	1.25	1.25	49,080	9,816	38,000	5,540	5,540	
(9	chubu	Osaka	_	640	009	20	20	12.00	9.50	1.25	1.25	51,580	10,316	40,500	5,540	5,540	
eitie		Okayama	_	768	728	20	20	14.00	11.50	1.25	1.25	59,580	11,916	48,500	5,540	5,540	
£T)		Hiroshima	_	925	885	20	20	18.00	15.50	1.25	1.25	66,580	13,316	55,500	5,540	5,540	
uede		Fukuoka	Tokyo	1,224	1,184	20	20	23.50	21.00	1.25	1.25	81,080	16,216	70,000	5,540	5,540	
scu 19		Saga	_	1,258	1,218	20	20	25.25	22.75	1.25	1.25	86,080	17,216	75,000	5,540	5,540	
este		Nagasaki	_	1,383	1,343	20	20	28.75	26.25	1.25	1.25	91,080	18,216	80,000	5,540	5,540	
۸	Kyushu	Kumamoto	_	1,347	1,307	20	20	29.00	26.50	1.25	1.25	91,080	18,216	80,000	5,540	5,540	
		Oita	_	1,292	1,252	20	20	25.50	23.00	1.25	1.25	86,080	17,216	75,000	5,540	5,540	•
		Miyazaki	_	1,418	1,378	20	20	28.50	26.00	1.25	1.25	91,080	18,216	80,000	5,540	5,540	,
		Kagoshima		1,549	1,509	20	20	32.50	30.00	1.25	1.25	100,580	20,116	89,500	5,540	5,540	

2.3 Three-Factor Calculation for Vessel Transportation

The following are formulas for the calculation of the three factors of vessel transportation. Distance of vessel transportation *SD*

$$SD = di + dj + dk \tag{11}$$

di: Distance of intercity vessel transportation.

dj: Distance of truck transportation from shippers to goods stations (goods collection distance).

dk: Distance of truck transportation from cargo ports to shippers (delivery distance).

Time necessary for vessel transportation ST

$$ST = ti + tj + tk \tag{12}$$

ti: Duration of intercity vessel transportation.

tj: Duration of truck transportation from shippers to cargo ports (time required for goods collection).

tk: Duration of truck transportation from cargo ports to shippers (time required for delivery).

Fares for vessel transportation SF

$$SF = fi + fj + fk \tag{13}$$

fi: Fares for intercity vessel transportation.

fj: Fares for truck transportation from shippers to cargo ports (charges for goods collection).

fk: Fares for truck transportation from cargo ports to shippers (delivery charges).

Vessel transportation assumes the use of roll-on – roll-off (RORO) vessels and 13-m trailer chassis (20 tons). Table 3 presents the results of three-factor calculation for vessel transportation from each city to Tokyo (data from 2023).

2.4 Calculation of Cargo Information

This study used data for total cargo volumes between cities in the Portal Site of official Statistics of Japan (e-Stat) 2024 provided by the Japanese government. Table 4 presents the results of cargo data calculations for truck transportation from each city to Tokyo (data from 2023), which correspond to the following conditions.

- (A) Annual cargo volume of truck transportation.
- (B) Number of trucks per year considering the load factor (average load factor is set to 70%) for the annual cargo volume.
- (C) Number of trucks per day.
- (D) Number of trucks per business day.

Table 5 presents the results of cargo data calculations for rail transportation from each city to Tokyo (data from 2023), which correspond to the following conditions.

- (E) Annual cargo volume of rail transportation.
- (F) Number of 12-foot containers (5 tons) per year considering the annual cargo volume (average load factor of rail container transportation is set to 70%).
- (G) Number of 12-foot containers per day.
- (H) Number of 12-foot containers per business day.

Table 3. Results of Three-Factor Calculation for Vessel Transportation from Each City to Tokyo

_	Dep	Departure			Bre	Breakdown (km)	n)		Bre	Breakdown (hour)	'ur)				Breakdown (JPY)	
			(;	Distance	Distance of	Distance	Distance	Time	Duration of		Duration	Fares per 13 m trailer chassis	Fares per	Fares for vessel per 13 m trailer	Fares for goods collection per 13 m	Fares for delivery per 13 m trailer
	Area	City	Arrival	(km)	maritime		_	necessary (hour)	maritime		of delivery	(20 tons)	TON (IDV)	chassis	trailer chassis	chassis
					(<i>di</i>)	collection (<i>dj</i>)	(dk)		(ti)	collection (<i>tj</i>)	(tk)	(JPY)	2	(20 tons)	(20 tons)	(20 tons)
		Kitami		C	C	c	c	c	C		c	C	C	(//)	(#)	(JK)
		Acabikawa										0		0		
		Kushiro		1,323	1,201	61	61	40.60	33.60	3.5	3.5	463,970	23,199	364,770	49,600	49,600
	Hokkaido			0	0	0	0	0	0	0	0	0	0	0	0	0
(səiti		Sapporo		0	0	0	0	0	0	0	0	0	0	0	0	0
१३३ ०		Muroran		1,178	1,056	61	61	45.75	38.75	3.5	3.5	424,010	21,201	324,810	49,600	49,600
ued		Hakodate	Tokyo	1,143	1,021	61	61	25.25	18.25	3.5	3.5	410,690	20,535	311,490	49,600	49,600
rn Ja		Aomori		1,219	1,097	19	61	35.80	28.80	3.5	3.5	424,010	21,201	324,810	49,600	49,600
ətse		Iwate		773	651	61	61	23.80	16.80	3.5	3.5	317,450	15,873	218,250	49,600	49,600
3		Akita		1,559	1,437	61	61	45.40	38.40	3.5	3.5	517,250	25,863	418,050	49,600	49,600
	DELOKO	Miyagi		647	525	61	61	21.40	14.40	3.5	3.5	277,490	13,875	178,290	49,600	49,600
		Yamagata		1,543	1,421	61	61	45.40	38.40	3.5	3.5	517,250	25,863	418,050	49,600	49,600
		Fukushima		514	392	61	61	16.60	9.60	3.5	3.5	237,530	11,877	138,330	49,600	49,600
		Shizuoka		438	316	61	61	16.6	9.6	3.5	3.5	224,210	11,211	125,010	49,600	49,600
		Aichi		755	633	61	61	23.8	16.8	3.5	3.5	304,130	15,207	204,930	49,600	49,600
	Chugoku,	Kyoto		1,811	1,689	61	61	52.6	45.6	3.5	3.5	583,850	29,193	484,650	49,600	49,600
	chubu	Osaka		942	820	61	61	28.6	21.6	3.5	3.5	357,410	17,871	258,210	49,600	49,600
eitie		Okayama		1,010	888	61	61	31.0	24.0	3.5	3.5	370,730	18,537	271,530	49,600	49,600
£1)		Hiroshima		1,147	1,025	61	61	14.2	7.2	3.5	3.5	410,690	20,535	311,490	49,600	49,600
uede		Fukuoka	Tokyo	1,369	1,247	19	19	40.6	33.6	3.5	3.5	463,970	23,199	364,770	49,600	49,600
st u J		Saga		1,450	1,328	61	61	43.0	36.0	3.5	3.5	490,610	24,531	391,410	49,600	49,600
veste		Nagasaki		1,706	1,584	61	61	50.2	43.2	3.5	3.5	557,210	27,861	458,010	49,600	49,600
٨	Kyushu	Kumamoto		1,844	1,722	61	61	52.6	45.6	3.5	3.5	597,170	29,859	497,970	49,600	49,600
		Oita		1,254	1,132	61	61	38.2	31.2	3.5	3.5	437,330	21,867	338,130	49,600	49,600
		Miyazaki		1,354	1,232	61	61	40.6	33.6	3.5	3.5	463,970	23,199	364,770	49,600	49,600
		Kagoshima		1,715	1,593	61	61	50.2	43.2	3.5	3.5	557,210	27,861	458,010	49,600	49,600

Table 4. Results of Cargo Data Calculations for Truck Transportation from Each City to Tokyo

	Depa	arture		(A)	(B) Number of trucks per year	(C)	(D)
	Area	City	Arrival	Annual cargo volume of truck transportation (ton)	considering the load factor for the annual cargo volume (Load factor set as 70%)	Number of trucks per day	Number of trucks per business day
		Kitami		16,584	1,668	5	7
		Asahikawa		11,499	1,157	3	5
		Kushiro		0	0	0	0
	Hokkaido	Obihiro		0	0	0	0
ities		Sapporo		135,389	13,621	37	56
(13 (Muroran		45,945	4,622	13	19
ıpan		Hakodate	Tokyo	52,155	5,247	14	22
Eastern Japan (13 cities)		Aomori		610,159	61,384	168	252
aste		Iwate		313,568	31,546	86	129
"	Tohoku	Akita		151,735	15,265	42	63
	TOTIONU	Miyagi		541,057	54,432	149	223
		Yamagata		365,835	36,804	101	151
		Fukushima		548,743	55,206	151	226
		Shizuoka		1,148,114	115,504	316	473
		Aichi		975,390	98,128	269	402
	Chugoku, Kansai and	Kyoto		94,093	9,466	26	39
(8)	Chubu	Osaka		1,003,443	100,950	277	414
Western Japan (13 cities)		Okayama		68,044	6,845	19	28
(13		Hiroshima		88,701	8,924	24	37
эрап		Fukuoka	Tokyo	408,038	41,050	112	168
ırn J		Saga		71,569	7,200	20	30
/este		Nagasaki		75,714	7,617	21	31
>	Kyushu	Kumamoto		102,656	10,328	28	42
		Oita		0	0	0	0
		Miyazaki		108,148	10,880	30	45
		Kagoshima		104,704	10,534	29	43

Table 5. Results of Cargo Data Calculations for Rail Transportation from Each City to Tokyo

	Depa	arture		(E)	(F) Number of 12-foot	(G)	(H)
	Area	City	Arrival	Annual cargo volume of rail transportation (ton)	containers per year considering the load factor for the annual cargo volume (Load factor set as 70%)	Number of 12-foot containers per day	Number of 12-foot containers per business day
		Kitami		21,900	6,257	17	26
		Asahikawa		25,703	7,344	20	30
		Kushiro		2,415	690	2	3
	Hokkaido	Obihiro		14,600	4,171	11	17
ities		Sapporo		121,454	34,701	95	142
Eastern Japan (13 cities)		Muroran		12,556	3,587	10	15
ıpan		Hakodate	Tokyo	25,359	7,245	20	30
rn Ja		Aomori		35,469	10,134	28	42
aste		lwate		32,485	9,281	25	38
"	Tohoku	Akita		9,584	2,738	8	11
	Tonoku	Miyagi		135,106	38,602	106	158
		Yamagata		1,329	380	1	2
		Fukushima		2,991	855	2	4
		Shizuoka		5,251	1,500	4	6
		Aichi		28,345	8,099	22	33
	Chugoku,	Kyoto		16,296	4,656	13	19
<u></u>	Kansai and Chubu	Osaka		373,109	106,603	292	437
Western Japan (13 cities)		Okayama		88,639	25,325	69	104
(13		Hiroshima		221,993	63,427	174	260
apan		Fukuoka	Tokyo	199,417	56,976	156	234
irn Ja		Saga		50,689	14,483	40	59
/este		Nagasaki		6,440	1,840	5	8
>	Kyushu	Kumamoto		16,459	4,703	13	19
		Oita		5,939	1,697	5	7
		Miyazaki		11,625	3,321	9	14
		Kagoshima		33,878	9,679	27	40

Table 6 presents the results of cargo data calculations for vessel transportation from each city to Tokyo (data from 2023), which correspond to the following conditions.

- (I) Annual cargo volume of vessel transportation.
- (J) Number of 13-m trailer chassis (20 tons) per year that considers the load factor (average load factor is set to 70%) for the annual cargo volume.
- (K) Number of 13-m trailer chassis per day.
- (L) Number of 13-m trailer chassis per business day.

Table 6. Results of Cargo Data Calculations for Vessel Transportation from Each City to Tokyo

	Depa	arture		(1)	(1)		
	Area	City	Arrival	Annual cargo volume of vessel transportation (ton)	Number of 13 m trailer chassis per year considering the load factor for the annual cargo volume (Load factor set as 70%)	(K) Number of 13 m trailer chassis per day	(L) Number of 13 m trailer chassis per business day
		Kitami		3,690	264	1	1
		Asahikawa		0	0	0	0
		Kushiro		109,840	7,846	21	32
	Hokkaido	Obihiro		920	66	0	0
ities		Sapporo		0	0	0	0
(13 0		Muroran		1,020,205	72,872	200	299
Eastern Japan (13 cities)		Hakodate	Tokyo	245,601	17,543	48	72
rn Ja		Aomori		544,567	38,898	107	159
aste		Iwate		748,085	53,435	146	219
ш		Akita		0	0	0	0
	Tohoku	Miyagi		275,767	19,698	54	81
		Yamagata		0	0	0	0
		Fukushima		67,130	4,795	13	20
		Shizuoka		147,289	10,521	29	43
		Aichi		269,749	19,268	53	79
	Chugoku,	Kyoto		0	0	0	0
_	Kansai and Chubu	Osaka		629,798	44,986	123	184
ities		Okayama		340,135	24,295	67	100
Western Japan (13 cities)		Hiroshima		39,653	2,832	8	12
pan		Fukuoka	Tokyo	2,208,521	157,752	432	647
ırı Ja		Saga		0	0	0	0
/este		Nagasaki		30,070	2,148	6	9
>	Kyushu	Kumamoto		0	0	0	0
		Oita		480,171	34,298	94	141
		Miyazaki		46,446	3,318	9	14
		Kagoshima		93,265	6,662	18	27

3. Analysis of Transportation Modes

Based on information from Table 1 to Table 6, Table 7 and Figure 3 present the relations between the shares of transportation (percentages of truck, rail and vessel transportation) from cities in Eastern Japan to Tokyo and three-factor calculations (distance, time required and fares). Table 8 and Figure 4 present the relation between shares of transportation (percentages of truck, rail and vessel transportation) from cities in Western Japan to Tokyo and three-factor calculations (distance, time required and fares).

In Eastern Japan, the share of cargo transportation from Hokkaido to Tokyo is characterized by a high percentage of rail transportation departing from Kitami and Asahikawa and a certain share of truck transportation. The percentages of vessel container transportation from Kushiro, Muroran and Hakodate are very high. Transportation departing from Obihiro shows an extremely high percentage of rail transportation. The percentages of rail transportation and truck transportation from Sapporo are mutually comparable. The share of cargo transportation from Tohoku to Tokyo is characterized

by the tendency that, basically, the closer to Tokyo, the more advantageous truck transportation becomes, whereas, in regions on the Pacific side of Japan (departing from Aomori, Iwate, Miyagi and Fukushima), the percentage of vessel transportation also tends to be high.

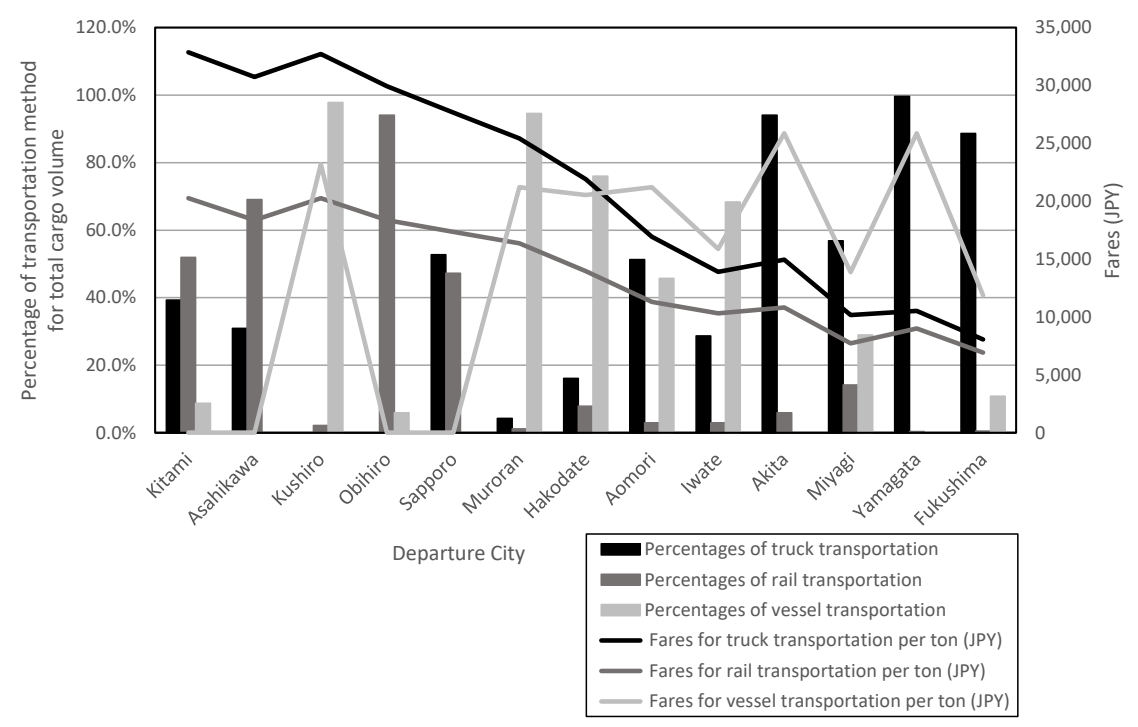


Figure 3. Graph of Relations Between Shares of Transportation and Three-Factor Calculation for Transportation from Eastern Japan to Tokyo

In Western Japan, the share of cargo transportation from Chugoku, Kansai and Chubu to Tokyo is characterized by the general advantage of truck transportation and the tendency by which the farther the origin is from Tokyo, the lower the percentage of truck transportation, and the higher the percentage of rail transportation. In addition, the use of vessel transportation is not necessarily low, although percentages are small. The share of cargo transportation from Kyushu to Tokyo is characterized by the overall high percentage of rail transportation. In regions facing the sea on the east side (departing from Fukuoka and Oita), the percentage of vessel transportation tends to be higher than that of truck transportation. The data suggest that transportation from Saga and Kumamoto uses trucks and railroads because of the sea on the west side that makes vessel transportation time-consuming.

The overall results reflect the characteristics of modes of transportation in each region. In view of the three factors, including distance, time required and fares, truck transportation proves to be advantageous in terms of distance and time required, whereas rail transportation is better in terms of fares. This finding suggests that, in general, effective modes of transportation for short distances are trucks. For medium distances, trucks and railroads hold the greatest benefit. For long distances, railroads and vessels are the most beneficial. Currently, modes of transportation prioritizing distance and time required are used. Goods affected by time required (i.e., perishables) are transported generally by trucks, but we propose a modal shift from trucks to railroads to transport items unaffected by time required (those other than perishables) to the greatest degree possible in light of fares and environmental impacts.

Table 7. Table of Relations Between Shares of Transportation and Three-Factor Calculation for Transportation from Eastern Japan to Tokyo

Transport Share	Transport Share				Distance		i		į		Fares	
Percentages of Percentages of Percentages of truck ruck ransportation transportation transportation (km)	Distance of truck transportation (km)	Distance of truck transportation (km)		Distance · transport (km)	of rail ation	Distance of vessel transportation (km)	Time necessary for truck transportation (hour)	Time necessary for rail for vessel transportation transportation (hour)	Time necessary for vessel transportation (hour)	Fares for truck transportation per ton (JPY)	Fares for rail transportation per ton (JPY)	Fares for vessel transportation per ton (JPY)
39.3% 51.9% 8.7% 1351.30 1581.00	8.7% 1351.30	1351.30		1581.0	0	0.00	19.25	49.00	00'0	32,865	20,256	0
30.9% 69.1% 0.0% 1233.30 1403.00	0.0% 1233.30	1233.30		1403.0	0	0.00	17.50	45.75	0.00	30,737	18,356	0
0.0% 2.2% 97.8% 1324.30 1545.00	97.8% 1324.30	1324.30		1545.0	0	1322.65	18.75	52.75	40.60	32,717	20,256	23,199
0.0% 94.1% 5.9% 1210.30 1419.00	5.9% 1210.30	1210.30		1419.00		0.00	17.25	45.75	00.0	726,62	18,356	0
52.7% 47.3% 0.0% 1089.30 1287.00	0.0% 1089.30	1089.30		1287.00		0.00	15.75	23.75	00:0	27,663	17,356	0
4.3% 1.2% 94.6% 968.30 1167.00	94.6% 968.30	968.30		1167.00		1178.35	14.00	41.25	45.75	25,423	16,356	21,201
16.1% 7.8% 76.0% 788.30 981.00	76.0% 788.30	788.30		981.00		1143.20	11.75	20.75	25.25	21,904	13,956	20,535
51.3% 3.0% 45.8% 713.30 729.00	45.8% 713.30	713.30	-	729.00		1219.05	10.00	32.50	35.80	16,929	11,316	21,201
28.7% 3.0% 68.4% 594.00 613.00	68.4% 594.00	594.00		613.00		773.20	8.50	18.00	23.80	13,888	10,316	15,873
94.1% 5.9% 0.0% 640.90 680.00	0.0% 640.90	640.90		680.00		1559.45	10.00	23.75	45.40	14,956	10,816	25,863
56.8% 14.2% 29.0% 414.30 390.00	29.0% 414.30	414.30	4.30	390.00		647.40	7.00	10.50	21.40	10,158	7,716	13,875
99.6% 0.4% 0.0% 426.40 501.00	0.0% 426.40	426.40		501.00		1542.80	7.25	18.00	45.40	10,532	9,016	25,863
88.7% 0.5% 10.8% 300.30 310.00	10.8% 300.30	300.30		310.00		514.20	5.75	15.50	16.60	8,056	6,916	11,877

Table 8. Table of Relations Between Shares of Transportation and Three-Factor Calculation for Transportation from Western Japan to Tokyo

		Transport Share			Distance			Time necessary			Fares	
City	Percentages of truck transportation	Percentages of Percentages of truck ransportation transportation	Percentages of vessel transportation	Distance of truck transportation (km)	Distance of rail transportation (km)	Distance of vessel transportation (km)	Time necessary for truck transportation (hour)	Time necessary for rail transportation (hour)	Time necessary for vessel transportation (hour)	Fares for truck transportation per ton (JPY)	Fares for rail transportation per ton (JPY)	Fares for vessel transportation per ton (JPV)
Shizuoka	88.3%	0.4%	11.3%	220.50	214.00	438.35	5.25	6.25	16.60	0:830	5,916	11,211
Aichi	76.6%	2.2%	21.2%	392.10	415.00	754.70	6.50	12.50	23.80	10,487	8,016	15,207
Kyoto	85.2%	14.8%	%0:0	500.10	552.00	1811.05	7.50	12.25	52.60	13,694	9,816	29,193
Osaka	20.0%	18.6%	31.4%	591.00	640.00	941.55	8.50	12.00	28.60	14,759	10,316	17,871
Okayama	13.7%	17.8%	68.5%	695.10	768.00	1010.00	9.75	14.00	31.00	16,576	11,916	18,537
Hiroshima	25.3%	63.4%	11.3%	846.70	925.00	1146.90	11.75	18.00	14.20	19,846	13,316	20,535
Fukuoka	14.5%	7.1%	78.4%	1122.60	1224.00	1368.90	15.00	23.50	40.60	25,855	16,216	23,199
Saga	58.5%	41.5%	%0:0	1149.30	1258.00	1450.30	15.25	25.25	43.00	25,793	17,216	24,531
Nagasaki	67.5%	5.7%	76.8%	1268.30	1383.00	1705.60	16.50	28.75	50.20	28,880	18,216	27,861
Kumamoto	86.2%	13.8%	%0:0	1223.30	1347.00	1844.35	16.00	29.00	52.60	27,839	18,216	29,859
Oita	%0:0	1.2%	98.8%	1176.10	1292.00	1254.20	15.75	25.50	38.20	26,857	17,216	21,867
Miyazaki	65.1%	7.0%	27.9%	1283.50	1418.00	1354.10	17.25	28.50	40.60	28,847	18,216	23,199
Kagoshima	45.2%	14.6%	40.2%	1394.50	1549.00	1714.85	18.25	32.50	50.20	31,117	20,116	27,861

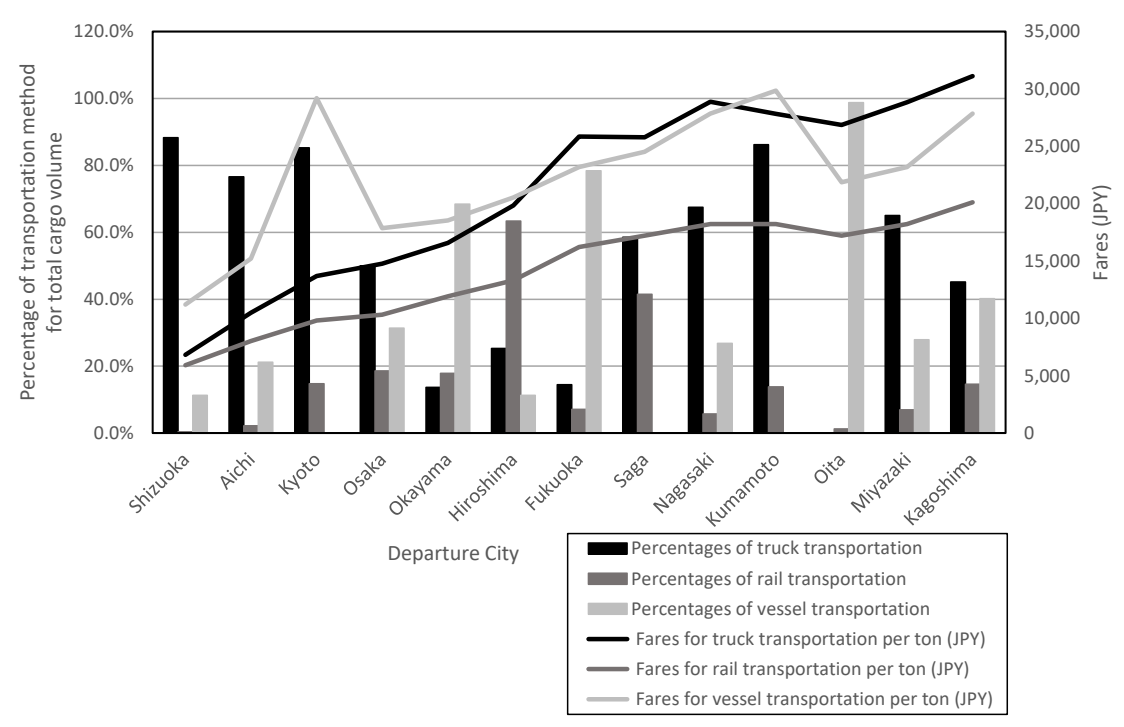


Figure 4. Graph of Relations Between Shares of Transportation and Three-Factor Calculation for Transportation from Western Japan to Tokyo

4. Conclusion

For this study, comparative analysis was performed of the characteristics of intercity truck, rail and vessel transportation in terms of the total cargo volume of Japan from the perspective of three factors including distance, time required and fares, with subsequent discussion of the effective modes of transportation (modal shift). Results suggest that, for goods distribution in Japan (total cargo volume), whereas transportation is mainstream in view of distance and time required, a modal shift to rail and vessel transportation is necessary considering fares and environmental impacts. To accelerate that modal shift, it is important to demonstrate its benefits from the perspective of small and medium-sized truck transportation companies and end-consumers who receive the transported products.

Issues left for future studies include analyses of three-factor calculation for routes between small and medium-sized cities and between Eastern Japan and Western Japan (direct transportation routes in Hokkaido and Kyushu without passing the Tokyo metropolitan area (route via the Sea of Japan)), which are purportedly present greater difficulty when calculating the benefit generated by modal shift.

Furthermore, although this study used total cargo volume data, modes of transportation for categories of goods must also be studied, such as those from agriculture, forestry and fisheries, forest products, metal and machine industrial products, chemical industrial products, miscellaneous manufactured articles, and special goods.

5. Acknowledgements:

This work was supported by the Japan Society for the Promotion of Science (JSPS) KAKENHI Grant Number JP24K07934.

6. Disclaimer Statements

Funding: None

Conflict of Interest: None

7. References

Japan Freight Railway Company (2024). Retrieved from: https://www.jrfreight.co.jp/en.html

Ministry of Land, Infrastructure, Transport and Tourism (MLIT) (2024). Retrieved from: https://www.mlit.go.jp/en/statistics/white-paper-mlit-index.html

Portal Site of Official Statistics of Japan (e-Stat) (2,024). Retrieved from: https://www.e-stat.go.jp/en

Sheth, J. (2020). Impact of COVID-19 on Consumer Behavior: Will the Old Habits Return or Die ?, Journal of Business Research, Vol.117, pp.280–283.

- Shirai, Y., Furihata, W. and Ono, H. (2016). Proposed Techniques for Capacitated Vehicle Routing Problem Considering Environmental Loads, Journal of Management and Engineering Integration, Vol.9, No.1, pp.64–73.
- Siskos, P. and Moysoglou, Y. (2019). Assessing the impacts of setting CO2 emission targets on truck manufacturers: A model implementation and application for the EU, Transportation Research Part A: Policy and Practice, Vol.125, pp.123–138.
- Sohoni, A.V., Thomas, M. and Rao, K.V.K. (2017). Mode Shift Behavior of Commuters due to the Introduction of New Rail Transit Mode, Transportation Research Procedia, Vol.25, pp.2603–2618.
- Tsuchiya, T. and Kurokawa, H. (2022). Discussions on A Framework for Policy Simulation to Deal with the Truck Driver Shortage in Japan, Proceeding to the Ninth International Conference on Transportation and Logistics (T-LOG 2022).
- Velázquez-Martínez, J.C., Fransoo, J.C., Blanco, E.E. and Valenzuela-Ocaña, K.B (2016). A new statistical method of assigning vehicles to deliver areas for CO2 emissions reduction, Transportation Research Part D: Transport and Environment, Vol.43, pp.133–144.
- Wang, H., Nozick, L., Xu, N. and Gearhart, J. (2018), Modeling Ocean, Rail, and Truck Transportation Flows to Support Policy Analysis, Maritime Economics & Logistics, Vol.20, pp.327–357.

The Journal of Management and Engineering Integration (JMEI) © 2025 by AIEMS Inc., is licensed under CC BY 4.0. To view a copy of this license, visit https://creativecommons.org/licenses/by/4.0/

CONCEPTS FOR A NEW CYBER-PHYSICAL SYSTEM: ADDRESSING NATIONAL DEFENSE CHALLENGES IN UAV OPERATIONS

Pedro Cordeiro Povoa Cupertino 1

Adam Carlton Lynch 1

¹ Wichita State University

pxcordeiropovoacupertino@shockers.wichita.edu; adam.lycnh@wichita.edu

Abstract

This research introduces a Cyber-Physical System for defense UAVs. Based on DOD research priorities, the solution can improve UAVs. The solution integrates KEEN concepts, aligning the system design with operational and strategic needs. Costs, suppliers, equipment, and compatibility with existing UAVs were analyzed. The Gantt Chart deploys in phases considering manufacturability and cost. This research explores financial and operational benefits to DoD UAVs. Combining systems engineering and KEEN, this research baselines the innovative CPS challenges in defense UAVs.

Keywords: Cyber-Physical Systems, UAVs, DoD, KEEN

1. Introduction

1.1 Background

Unmanned Aerial Vehicles (UAVs) have emerged as fundamental components of modern military operations. This evolution is evident in recent conflicts in Syria, Libya, Nagorno-Karabakh, and Ukraine, marking what is popularly referred to as the era of "Dronization" (Vallée, 2023). In such a setting, Cyber-Physical Systems (CPS) are crucial for integrating UAV's physical components with its processing capabilities. However, as military operations become more complex, advancing next-generation CPS to enhance defense capabilities has become a strategic necessity.

The U.S. Department of Defense (DoD) Cyber Strategy emphasizes the necessity of developing systems capable of defending the nation, winning wars, protecting allies, and maintaining a technological edge in cyberspace (Department of Defense, 2023). One key element to facilitate this vision is possessing a secure and robust supply chain base. It is noted that the last decades of outsourcing significant sectors of U.S. manufacturing have come with important vulnerabilities (Joint Economic Committee, 2022) and growing geopolitical competition has exposed this risk. Consequently, there is a renewed national urgency to reestablish domestic manufacturing capabilities, especially for systems related to defense and national interests.

Guided by the Kern Entrepreneurial Engineering Network (KEEN) and its emphasis on Creating Value, this study examines US-based costs, components, and suppliers to determine whether the entire CPS can be designed and manufactured in the US. The objective is to offer an actionable plan for a new CPS development that benefits defense, industry, and academia.

1.2 Cyber-Physical Systems (CPS) and Unmanned Aerial Vehicles (UAVs)

Cyber-Physical Systems in UAVs enable dynamic reconfiguration, autonomous operation, and adaptability of missions. These systems integrate computational intelligence and physical

Submitted: April 29, 2025 Revised: September 6, 2025 components to offer the monitoring, data processing, and control of UAV operations. CPS technologies are critical in contested or infrastructure-constrained environments, offering edge computing, secure communication, and autonomous decision-making.

Despite their capabilities, CPS technologies can face many intricate challenges. These include dependability, maintainability, availability, safety, reliability, robustness, predictability, reconfigurability, security, confidentiality, heterogeneity, and scalability (Awotunde et al., 2022). These features significantly affect the performance of CPS-enabled UAVs in military applications and must be considered as part of the system design. Also, most of these problems are compounded by the global nature of supply chains, which are susceptible to disruption by geopolitical tensions, regulatory differences, and logistical bottlenecks.

1.3 Kern Entrepreneurial Engineering Network (KEEN)

The KEEN mindset drives engineers beyond the realm of technical feasibility by infusing value creation, curiosity, and connectivity in the quest for solutions that work in real-life (Engineering Unleashed, n.d.). This research is grounded in value creation and innovation, and proposes an idea that can bring both technical and financial benefits to defense, industry, and academia.

1.3.1 Creating Value

The value creation mindset is embedded throughout the design, integration, and implementation stages of the system, serving as a catalyst for cross-disciplinary innovation and strategic decision-making (Rae and Melton, 2017). To clearly demonstrate the value generated, this study uses the Cost-Quality-Delivery (CQD) model. This approach evaluates not only technical performance but also each decision's capacity to generate quantifiable and long-term effects across industry, academia, and defense (Manalo & Manalo, 2010).

1.4 Problem Statement

There is a need to develop a new Cyber-Physical System (CPS). If tailored for integration with current Unmanned Aerial Vehicles (UAVs) operated by the DoD, it can also be faster and easier to implement. As military operations become more sophisticated and cyber threats intensify, one problem is the continued dependence on multinational supply chains that are vulnerable to disruption. Therefore, a critical question remains: Is it feasible to design, procure, and produce an entire CPS using only U.S.-based suppliers?

1.5 Research Questions (RQ)

RQ1: (Cost) What are the cost implications of developing a new CPS domestically?

RQ2: (Quality) Does the United States have the necessary suppliers to support CPS

development?

RQ3: (Delivery) How will a new CPS be produced, integrated, and deployed?

1.6 Contribution

This research contributes to U.S. national defense goals by providing a CPS solution that is cost-designed, quality-assured, and delivery-focused. It incorporates KEEN to promote innovation in a domestically based U.S. supply chain. The initiative considers interdisciplinary collaboration and real-world relevance and creates value for the government, industry, and academia.

1.7 Structure of the Study

In the remaining sections of this study, we present the Literature Review (Section 2.0), Methods (Section 3.0), Results (Section 4.0), Discussion (Section 5.0), and Conclusion (Section 6.0).

2. Literature Review

2.1 CPS challenges faced by the Department of Defense (DoD)

In the wake of a locally developed Cyber-Physical Systems (CPS) in defense Unmanned Aerial Vehicles (UAVs), it is essential to understand the specific operational and technical matters that the U.S. Department of Defense (DoD) wants to address through its budgetary initiatives. DoD is investing significant funds in Research, Development, Test, and Evaluation (RDT&E) to fund the development of new CPS technologies for UAV platforms.

An in-depth analysis of the elements of new DoD programs indicates that security, reliability, and sustainability are the top three concerns for CPS development (Cupertino & Lynch, in press). They are not only critical to mission' success but also encompass the greater strategic interests of maintaining cyber and operational superiority in contested environments.

2.2 UAV systems in Military Operations

To ensure the feasibility of CPS integration, it is necessary to evaluate the diversity and operational demands of the UAVs currently deployed by the Department of Defense. These UAVs serve a broad range of mission profiles, including Intelligence, Surveillance, and Reconnaissance (ISR) and precision strike operations (Army Technology, n.d.; Designation-Systems.Net, n.d.; Military Factory, n.d.; U.S. Air Force, n.d.-a through n.d.-e; U.S. Army, n.d.).

UAV platforms vary in payload capacity, endurance, size, and onboard computing power. The proposed CPS must be compact, lightweight, and adaptable to fit a broad range of systems without affecting performance. Table 1 summarizes the key UAV platforms and their estimated capabilities. Because official data are limited, this study used open-source estimates.

Drone	Mission	Approx. Quantity	Approx. Payload Volume (ft³)	Approx. Payload Capacity (lbs)
RQ-11 Raven	Reconnaissance, Surveillance	7362	0.10	5.0
AeroVironment Wasp III	Close-Range ISR	990	0.05	2.5
RQ-20 Puma	Tactical ISR, Maritime Patrol	1137	0.30	15.0
RQ-16 T-Hawk	Recon, IED Detection (hover-capable)	306	0.20	9.0
MQ-1 Predator / Gray Eagle	ISR + Precision Strike	246	29.00	450.0
MQ-9 Reaper	Strategic ISR + Attack Missions	126	66.00	3,750.0
RQ-7 Shadow	Tactical Recon/Surveillance	491	2.50	60.0
RQ-4 Global Hawk	High-Altitude, Long-Endurance ISR		420.00	3,000.0
	TOTAL	10691	-	

Table 1. Drones Operated by the DoD and their Estimated Capabilities

3. Methods

3.1 Components Selection

CPS development and component selection were guided by the top three DoD CPS priorities: Security, Dependability, and Sustainability. The system includes processors, encrypted communication modules, and high-efficiency power regulation units. The components were checked to see if they were available domestically, after some domestic suppliers were identified, complying with defense contracting standards, which facilitated purchasing and integration.

3.2 Supply Chain Analysis and Components Cost

After identifying the necessary components, a more comprehensive quantity of suppliers was identified. It was checked whether established U.S.-based companies were already under DoD contracts (Defense News, n.d.). Suppliers were selected based on their relationships with the current top DoD contractors (e.g., Lockheed Martin, RTX, and Northrop Grumman). This approach minimizes foreign dependency and enhances logistics resilience. Public data enabled the identification of the component models and their physical characteristics. Using this data, other information such as the total weight, volume, and cost was estimated using the following equations:

$$W_{Total} = \sum_{i=1 \atop n}^{n} W_i = W_1 + W_2 + W_3 + \dots + W_n$$
 (1)

$$V_{Total} = \sum_{i=1}^{n} V_i = V_1 + V_2 + V_3 + \dots + V_n$$
 (2)

$$C_{Total} = \sum_{i=1}^{n} C_i = C_1 + C_2 + C_3 + \dots + C_n$$
 (3)

3.3 Implementation Planning

To determine the suitability of the Cyber-Physical System, the drone payload and volume limits were compared with CPS requirements. A Gantt chart was developed, covering procurement, subsystem integration, UAV integration/testing, and full deployment.

4. Results

4.1 Selected Components

The components selected for the idealized CPS are listed in Table 2. These were chosen to address the DoD's priorities in security, reliability, and sustainability.

Component	Function in CPS
Mesh Network Radio	Enables self-healing, decentralized communication between UAVs without relying on a central node
High-Gain Antenna	Ensures long-range, high-throughput signal transmission in contested or low-signal environments
Edge Computing Processor	Provides real-time, onboard computation for autonomy, decision-making, and data filtering
Encryption Hardware	Delivers secure cryptographic operations, including data encryption, authentication, and node identity
Power Management Module	Maintains stable voltage and power delivery to all CPS components, with protection from power surges

Table 2. CPS Required Components

Some UAVs possess onboard systems, and to prevent overloading of drones, Table 2 presents only the necessary hardware parts that are required in the proposed CPS. These include: a mesh network radio for decentralized communication, high-gain antenna for a wider signal range, edge computing processor for autonomy, encryption hardware for safe data processing, and power management module for voltage control.

4.2 Strategic Supply Chain Configuration (RQ2) and Components Cost (RQ1)

All selected components were sourced from local suppliers. The suppliers are CMMC or ITAR-certified, enabling secure and efficient integration with national defense efforts. This enhances the U.S. industrial base and long-term supply chain resilience. Table 3 shows the total weight, space

occupied, and cost of the components found in the domestic suppliers (Ezurio, n.d.; Intel Corporation, n.d.; Microchip Technology Inc., n.d.; Silvus Technologies, n.d.; Texas Instruments, n.d.).

Components	Companies	Products	Weight (lbs)	Space Occupied (ft ³)	ost/Unity (Dollars)
Mesh Network Radios	Silvus Technologies	Silvus Technologies StreamCaster 4200	1.50	0.035	\$ 30,000.00
High-Gain Antennas	Ezurio(Former Laird Connectivity)	Laird Phantom High-Gain Antenna	0.20	0.007	\$ 75.00
Edge Computing Processor	Intel Corporation	Intel Movidius Myriad X	0.50	0.002	\$ 400.00
Encryption Hardware	Microchip Technology Inc	Microchip AT97SC3205T TPM	0.01	0.003	\$ 10.00
Power Management Module	Texas Instruments	TPSM843820 8A SWIFT™ Step-Down Power Module	0.15	0.005	\$ 20.00
		TOTAL	2.36	0.052	\$ 30,505.00

Table 3. CPS Weight, Volume, and Estimated Cost

The proposed Cyber-Physical System takes up only 0.052 ft³ of space and has a weight of 2.36 lbs., which make it possible to be implemented in 90% of the UAVs already in use by DoD. The overall cost per unit is \$30,505.00. Figure 1 shows the geographic locations of the domestic suppliers identified, illustrating that the U.S. has the production capability to manufacture a new CPS domestically.

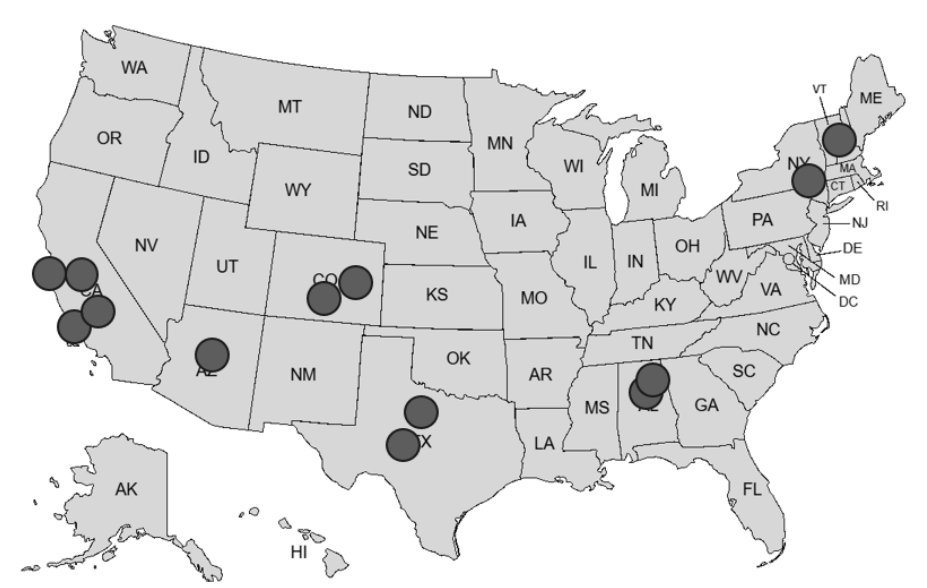


Figure 1. Locations of Identified U.S. Suppliers

4.3 System Integration Timeline (RQ3)

The Gantt Chart, in Figure 2, was derived from the standard subsystem development and integration practices in DoD UAV programs. The 5-month duration was estimated by breaking the process into 4 phases: System Architecture & Requirements, Hardware Integration & Bench Testing, UAV Integration and Field Testing, and Deployment & Monitoring.

Phases		Months					
rilases	1	2	3	4	5		
System Architecture & Requirements							
Hardware Integration & Bench Testing							
UAV Integration & Field Testing							
Deployment & Monitoring							

Figure 2. CPS Implementation Timeline

5. Discussion

5.1 Interpretation of results

RQ1: (Cost) What are the cost implications of developing a new CPS domestically?

The proposed Cyber-Physical System is a comparatively low-cost alternative to the full redesign of UAV or new platform construction. The unit cost of production was approximately \$30,505.00. Acquisition from credible U.S. defense corporations avoids import tariff costs, regulatory delays, and geopolitics-driven costs. This initiative promotes collaborative innovation by involving U.S.-based suppliers and local workforce ecosystems. Academic institutions located near these supplier hubs can contribute to testing, prototyping, and process improvement, directly supporting KEEN's goal of connecting engineering education to industry and government needs.

RQ2: (Quality) Does the United States have the necessary suppliers to support CPS development?

System quality is improved using CMMC and/or ITAR-compliant U.S.-based suppliers. This is in line with defense processes without exposing the firm to threats from supply chain disruptions. Furthermore, the CPS modular design improves operational reliability through decreased complexity, ease of rapid field replacement, and seamless accommodation of platform upgrades.

RQ3: (Delivery) How will a new CPS be produced, integrated, and deployed?

The idealized CPS design supports rapid integration, requiring approximately five weeks from development to deployment. The four-phase implementation framework offers flexibility in the mission profile. System modularity minimizes the retraining needs and engineering overhead. The delivery strategy reflects the KEEN mindset of innovation, balancing systems engineering, lean thinking, and an entrepreneurial mindset to deliver value to government, industry, and academia.

5.2 Implications

5.2.1 For Academia

This project creates a bridge between academic research and national defense initiatives. It uses systems engineering and the KEEN concepts. It creates a foundation for hands-on research, capstone projects, and curriculum development, aligned with real-world challenges. It encourages students and faculty to engage with emerging defense technologies and supply chain realities.

5.2.2 For Industry

The system offers a deployable and scalable solution that aligns with real-world production needs. This opens opportunities for manufacturing contracts, dual-use technology transfer, and system expansion across various UAV platforms. By fostering strategic collaboration among domestic suppliers, CPS design also contributes to national innovation and an industrial base that supports defense logistics.

5.2.3 For Government

This study supports government initiatives to embed secure, locally manufactured systems, to enhance supply base independence and mission robustness. The idealized CPS enforces DoD modernization initiatives through the establishment of a modular platform that can resist geopolitical risks and face technologically developments in other nations.

5.3 Limitations of the Study

This research focuses on the integration, manufacturing, and domestic sourcing of a new CPS aligned with DoD priorities. Information on cybersecurity, such as intrusion detection systems, encrypted software protocols, and secure firmware mechanisms, is beyond the scope of this study and warrant further research. Not all the suppliers and cost information are publicly available, and therefore some lack certainty crept into cost modeling. As partnerships are created and proprietary data becomes available, the CPS component list and system architecture may evolve.

5.4 Suggestions for future work

Future research can include a SysML approach to validate system functionality. Conduct a Design Failure Mode and Effects Analysis (DFMEA) using the 6M methodology to assess risks. It is recommended to analyze how cybersecurity resilience and adaptive behavior can be achieved.

6. Conclusion

This paper presents a domestically sourced CPS solution with preliminary results suggesting affordability and alignment with the cost, quality, and delivery requirements. Further validation using proprietary supplier data would strengthen this assessment. This solution offers a scalable concept for real-world development and deployment, focusing on national defense demands.

7. Disclaimer Statements

Funding: None

Conflict of Interest: None

8. References

Amentum. (n.d.). Amentum: Global engineering and technology solutions. Retrieved January 31, 2025, from https://www.amentum.com/

Army Technology. (n.d.). MQ-1C Gray Eagle ER/MP Unmanned Aircraft System (UAS). Retrieved January 3, 2025, from https://www.army-technology.com/projects/mq1c-gray-eagle-uas-us-army/

Awotunde, J. B., Amuda, K. A., Oguns, Y. J., Nigar, N., Adeleke, T. A., Olagunju, K. M., & Ajagbe, S. A. (2022). Cyber-physical systems security: Analysis, opportunities, challenges, and future prospects. Springer. https://link.springer.com/content/pdf/10.1007/978-3-031-25506-9 2.pdf

Boeing. (n.d.). The Boeing Company official website. Retrieved Jan 31, 2025, from https://www.boeing.com/

- Booz Allen Hamilton. (n.d.). Booz Allen Hamilton: Consulting services. Retrieved January 31, 2025, from https://www.boozallen.com/
- Cupertino, P. C. P., & Lynch, A. C. (in press). Cyber-Physical Systems Challenges for UAVs: Defense Industry Insights. Proceedings of the 2025 ASEE Gulf-Southwest Annual Conference, The University of Texas at Arlington. American Society for Engineering Education.
- Defense News. (n.d.). Top 100 defense companies. Retrieved January 5, 2025, from https://people.defensenews.com/top-100/
- Department of Defense. (2023). 2023 DoD Cyber Strategy Summary. U.S. Department of Defense. https://media.defense.gov/2023/Sep/12/2003299076/-1/-1/2023_DOD_Cyber_Strategy_Summary.PDF
- Designation-Systems.Net. (n.d.). AeroVironment RQ-20 Puma. Retrieved January 3, 2025, from https://www.designation-systems.net/dusrm/app2/q-20.html
- Engineering Unleashed. (n.d.). What is KEEN? https://engineeringunleashed.com/what-is-keen
- Ezurio. (n.d.). Laird Phantom high-gain antenna product page. Retrieved April 7, 2025, from https://www.ezurio.com/internal-antennas
- General Dynamics. (n.d.). General Dynamics: Aerospace and defense company. Retrieved January 31, 2025, from https://www.gd.com/
- HII. (n.d.). HII: Global, all-domain defense provider. Retrieved January 31, 2025, from https://hii.com/
- Intel Corporation. (n.d.). Intel® Movidius™ Myriad™ X VPU. Retrieved April 7, 2025, from https://www.intel.com/content/www/us/en/products/details/processors/movidius/myriad-x.html
- Joint Economic Committee. (2022, February 1). Decades of Manufacturing Decline and Outsourcing Left U.S. Supply Chains Vulnerable to Disruption. United States Congress. https://www.jec.senate.gov/public/index.cfm/democrats/2022/2/decades-of-manufacturing-decline-and-outsourcing-left-u-s-supply-chains-vulnerable-to-disruption
- L3Harris Technologies. (n.d.). L3Harris: Fast. Forward. Retrieved Jan 31, 2025, from https://www.l3harris.com/
- Leidos. (n.d.). Leidos: Innovative solutions through information technology. Retrieved January 31, 2025, from https://www.leidos.com/
- Lockheed Martin. (n.d.). Lockheed Martin: Leading aerospace and defense Retrieved January 31, 2025, from https://www.lockheedmartin.com/
- Manalo, R. G., & Manalo, M. V. (2010). Quality, cost and delivery performance indicators and activity-based costing. 2010 IEEE International Conference on Management of Innovation & Technology, 869–874. IEEE. https://ieeexplore.ieee.org/abstract/document/5492805
- Microchip Technology Inc. (n.d.). AT97SC3205T: Trusted Platform Module. Retrieved April 7, 2025, from https://www.microchip.com/en-us/product/AT97SC3205T
- Military Factory. (n.d.). Honeywell RQ-16 T-Hawk. Retrieved January 3, 2025, from https://www.militaryfactory.com/aircraft/detail.php?aircraft_id=1025
- Northrop Grumman. (n.d.). Northrop Grumman: Aerospace and defense technology. Retrieved April 7, 2025, from https://www.northropgrumman.com/
- Rae, D. & Melton, D. E. (2017). Developing an entrepreneurial mindset in US engineering education: an international view of the KEEN project. The Journal of Engineering Entrepreneurship, 7(3). https://bgro.repository.guildhe.ac.uk/id/eprint/161/
- RTX. (n.d.). RTX: Home. Retrieved Jan 31, 2025, from https://www.rtx.com/
- Silvus Technologies. (n.d.). StreamCaster 4200 radios for tactical mesh networking. Retrieved April 7, 2025, from https://silvustechnologies.com/products/streamcaster-4200/
- Texas Instruments. (n.d.). TPSM843820 8A SWIFT™ Step-Down Power Module. Retrieved April 7, 2025, from https://www.ti.com/product/TPSM843820
- U.S. Air Force. (n.d.-a). MQ-1B Predator. Retrieved January 3, 2025, from https://www.af.mil/About-Us/Fact-Sheets/Display/Article/104469/mq-1b-predator/
- U.S. Air Force. (n.d.-b). MQ-9 Reaper. Retrieved January 3, 2025, from https://www.af.mil/About-Us/Fact-Sheets/Display/Article/104470/mq-9-reaper/
- U.S. Air Force. (n.d.-c). RQ-4 Global Hawk. Retrieved January 3, 2025, from https://www.af.mil/About-us/Fact-Sheets/Display/Article/104516/rq-4-global-hawk/

- U.S. Air Force. (n.d.-d). RQ-11B Raven. Retrieved January 3, 2025, from https://www.af.mil/About-Us/Fact-Sheets/Display/Article/104533/rq-11b-raven/
- U.S. Air Force. (n.d.-e). Wasp III. Retrieved January 3, 2025, from https://www.af.mil/About-Us/Fact-Sheets/Display/Article/104480/wasp-iii/
- U.S. Army. (n.d.). RQ-7B Shadow Tactical Unmanned Aircraft System (TUAS). Retrieved January 3, 2025, from https://www.army.mil/article/137609/rg 7b shadow tactical unmanned aircraft system tuas
- Vallée, P. (2023). The role of unmanned aerial vehicles in current and future conflicts. Revue Défense Nationale. https://www.defnat.com/e-RDN/vue-article-cahier.php?carticle=585&cidcahier=131

The Journal of Management and Engineering Integration (JMEI) © 2025 by AIEMS Inc., is licensed under CC BY 4.0. To view a copy of this license, visit https://creativecommons.org/licenses/by/4.0/

THE EFFECT OF PILOT MENTAL HEALTH ON PASSENGER WILLINGNESS TO FLY

Isabella Laurynn DeLoach1

Sara Bergamini 1

Dowon Choi¹

Vivek Sharma¹

Brooke E. Wheeler 1

¹ Florida Institute of Technology

deloachisabella5@gmail.com; bwheeler@fit.edu

Abstract

This study explored how passengers' willingness to fly is affected by the mental health condition of pilots and their various coping mechanisms. Data were collected from 76 participants at a university in the Southeastern United States via a Qualtrics questionnaire. Participants received four scenarios regarding pilot mental health: no history of mental health issues, history of mental health issues with medication as a coping mechanism, history of mental health issues with therapy as a coping mechanism, and history of mental health issues with no coping mechanism. Participants rated their willingness to fly for each scenario. The data were analyzed through a one-way, repeated-measures ANOVA. Results indicated that participants' most preferred scenario was no history of mental health issues. The least preferred scenario was the pilot with no coping mechanism. A significant difference in passenger willingness to fly was found between all pairs of pilot mental health scenarios except therapy compared to medication. The findings emphasized the impact of pilot mental health condition on passenger preferences and provided insight into public perception of pilot mental health.

Keywords: Pilot Mental Health, Coping Mechanisms, Therapy, Medication, Pilot Health, Willingness to Fly, Consumer Perceptions, Passenger Willingness to Fly.

1. Introduction

The aviation industry is constantly growing and changing; because of this, there is a great need to increase awareness of mental health and create resources for pilots struggling with mental disorders. The stigma of mental health has a societal impact on all industries, but for the aviation industry, it may lead to problems, such as reluctance to report mental health issues or pilots struggling without assistance or support. This study explored how passengers' willingness to fly on airlines in the United States was affected by different mental health scenarios.

The purpose of this research was to determine a person's willingness to fly (Rice et al., 2020) when presented with different information regarding a pilot's mental health status and their various coping strategies. Participants were given a questionnaire consisting of four scenarios: no history of mental health issues, a history of depression and attends therapy to cope, a history of depression and uses medication to cope, and a history of depression with no coping mechanism. The research

Submitted: April 29, 2025 Revised: September 8, 2025 question was the following: how does a pilot's mental health status (no history of mental health issues, a history of depression and attends therapy to cope, a history of depression and uses medication to cope, and a history of depression with no coping mechanism) affect passenger willingness to fly? Participants' willingness to fly was expected to differ, depending on the pilot's mental health status.

This study provided data on passenger willingness to fly with pilots using various coping mechanisms to manage mental health conditions. This research improved the understanding of the social acceptance of pilot mental health issues and the degree pilots can receive aid with mental health conditions. Findings from this research study may have broader implications, as a greater understanding of social acceptance is discovered. This information may be used to improve the coping mechanisms pilots can access. This could also decrease the stigma around conversations of pilot mental health. This study could help improve the openness in communication between pilots and airlines surrounding mental health. The results of this study are generalizable to collegiate students in the Southeastern United States due to the sample being representative of that population in age and other characteristics.

2. Literature Review

This section will review past studies on topics related to willingness to fly in relation to pilot mental health. Researchers reviewed willingness to fly, perception of mental health from a public and aviation standpoint, and aeromedical factors. These factors play a vital role in understanding passengers' willingness to fly and the mental health challenges faced by pilots.

2.1 Willingness to Fly

Rice and Winter (2015) investigated if there were emotions that mediated passenger decisions to fly. They found that the emotions of anger, fear, and happiness played a role unconstrained by the dependent variable pilot configuration (Rice & Winter, 2015). Lerner et al. (2014) illustrated that there was a new pattern in the relationship between emotion and decision-making. Learner et al. (2014) can be linked to the research conducted by Rice and Winter (2015) as they investigated emotions used in passengers' decisions to fly because both found that decisions were developed from the emotions the person was experiencing. Lamb et al. (2020) and Rice and Winter (2015) demonstrated the need for a scale to provide accurate information about passengers, leading to the validated willingness to fly scale (Rice et al., 2020). Rice et al. (2020) developed and validated a scale that can be used to determine passenger willingness to fly and another scale determining willingness to pilot to fill the gaps of previous measures.

Willingness to fly is widely affected by both internal (Lamb et al., 2020) and external factors (Graham et al., 2020). Graham and colleagues (2020) demonstrated that safety measures could foster the motivation of aging passengers to travel. Over 60 percent of participants reported that the COVID-19 pandemic influenced their trip decisions. Research found that health safety measures, such as social distancing, regular sanitization, and mask mandates, were the primary factors that affected willingness to fly. The COVID-19 pandemic not only influenced passengers' willingness to fly, but also pilots' willingness to pilot. Wheeler et al. (2021) determined willingness to pilot when presented with different aircraft sanitation scenarios. The results showed that pilots were most willing to pilot when the aircraft was assigned to one certified flight instructor (CFI) and the CFI was responsible for plane sanitation (Wheeler et al., 2021). These studies of willingness to fly and pilot demonstrated that both pilots and passengers want to fly in the safest possible conditions.

2.2 Perception of Mental Health

Mental health is a sensitive topic in many industries. In some instances, industries even go as far as to avoid hiring people with pre-existing mental disorders or conditions. Individuals, who have a diagnosed mental health disorder or condition, can experience changed behavior from people around them based on perceptions they have. People are likely to have prejudices towards others with diagnoses due to a lack of education surrounding mental health (Thornicroft et al., 2016). Although having mental health conditions can cause difficulties, there are options to help manage these conditions, such as medication and therapy. While these options are available, they are not always easily accessible, causing greater difficulty coping with conditions. Other people may have access to these types of services but choose to opt out because of the stigma surrounding coping tools. Typically, people recognized stigma as a treatment barrier and avoided treatment due to the public's discernment (Glazer et al., 2023). Understanding how stigma affects the individual's perception of themself and providing strategies to educate others about mental health disorders helped to reduce stigmas (Gaddis et al., 2018; Thornicroft et al., 2016). Providing the necessary resources may help people manage their symptoms and aid in their day-to-day functions.

It is important to provide useful tools for people with mental health conditions to help them cope. Mental health services provide resources that decrease symptoms and disabilities, but people avoid use of services because of the societal stigmas around mental illness (Corrigan et al., 2014). Stigmas can present themselves in different ways (Corrigan et al., 2014), such as internal factors that may impact a passenger's willingness to fly (Lamb et al., 2020). Although stigma surrounds the issue of mental health and treatment, it is important to provide services and tools to support those with mental health issues.

Medications, such as selective serotonin reuptake inhibitors (SSRI), can help people with mental conditions balance the chemicals in their brains to regulate the correct hormones. Although medication can be helpful, this is not always right for everyone. If desired as an alternative to medication, therapy can be another useful coping mechanism. Therapy can be used to maintain mental health levels or as a more serious treatment. Both medication and therapy can act as a coping mechanism, but this is only an option if it is affordable or covered by health insurance. Many people have trouble accessing mental healthcare. According to Hester (2017), many U.S. veterans had access issues to mental healthcare. This lack of access led to an 18% increase in suicide rates within the span of 4 years (Hester, 2017). Access issues can be present no matter where a person is in the world. Øien-Ødegaard (2024) found that people had access issues to mental health services even in countries where universal healthcare was available. This was due to a lack of understanding of mental healthcare, socio-economic status, support seeking behavior, public and personal stigmas, and other factors (Øien-Ødegaard et al., 2024). Providing the proper education on options can help reduce stigma and promote the usage of mental healthcare.

Mental health stigmas extend to all industries and individuals, despite research that has shown there are many ways to destigmatize treatment. One of the most effective strategies is altering cognitive-behavioral strategies to change self-perception of treatments (Glazer et al., 2023; Thornicroft et al., 2016). Further research is needed to investigate the stigma surrounding mental health and treatments. Urging help-seeking behavior and affirming self-compassion (Glazer et al., 2023) should be encouraged throughout all industries and people to assist in destigmatization, while aiding to provide a positive perception of mental health.

2.3 Aeromedical Factors

Aeromedical factors are a crucial component of aviation safety. Aeromedical certifications ensure

that pilots and crew members are physically and mentally fit to fulfill their duties. Currently, there are no procedural evaluations for pilot mental health, and it is based on self-reporting. Vuorio et al. (2024) suggested conducting a neurocognitive evaluation to determine effects on performance. The test did not determine a pilot's mental health but provided better insight into pilot performance (Vuorio et al., 2024). In one case, Martinez et al. (2022) placed a mental health specialist in operational units within the United States Air Force. They described that airmen avoided getting the assistance they needed because they did not want to jeopardize their careers. Martinez et al. (2022) showed a baseline for what it would be like to have embedded professionals that would allow medical leadership to strategize implementation to improve upon efforts regarding airman mental health. Implementing proper procedures and resources for airmen is needed for the betterment of the industry.

Past research has analyzed the use of medication in pilots. Kelley et al. (2020) investigated the use of SSRI drugs in the military over the past 10 years. These cases are critical in determining the safety of SSRI use. The use among females was higher, supporting that of the normal population with SSRI use being higher in women. Many of those using SSRI drugs were not given a waiver to fly and instead recommended for suspension. It is important for aviators to seek support and not suffer in silence. SSRI use has a place in safe aviation operations when the proper screening and precautions are taken (Kelley et al., 2020). Although past research provides some support, further research is needed to show how the use of coping mechanisms can be integrated into the aviation industry without jeopardizing the safety of pilots and passengers.

2.4 Aviation Industry Perception of Mental Health

The aviation industry is one of the most demanding and high-risk industries, where pilot well-being directly impacts safety. After the Germanwings accident, in which the co-pilot crashed the plane intentionally with passengers on board, people showed increased awareness of the importance of mental health care for pilots. The accident emphasized the need for improved management of pilot mental health (Wu et al., 2016).

One of the dilemmas in managing pilot mental health is balancing medical confidentiality and public safety. Confidentiality is a cornerstone of ethical medical practice; however, some airmen think that by talking to a medical professional they are putting their career at stake.

The International Civil Aviation Organization (ICAO) provides guidelines for pilots' mental health, but reporting policies vary depending on countries (Kenedi et al., 2019). Some countries, such as Canada and New Zealand, enforce mandatory reporting of mental health concerns that could risk aviation safety. In other countries, the responsibility to report is on the medical examiner (Kenedi et al., 2019). Research conducted by Wu et al. (2016) discovered that 12.6 percent of airline pilots satisfied the depression threshold. In addition, 4.1 percent of participants answered that they had considered suicide in the past two weeks from the survey date. Participants answered that the reason they did not report their mental concerns was because they feared it might negatively impact their careers. This finding showed that airlines must prioritize pilot mental health treatment to prevent unexpected accidents (Wu et al., 2016). Kenedi et al. (2019) and Wu et al. (2016) demonstrated that in some cases pilots did not have the opportunity to speak on issues without the fear of being reported to other parties. This lack of communication can lead to safety issues that can cause accidents.

Safety issues for airmen can arise from pilots experiencing mental deterioration due to stress and fatigue. Pilots are exposed to irregular work hours and long flights, which can lead to increased levels of anxiety due to changing circadian rhythms (Tsismalidou & Kondilis, 2024). Tsismalidou and

Kondilis (2024) demonstrated that working long hours could influence pilots' increased anxiety and depression. However, even a short-haul flight could affect the pilot's well-being. According to Roach et al. (2012), pilots experienced severe fatigue due to short layovers. This led to malfunctioning in their body conditions. According to Tsismalidou and Kondilis (2024), stress was a key factor in pilots' anxiety levels. In their study, 88.3 percent of participants stated that work was a crucial personal factor to stress. Tsismalidou and Kondilis (2024) highlighted that managing stress and fatigue in the workplace is important to support airmen's mental health.

The stigma of mental illness remains a significant barrier to reporting and seeking help for mental health conditions in aviation. Pilots hesitate to report their conditions due to concerns about losing their careers (Cross et al., 2024). According to Cross et al. (2024), all participants in their study answered that the most mentioned mental health issue was depression for pilots. One of the participants said the reason they avoided talking about mental issues was that they could face consequences (Cross et al., 2024). Public perception is another factor that pilots avoid reporting their mental issues. The stigma surrounding mental health issues creates a barrier to a willingness to seek care and treatment (Corrigan et al., 2014). Cross et al. (2024) and Corrigan et al. (2014) found compounding reasons that pilots wanted to avoid reporting their mental health conditions.

Pilots did not report their mental condition because they believed the current systems, such as company resources or Aviation Medical Examiners (AME), were unreliable (Cross et al., 2024). They were concerned about the possibility of the stigma of mental issues regardless of their severity. The Federal Aviation Administration (FAA) and airlines are required to consider the change in their reporting systems, which pilots can trust (Cross et al., 2024). Airlines must implement effective mental health support programs that address both the stigma of mental illness and the barriers to seeking care. Airlines can do this by providing resources, such as peer support networks, which will help in guiding them to appropriate treatment (Kenedi et al., 2019). Cross et al. (2024) and Kenedi et al. (2019) highlighted the need for support systems that minimize the career risks that pilots encounter when reporting their mental health concerns for flight safety. Further research is needed to determine the safest and most effective reporting strategies for pilots. Improving pilot reporting will allow for more honesty and less fear in the realm of mental health.

It is critical to understand the issue of pilot mental health (Wu et al., 2016) and to define the blurry guidelines in the industry (Kenedi et al., 2019). There is a need to ensure the safety of pilots and passengers with regard to pilot mental health. Past studies have shown success surrounding the use of medication in aviation (e.g., Kelley et al., 2020); however, more research is needed to determine current passenger willingness to fly with pilots, who have reported mental health issues. Understanding the public's willingness to fly with different coping mechanisms is the first step towards reducing the stigma surrounding pilot reporting, and aid in developing accessible mental health resources in aviation. This study aims to investigate passenger willingness to fly when presented with different pilot mental health scenarios.

3. Methodology

The target population for this study was passengers traveling on airlines in the United States. The accessible population was collegiate students at a university in the Southeastern United States that are mostly within the ages of 18 to 23. The university is made up of 37% females, 62.9% males, and 0.1% non-binary (Florida Tech, Fall 2022). Most of the accessible population identifies as white at 53.8%. The rest of the population identifies as American Indian or Alaska Native, Asian, black, or African American, Native Hawaiian or Pacific Islander, two or more races, unknown, or international

(Florida Tech, Fall 2022).

This study gathered data through purposive cluster sampling and used a questionnaire on Qualtrics. Researchers asked college professors for permission to recruit their class to be participants in this study. After permission was granted, researchers visited the class, distributed the survey to students, and gave them a candy incentive for participating. Professors, who did not allow the researchers to visit class, were able to distribute the questionnaire via the learning management system (LMS). In this situation, the researchers emailed the professor a recruitment announcement to post on the LMS.

This study utilized a within-subjects design, and all participants rated their willingness to fly for each pilot mental health scenario. Participants were asked questions about their willingness to fly in four different scenarios regarding pilot mental health. The scenarios are no history of mental health issues, history of depression and attending therapy to cope, history of depression and uses medication to cope, and history of depression with no coping mechanism. Participants rated their willingness to fly with the validated Willingness to Fly scale (Rice et al., 2020). This scale was developed and fully tested for internal reliability (Cronbach's alpha = .97) and sensitivity. The scale was determined to be both valid and reliable (Rice et al., 2020). Prior to starting the project, an IRB exemption was approved (24-186) as the study was of minimal risk, voluntary, fully anonymous, conducted in a population of adults, and allowed participants to withdraw at their discretion. Demographic information was collected, and participants were offered candy as an incentive.

Data were exported from Qualtrics as a Microsoft Excel file. Participants' rated willingness to fly on a scale of 1 (Strongly Disagree) to 5 (Strongly Agree) after reading each scenario. To calculate the overall score for each scenario, all seven items from the willingness to fly scale (Rice et al., 2020) were averaged together per participant. Once each participant's scenario rating was calculated, all participants' ratings were averaged to calculate the overall average per scenario. Descriptive statistics including mean, median, mode, range, and standard deviation were calculated both overall and by scenario. JMP Pro 18.0.2. was used to calculate measures of central tendency and variability. Data were evaluated in RStudio Version 4.4.1 using a one-way, repeated measures ANOVA. This test was appropriate because this research utilized a numeric dependent variable and a within-subjects design giving each participant a total of four scenarios (Gallo et al., 2023): no history of mental health issues, a history of depression and attends therapy to cope, a history of depression and uses medication to cope, and a history of depression with no coping mechanism.

4. Results

At a university in the Southeastern United States, 134 students were asked to participate through cluster sampling of existing class sections. A total of 88 responses were collected, giving the study a 65% response rate. Twelve participants were excluded due to mortality, yielding a sample size of n = 76 (26 females) collegiate students. Academic years ranged from freshman to seniors: 30 freshman, 17 sophomores, 19 juniors, and 10 seniors. This is a representative sample; the sample has a population of 39.47% freshman. The accessible population of on-campus undergraduate students is 38.82% freshman (Florida Tech, Fall 2023).

The participants were asked to complete the questionnaire during class time professors set aside for the research group to visit. Of 76 participants, eight participants did not answer the demographic question asking the approximate commercial flights they took per year with a numeric value. Additionally, eight participants did not understand the demographic questions asking participants to state approximately how many commercial flights they take a year. Instead, these participants listed the date of the last commercial flight they were on. For these participants, their answers were substituted with the average for all other participants, which is 4.5 flights per year, showing the accessible population is representative of target population because this frequency of flights per year is similar to other aviation consumers. Answers from participants ranged from 0 to 20.

Table 1 shows the descriptive statistics for willingness to fly by pilot mental health scenario. Figure 1 displays all mean willingness to fly values by pilot mental health condition. The no history scenario reported the highest mean (4.76) and a left-skewed distribution. Both the medication scenario and the therapy scenario showed a more normal distribution with slight skews to the left as well as similar means. The no coping scenario showed a right-skewed distribution and reported the lowest mean (2.38).

Scenario	Mean	Median	Standard Deviation	Range
No History	4.76	5	0.64	1-5
Medication	3.33	3.34	1.08	1-5
Therapy	3.62	3.71	1.03	1-5
No Coping	2.38	2.29	1.07	1-5
Overall	3.52	3.71	1.29	1 – 5

Table 1. Descriptive Statistics for Passenger Willingness to Fly by Pilot Mental Health Scenario

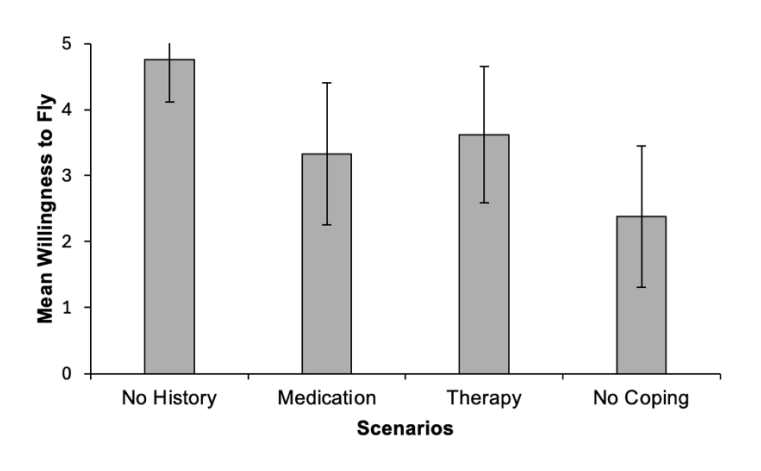


Figure 1. Willingness to Fly by Pilot Mental Health Scenario

Note: Participants rated each scenario with seven items ranging from 1 (strongly disagree) to 5 (strongly agree). The items were from the willingness to fly scale (Rice et al., 2020). All seven items were averaged to determine the participants' willingness to fly per scenario. Each participants' score was averaged with other participants within each condition to equal the sample mean per scenario.

Table 2. Tukey's Pairwise Test

Pair	p value		
No Coping vs.	< .001 ***		
Medication	1.001		
No History vs.	< .001 ***		
Medication	< .001		
Therapy vs. Medication	.27		
No History vs. No	< .001 ***		
Coping	1.001		
Therapy vs. No Coping	< .001 ***		
Therapy vs. No History	<.001 ***		

Note: All pairs of coping mechanisms were statistically different on willingness to fly, except for Therapy vs. Medication.

Due to the number of testing scenarios (no history, medication, therapy, and no coping), a oneway, repeated measures ANOVA was the desired testing statistic. All data points are independent of each other, and data points have no influence on one another. Levene's test for heterogeneity of variances was conducted (p < .001). The null hypothesis could not be accepted and equal variances in the data set cannot be assumed. However, Welch's test was conducted to meet the assumption. Welch's test concluded the F-statistic to be 129.9. This suggests that variation between scenarios may exist, and it is likely that differences are not due to chance. The Shapiro-Wilk's test for normality indicated that the null hypothesis, normal distribution of the data, could not be accepted (p < .001). Due to this, the analysis proceeded under the central limit theory. This experiment utilized a withinsubjects design, and 76 participants can be considered large enough to assume normality. Under the Central Limit Theorem, samples over 30 should begin to approximate a normal distribution (Gallo et al., 2023). A one-way ANOVA was conducted to determine if there were statistical differences in passenger willingness to fly between pilot mental health scenarios. The ANOVA indicated there was a significant effect of pilot mental health scenario on passenger willingness to fly (F(3, 73) = 77.47, p)< .001). Post hoc comparisons between all pairs of scenarios using Tukey's HSD showed that all pairs of scenarios had statistically significant differences in mean willingness to fly (p < .001), except the medication vs. therapy comparison (p = .27). Tukey's test results can be found in Table 2. These results indicate that pilot mental health scenario affected participants' willingness to fly. The etasquared was .44, indicating a large effect size. The post-hoc power analysis indicated high power (1 $-\beta = > .99$).

5. Discussion and Future research

The findings of this study support the hypothesis that the mean willingness to fly will vary based on pilot mental health status. No history of mental health issues was reported as the most preferred scenario, and the lowest was the no coping mechanism scenario. Tukey's HSD showed that all pairs had statistically significant differences in mean willing to fly (p < .001), except the medication vs. therapy pairwise comparison. This may be due to lack of knowledge on treatments, or due to stigmas surrounding mental health in aviation. However, there are some probable explanations for why participants responded the way they did. Although no statistically significant difference was found between therapy and medication coping scenarios, the therapy scenario rated slightly higher on average

for willingness to fly than the medication scenario. This may be because both scenarios are treatments for depression and participants were not primed with the type of medication a pilot was taking or the amount of time a pilot was in therapy. This may also be due to stigma and lack of education of mental health resources (Thornicroft et al., 2016). Participants may not have seen a large difference in the type of treatment and gave similar ratings to both the medication and therapy scenario. Likewise, the fact that the pilot had some coping mechanism as opposed to none may be the important point for an aviation consumer. Although no statistically significant difference was found in this comparison, all other pairwise comparisons were found to have significant differences.

In the comparison between the therapy and no history groups, participants rated the no history group with a higher willingness to fly. Thus, participants were more willing to fly with pilots that had no mental health history when juxtaposed to a pilot with history, who is receiving therapy as treatment. Similar results were determined for the no history scenario when compared to the medication as a treatment scenario. Participants on average rated no history with a higher willingness to fly. This is likely due to the stigma surrounding pilot mental health issues. Stigma remains a barrier to pilots reporting mental health issues (Cross et al., 2024). Another possible explanation for this could be a lack of education surrounding mental health and treatment options (Thornicroft et al., 2016). Many people may think therapy is not an effective treatment, while others may think any treatment for mental health problems is hopeless and does not positively impact the mental state of the patient. This could come from improper education or an individuals' own experience with improper treatment and stigmas surrounding mental health in the public view.

Significant differences between therapy and no coping mechanism were also found; however, in this case, therapy was generally rated higher than the no coping mechanism scenario. This supports the hypothesis that passengers' willingness to fly differs based on pilot mental health scenario, showcasing that passengers are more willing to fly when a pilot is being treated as opposed to not being treated. Participants also generally rated willingness to fly higher for the medication scenario compared to the no coping mechanism scenario. This supports the claim that passengers would rather fly with a pilot being treated for mental health issues rather than fly with a pilot, who is suffering in silence and receiving no treatment.

The pairwise comparison between no history of mental health issues scenario against the no coping mechanism scenario was also statistically significant. Participants rated the no history scenario significantly higher on average than the no coping mechanism scenario. This outcome supports the claim that people show higher preference to others when no mental health history is present compared to people with prior mental health issues. The overall findings of the study indicate a preference for treatments over no coping mechanism demonstrating the importance of research on pilots using medication such as SSRI's (Kelley et al., 2020). Additionally, the large effect size suggests a strong difference in willingness between scenarios; the pilot mental health scenario had a meaningful impact on passenger willingness to fly. This analysis is crucial for future changes in the aviation industry.

This study utilized students at a college in the Southeastern United States, so it can be assumed that results may be applicable to anywhere with matching demographics. The college utilized consists of varying backgrounds; however, the sample was not entirely representative of U.S. aviation consumers. The study included 50 male participants and 26 female participants. An additional demographic question asked about ethnicity with the study including 54 Caucasian participants, 2 participants of African American descent, 7 participants of Asian descent, 8 participants of Latino/Hispanic descent, 2 participants reporting other, and 3 preferring not to say.

It is also important to note that this college has a Part 141 flight school, so some participants may have strong views about mental health in aviation and have shown slight bias in their responses. Of the

76 participants, 36 were flight students or held a flight certificate. Further examination of the data could exclude participants with a flight certification to look for a change in results. This research has a generalizability limitation due to the sample's age, education level, and location. The accessible population provided participants at a university in the Southeast United States, mostly in the age range of 18 to 23 with a majority of males 62.9% (Florida Tech, Fall 2022). Additional limitations, such as attrition/mortality, can be found in this study. Due to the number of questions per scenario in the questionnaire as well as asking for demographic information, twelve participants failed to complete the questionnaire and were excluded from analyses.

The findings demonstrated that there was a preference for pilots without any mental health issues. Passengers were willing to accept pilots with mental health issues if they use mental health treatments, such as therapy or medication, as indicated by the positive average willingness to fly values. Positive averages for therapy or medication may also be influenced by participants biases. Twenty-nine participants responded yes to the question asking, "Have you or anyone in your immediate family been prescribed medication for mental health?" and thirty-six participants responded yes to the question asking, "Have you or anyone in your immediate family attended therapy?" However, further research is needed to understand this topic more deeply. Mental health can be a very sensitive topic, but it is important to shed light on this within the aviation industry. Further research may allow pilots to feel more comfortable reporting mental health problems. The research may also contribute to an overall change in safety culture relating to mental health. If this can be achieved, pilots may be able to be treated for depression and other mental health issues without fear of losing their licenses and certifications. These developments may also make aviation a more accessible career path for those struggling with mental health problems. Airline contribution to and collaboration on research surrounding this issue would indicate support and openness to change. If possible, airlines may also offer alternatives to suspension if the pilot chooses to seek treatment. This may not be an immediate possibility due to certain regulations and confidentiality issues; however, beginning the process to support pilots in need may create a healthier and safer environment that allows pilots to seek mental health support if and when needed.

Future research should examine if participant age influences passengers' willingness to fly with pilots, who have different mental health conditions and coping mechanisms. Diverse perspectives regarding age may provide various insights into differences between generations in mental health conditions. Additionally, a larger and more diverse sample will increase the generalizability of the results and provide a more accurate public perception of mental health problems in aviation.

It may be beneficial for future research to collect qualitative responses for each scenario to understand the reason for participants' ratings. This approach will provide a better understanding of factors affecting passengers' preferences. The same questionnaire could be utilized with free response questions after each scenario. The same analyses would be run to examine quantitative data and compared to the results of this study. A thematic analysis would be conducted to extract themes from participant responses and coded accordingly. This study would provide a more in-depth understanding of how individual differences affect willingness to fly in the different pilot mental health scenarios.

6. Disclaimer statements

Funding: None

Conflict of Interest: None

7. References

- Corrigan, P. W., Druss, B. G., & Perlick, D. A. (2014). The impact of mental illness stigma on seeking and participating in mental health care. *Psychological Science in the Public Interest*, *15*(2), 37–70. https://doi.org/10.1177/1529100614531398
- Cross, D. S., Wallace, R., Cross, J., & Mendonca, F. C. (2024). Understanding pilots' perceptions of mental health issues: a qualitative phenomenological investigation among airline pilots in the United States. *Cureus*, *16*(8). https://doi.org/10.7759/cureus.66277
- Gaddis, S. M., Ramirez, D., & Hernandez, E. L. (2018). Contextualizing public stigma: Endorsed mental health treatment stigma on college and university campuses. *Social Science & Medicine*, 197, 183-191. https://doi.org/10.1016/j.socscimed.2017.11.029
- Gallo, M. A., Wheeler, B. E., & Silver, I. M. (2023). Fundamentals of Statistics for Aviation Research. Routledge. https://www.taylorfrancis.com/books/mono/10.4324/9781003308300/
- Glazer, J. V., Oleson, T., Campoverde, C., & Berenson, K. R. (2023). Effects of affirming values on self-compassion and mental health treatment stigma. *Stigma and Health*, 8(2), 252. https://doi.org/10.1037/sah0000307
- Graham, A., Kremarik, F., & Kruse, W. (2020). Attitudes of ageing passengers to air travel since the coronavirus pandemic. *Journal of Air Transport Management*, *87*, 101865. https://doi.org/10.1016/j.jairtraman.2020.101865
- Hester, R.D. (2017). Lack of access to mental health services contributing to the high suicide rates among veterans. *International Journal of Mental Health Systems* 11(1), 47. https://doi.org/10.1186/s13033-017-0154-2
- Florida Tech. (Fall 2022). *Student Diversity Data*. https://www.fit.edu/institutional-research/student-diversity-data/
- Florida Tech. (Fall 2023). *Institutional Data Reports*. https://www.fit.edu/media/site-specific/wwwfitedu/oir/documents/Fall-2023-OCR-Report.pdf
- Kelley, A. M., Bernhardt, K., McPherson, M., Persson, J. L., & Gaydos, S. J. (2020). Selective serotonin reuptake inhibitor use among army aviators. *Aerospace Medicine and Human Performance*, *91*(11), 897–900. https://doi.org/10.3357/amhp.5671.2020
- Kenedi, C. A., Appel, J. M., & Friedman, S. H. (2019). Medical privacy versus public safety in aviation. *The journal of the American Academy of Psychiatry and the Law, 47*(2), 224-232. https://doi.org/10.29158/JAAPL.003839-19
- Lamb, T. L., Winter, S. R., Rice, S., Ruskin, K. J., & Vaughn, A. (2020). Factors that predict passengers willingness to fly during and after the COVID-19 pandemic. *Journal of Air Transport Management*, 89, 101897. https://doi.org/10.1016/j.jairtraman.2020.101897
- Lerner, J. S., Li, Y., Valdesolo, P., & Kassam, K. S. (2014). Emotion and decision making. *Annual Review of Psychology*, 66(1), 799–823. https://doi.org/10.1146/annurev-psych-010213-115043
- Martinez, R. N., Galloway, K., Anderson, E., Thompson, C., & Chappelle, W. L. (2023). Perspectives of mental health professionals on the delivery of embedded mental health services for U.S. air force airmen. *Psychological Services*, 20(4), 988-1000. https://doi.org/10.1037/ser0000727
- Øien-Ødegaard, C., Christiansen, S. T. G., Hauge, L. J., Stene-Larsen, K., Bélanger, S. M., Bjertness, E., & Reneflot, A. (2024). Variations in healthcare utilization for mental health problems prior to suicide by socioeconomic status: a Norwegian register-based population study. *BMC health services research*, 24(1), 648. https://doi.org/10.1186/s12913-024-11113-w
- Rice, S., Winter, S. R., Capps, J., Trombley, J., Robbins, J., Milner, M., & Lamb, T. L. (2020). Creation of Two Valid Scales: Willingness to Fly in an Aircraft and Willingness to Pilot an Aircraft. *International Journal of Aviation, Aeronautics, and Aerospace, 7*(1). https://doi.org/10.15394/ijaaa.2020.1440
- Rice, S., & Winter, S. R. (2015). Which passenger emotions mediate the relationship between type of pilot configuration and willingness to fly in commercial aviation? *Aviation Psychology and Applied Human Factors*, 5(2), 83–92. https://doi.org/10.1027/2192-0923/a000081
- Roach, G. D., Petrilli, R. M. A., Dawson, D., & Lamond, N. (2012). Impact of layover length on sleep, subjective fatigue levels, and sustained attention of Long-Haul airline pilots. *Chronobiology*

- International, 29(5), 580–586. https://doi.org/10.3109/07420528.2012.675222
- Thornicroft, G., Mehta, N., Clement, S., Evans-Lacko, S., Doherty, M., Rose, D., Koschorke, M., Shidhaye, R., O'Reilly, C., & Henderso, C. (2016). Evidence for effective interventions to reduce mental-health-related stigma and discrimination. *The Lancet*, *387*(10023), 1123-1132. https://doi.org/10.1016/S0140-6736(15)00298-6
- Tsismalidou, G. K., & Kondilis, B. K. (2024). The effects of stress and fatigue on levels of anxiety in pilots: an aviation industry sample. *Journal of Organizational Psychology*, 24(2). 66-77. https://doi.org/10.33423/jop.v24i2.7084
- Vuorio, A., Suhonen-Malm, A., Budowle, B., & Bor, R. (2024). European and US aeromedical authority guidance for neurocognitive evaluation of airline pilots with mental disorders. *Aviation Psychology and Applied Human Factors*, 14(1), 57-68. https://doi.org/10.1027/2192-0923/a000271
- Wheeler, B., Shacknai, J., Valluzzi, N., & Li, T. (2021). Collegiate Flight Students' Willingness to Pilot in Different Aircraft Sanitization Scenarios. *Journal of Management & Engineering Integration*, 14(1), 1-8. https://doi.org/10.62704/10057/24763
- Wu, A. C., Donnelly-McLay, D., Weisskopf, M. G., McNeely, E., Betancourt, T. S., & Allen, J. G. (2016). Airplane pilot mental health and suicidal thoughts: a cross-sectional descriptive study via anonymous web-based survey. *Environmental Health*, 15(1). https://doi.org/10.1186/s12940-016-0200-6

The Journal of Management and Engineering Integration (JMEI) © 2025 by AIEMS Inc., is licensed under CC BY 4.0. To view a copy of this license, visit https://creativecommons.org/licenses/by/4.0/

AUTHENTIC CRISIS LEADERSHIP & EMPLOYEE MOTIVATION: COMPARING DIVERGENT COVID-ERA EXECUTIVE COMPENSATION STRATEGIES IN THE CRUISE LINE INDUSTRY

Tony Lewis ¹

Joshua Shackman ¹

¹ California State University – Maritime

<u>tlewis@csum.edu</u>

Abstract

The COVID-19 pandemic exposed the cruise line industry to an unprecedented crisis. Recovery required sustained discretionary effort from employees, simultaneously balancing safety concerns and extreme financial hardship. However, not all firms in the industry were affected equally. From January 2019 to January 2025, among the three dominant players in the industry, Norwegian Cruise Lines (NCLH) and Carnival Cruise Lines (CCL) saw their stock prices drop by approximately half. During the same period, Royal Caribbean Cruise Lines (RCL) achieved extraordinary stock market performance, more than doubling their 2019 valuation. This inductive study explores whether generous executive pay increases awarded during the COVID-19 crisis may have diminished managers' abilities to engage in authentic leadership (AL). Conceptual findings raise questions about whether the absence of rigorous AL may undermine employee motivation, resulting in depressed firm performance. Emergent themes primarily conform with the rent extraction and signaling views of executive compensation. Little support for the efficient contracting view is detectable. Inauthentic executive messaging and perceived executive opportunism at NCLH and CCL were associated with reduced employee motivation and poor share price performance, despite a full market rebound. In contrast, RCL's more congruent executive actions and communications were accompanied by a stronger recovery aided by higher employee productivity. This analysis contributes to the AL literature by illustrating how compensation practices can constrain authentic communication and leadership efficacy in crisis situations. Implications for corporate governance, organizational resilience, and leadership development are discussed.

Keywords: Authentic Leadership, Employee Motivation, Crisis Management, Executive Compensation, Rent Extraction, Signaling, Efficient Contracting

1. Introduction

The COVID-19 pandemic has thrust crisis management into the spotlight of leadership research, raising pressing questions about how to sustain employee motivation during periods of organizational tumult. Authentic leadership (AL) plays a pivotal role in enhancing employee motivation and firm performance (Maunz et al., 2024). Authentic leaders are honest, transparent, just, and truthful (Lux & Lowe, 2025). They are characterized by self-awareness, unbiased information processing, and internalized moral systems that comport with observed behaviors (Gardner et al., 2021). Crises disrupt established organizational routines and demand exceptional discretionary effort from employees, sometimes at risk to personal safety. In such contexts, trust in leadership may have an inordinately strong effect on employee motivation. We draw on efficient

Submitted: April 30, 2025 Revised: September 9, 2025 contracting, rent extraction, and signaling views of executive pay to investigate whether compensation decisions may erode leaders' capacity to engage in AL during crises and whether these antecedents may affect motivation and performance.

With some notable exceptions (e.g., Kvasić et al., 2021; Hendriks et al., 2023), few studies have examined how executive pay structures influence employee motivation during crises. Even fewer studies have investigated whether disproportionate or rapidly increasing executive compensation may undermine leaders' perceived authenticity, yet previous research suggests that executive compensation may influence leaders' capacity to engage in AL (e.g., Fisher, 2017).

Consistent with research that has criticized past AL scholarship for confusing antecedents and outcomes (e.g., Lux & Lowe, 2025), we also explore the opposite causal path, the possibility that inauthentic leaders may seek incongruous or excessive pay. Prior research has found that leadership style can affect the compensation package that executives demand (e.g., Du, et al., 2025). Emergent themes from this analysis suggest that an executive's compensation negotiating position may be a potent signal of managerial competence and capacity for AL, particularly during a crisis. Consistent with other research findings (e.g., Rodriguez et al., 2024), we explore whether crises amplify the harmful consequences of inauthentic leadership and contribute to firm performance disparities.

Scholars have identified at least two firm-level conditions under which AL may exert heightened influence on motivation: (1) when a firm is experiencing a crisis (Rodriguez et al., 2024), and (2) when it operates within a service-intensive industry (Kvasić et al., 2021). However, empirical studies focusing on AL in service sectors are rare (Kvasić et al., 2021; Schuckert et al., 2018). Research on how AL operates during crisis scenarios is slightly more accessible (e.g., Chully, et al., 2022; Lopes, et al., 2024) but seldom focuses on service industries. By focusing on cruise lines, a service industry severely affected by the pandemic, this study provides a unique empirical window into how leadership authenticity and executive compensation interact under extreme organizational stress.

We present an inductive industry-wide analysis of the three dominant cruise companies and their divergent managerial responses to the COVID-19 crisis. Inductive approaches do not prove theoretical claims, but are useful for uncovering complex, context-specific dynamics that are often overlooked by deductive methods (Bradley et al., 2023; Buetow, 2025). Over the past three decades, leadership and corporate governance research has been largely framed by agency theory, which emphasizes structural and macro-level variables, such as executive compensation contracts, board composition, and market performance (Aguilera & Castillo, 2025; Al-Faryan, 2024). While this paradigm has produced valuable insights, it neglects the role of emotion and perception in organizational behavior.

However, emotions, such as shame, pride, belonging, and alienation are central to understanding both employee motivation (Ashkanasy & Daus, 2005; Reizer et al., 2019) and AL (Els & Jacobs, 2023). One reason for the neglect of such essential variables may be the methodological challenge of capturing subjective, emotionally rich phenomena using conventional quantitative models. Organizational behavior is deeply embedded in context and is often fluid, tacit, and confusing (Lewis, 2000). Nevertheless, understanding these nuances is crucial for developing leadership theories that reflect real-world dynamism and complexity. We advance both theory and practice by illustrating how executive compensation may influence perceived leader authenticity in crisis situations, thereby significantly shaping employee motivation and firm performance. This perspective has practical implications for leadership development and compensation design. Emergent themes may help organizations build resilience to systemic shocks.

This analysis begins by describing tension in the literature about what motivates executive pay

decisions during crises. An overview of the cruise line industry follows. We explain why this industry is uniquely suited to inductive analysis. Divergent responses to the COVID-19 crisis and the disparate performance outcomes of the three major cruise lines are then presented. Next, we investigate what lessons about employee motivation can be gained by exploring firms' labor costs. We conclude with a discussion about these illustrative examples and explore promising avenues for future research.

2. Contrasting Views on What Motivates Executive Pay Decisions During Crises

Three frameworks may explain what motivates executive pay decisions during crises (Carter et al., 2024). The efficient contracting view holds that pay adjustments advance shareholder interests (Carter et al., 2024). In support, scholars have found that crisis-related compensation changes are largely market-driven (e.g., Gabaix et al., 2013) and that higher pay can reduce insolvency risk and managerial moral hazard (Guo et al., 2014). This perspective assumes directors and executives act in the firm's best interest, implying minimal tension between pay decisions during crises and executives' capacity for AL.

By contrast, the rent extraction view suggests that executives exploit crises to consolidate power and raise compensation irrespective of shareholder interests (Carter et al., 2024). Evidence indicates that pay decisions during crises can encourage management actions detrimental to shareholder interests (e.g., Bebchuk, et al., 2010). Governance strength emerges as a key determinant of pay outcomes during crises (Carter et al., 2024; Edmans et al., 2023), yet it is often insufficient. 67% of directors report a willingness to sacrifice shareholder value to avoid controversy over executive pay (Edmans et al., 2023). Opportunistic behavior is difficult to communicate authentically. Consistent with the rent extraction view, executive pay increases during crises may predictably undermine shareholder interests, thereby restricting managers' abilities to communicate and lead authentically.

A third framework, signaling theory, posits that pay adjustments serve as signals of legitimacy to stakeholders (Carter et al., 2024). Crises often require unpopular managerial decisions, such as furloughs and layoffs, which heighten stakeholder sensitivity to signals of accountability and competence (Carter et al., 2024). Executive pay decisions may therefore affect firm performance, with employee motivation moderating this relationship (Hendriks et al., 2023).

Signaling theory suggests that executive pay increases during crises can erode executives' capacity for AL. This view theoretically overlaps with both efficient contracting and rent extraction. High pay may serve as a price signal of managerial competence, but it may also convey a lack of empathy toward employees and other stakeholders. Empirical (e.g., Carter, et al., 2024; Edmans, et al., 2023; Hendriks et al., 2023) and journalistic evidence (e.g., Francis & Broughton, 2021; Gelles, 2021; Kerber, 2022; Melin, 2021; Jean Kaiser, 2022) support the interpretation that executive pay increases during crises signal opportunism. Little published evidence supports the alternative.

3. The Cruise Line Industry and the COVID-19 Pandemic

The cruise line industry is a natural fit for inductive analysis. As of 2019, the industry was dominated by just three firms: Norwegian Cruise Line Holdings (NCLH), which held a 9% share of global cruise passengers; Carnival Cruise Lines (CCL), which had a 43% share; and Royal Caribbean Cruise Lines (RCL), which had a 22% share (Cruise Industry Worldwide, 2024). All three major cruise lines were undiversified and, with minor exceptions, almost entirely focused on the cruise industry.

As the reality of the COVID-19 crisis became apparent, share prices for major cruise lines fell dramatically (Figure 1). However, while RCL quickly recovered, achieving much better share price performance than before the pandemic, the performance of NCLH and CCL worsened compared to their pre-pandemic valuations. NCLH and CCL held roughly the same share price through 2024 as

during the worst of the pandemic when there was significant uncertainty about whether cruise ships would ever sail again. From January 2019 to January 2025, NCLH witnessed a 45% drop in its share price. CCL saw a 52% drop. However, RCL celebrated a 122% share price increase. This dramatic performance disparity emerged despite generally consistent pre-COVID relative share price performance among the firms and nearly identical share price declines as the seriousness of COVID-19 became apparent (Figure 1).

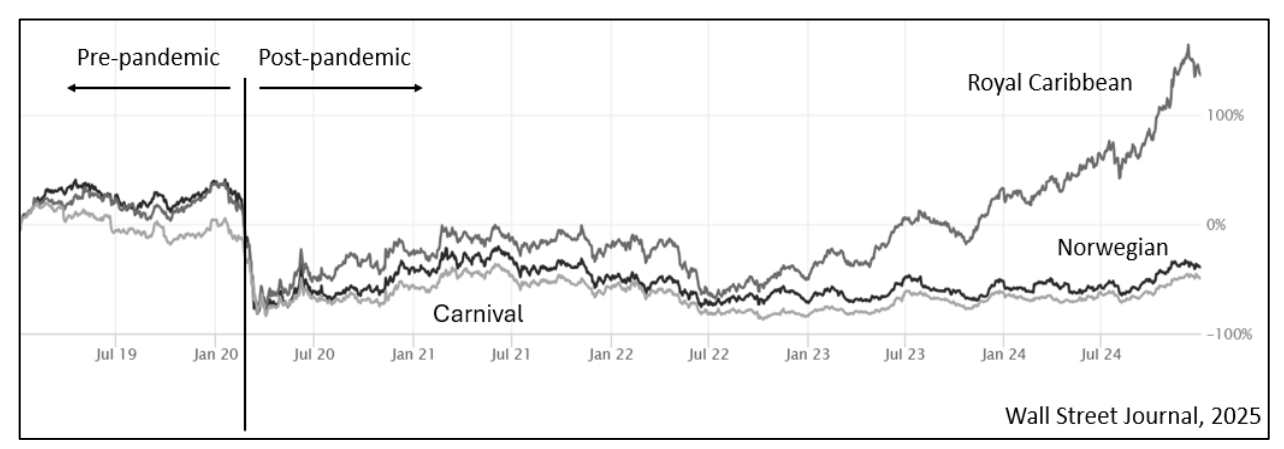


Figure 1. Cruise Industry Stock Price Comparison (January 1, 2019 – January 1, 2025)

During the COVID-19 emergency, the cruise industry also experienced a sharp decline in passengers, from approximately 30 million in 2019 to approximately 5 million in 2020 and 2021 (Figure 2). However, by 2023 the cruise industry had rebounded, logging over 30 million passengers worldwide, a record high number with stronger demand projected ahead (Figure 2). While NCLH and CCL both declined, RCL's portion of global cruise line sales increased by 30% between 2019 and 2021 (Perri, 2021).

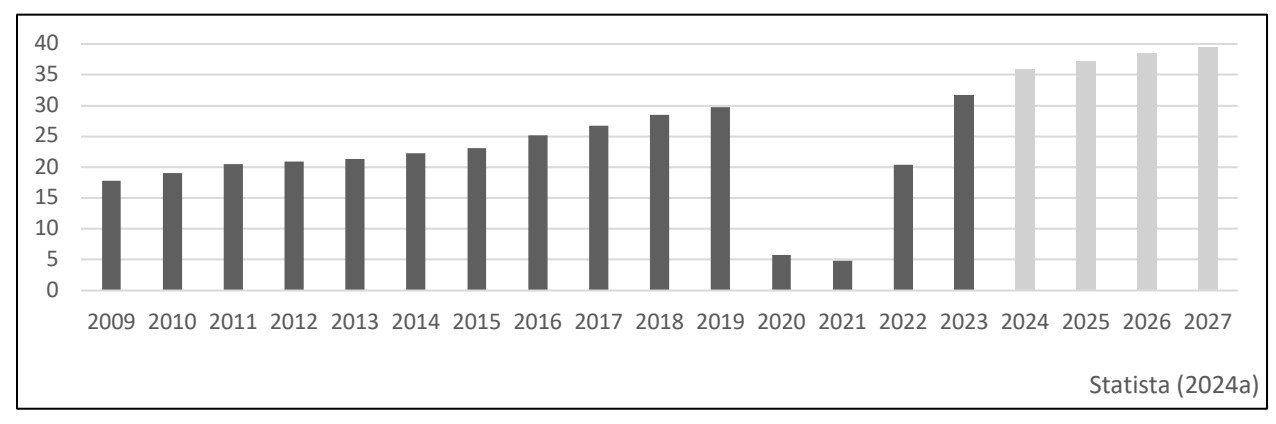
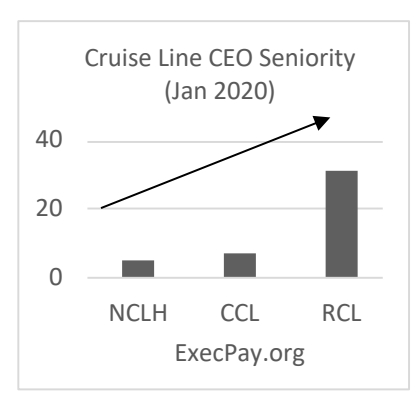
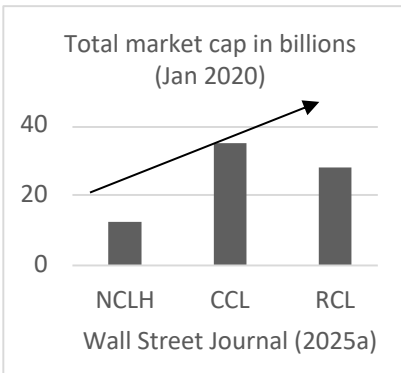


Figure 2. Annual Global Cruise Line Passengers 2009-2023 With a Forecast To 2027 (In Millions)

There are interesting idiosyncrasies in the COVID-era pay structures of cruise industry CEOs. Executive compensation is generally positively correlated with managerial seniority (Hill & Phan, 2017). However, in the cruise line industry, this correlation was reversed such that the longest serving CEO made the least, while the shortest serving made the most (Figure 3). Furthermore,

research suggests that executive pay is normally positively correlated with market capitalization (Bebchuk & Grinstein, 2005). In the cruise industry during the pandemic, this correlation also reversed (Figure 3).





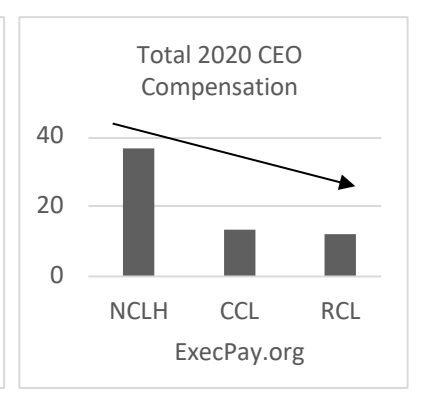


Figure 3. Cruise Line Market Capitalization & CEO Seniority Vs. CEO Total Compensation

4. Norwegian Cruise Line Holdings Pandemic Response

In May 2020, during the height of the COVID-19 pandemic, managers at NCLH acknowledged the company's vulnerability to imminent bankruptcy, citing "substantial doubt" that the firm could continue as a "going concern" (Feuer, 2022). In April 2020, NCLH announced that it would furlough 20% of its shoreside workforce (Dolven, 2020). Further layoffs followed in December 2022, with an additional 9% of the workforce losing their jobs (Jean Kaiser, 2022). These numbers do not account for shipboard employees, whose contracts were often not renewed, a common but less transparent means of workforce reduction in the cruise industry.

Employees who remained at NCLH faced significant financial hardship. In 2020, NCLH implemented a four-day workweek with a corresponding 20% salary reduction (Kalosh, 2020; Melin, 2021) and suspended 401(k) matching contributions (Peterson, 2020). All NCLH executives also suffered a nominal 20% salary reduction (Melin, 2021). NCLH managers emphasized solidarity and shared sacrifice, issuing the following public statement: "Part of adapting is making sacrifices and difficult decisions... we are thus implementing the following changes to our compensation policy" (Peterson, 2020).

NCLH employees who were promised shared sacrifice soon learned that their executive team secured enormous COVID-era financial rewards. Executive base salaries were reduced as promised. However, in 2020, salary only comprised an average of 5.3% of cruise industry executives' total compensation (Dolven & Wile, 2021). The NCLH Board of Directors implemented retention bonuses and adjusted performance metrics, leading to substantial increases in total executive compensation (Melin, 2021; Mullaney, 2022). New metrics focused on resuming operations, environmental goals, and cash management (Mullaney, 2022). Consequently, the average compensation of NCLH executives doubled from 2019-20 (NCLH Compensation History, 2025). NCLH CEO Jack Del Rio's total compensation more than doubled, from \$17.8 million in 2019 to \$36.4 million in 2020, even as NCLH posted a \$5 billion loss, a 50% drop in share price, and widespread layoffs (Jean Kaiser, 2022).

The Miami Herald criticized Del Rio's 2020 pay package, noting its contrast with the company's ongoing layoffs and urgent messaging about looming bankruptcy (Jean Kaiser, 2022). The paper also disparaged internal promotions, including Del Rio's son's appointment as President of Oceania Cruises, an NCLH subsidiary brand (Jean Kaiser, 2022). This move was a potential violation of the

company's Code of Ethical Business Conduct which precludes family members working in a position where NCLH believes that a conflict of interest may exist (Code of Ethical Business Conduct, n.d.).

The outgoing president of Oceania received \$6.6 million in severance pay upon accepting a special advisor role (Kalosh, 2023; Jean Kaiser, 2022). The outgoing President of Regent Seven Seas, another NCLH subsidiary brand, received an identical severance deal after an NCLH insider was promoted to their position (Kalosh, 2023; Jean Kaiser, 2022). These payouts contributed to shareholder dissatisfaction. In 2020, 83% of shareholders opposed CEO Del Rio's pay package, the lowest support ever recorded for an S&P 500 company (Kerber, 2022; Mullaney, 2022). NCLH stated that \$10 million of the package was contractually obligated, but acknowledged \$8.8 million in discretionary retention bonuses (Melin, 2021). After approving Del Rio's pay package over the loud objections of shareholders, NCLH managers released a statement pledging to "carefully consider" shareholder concerns when making future compensation decisions (Kerber, 2022).

The revised compensation framework was extraordinarily complex, spanning 38 pages in the SEC proxy statement, whereas only four pages were dedicated to the election of new board members (Mullaney, 2022). Despite exhaustive documentation, shareholder skepticism persisted, especially as NCLH's recovery lagged. In 2021, only 57% of its fleet was operational, compared to 85% at RCL, inflaming stakeholder concerns about perverse executive incentive structures (Mullaney, 2022). Del Rio's compensation was widely criticized in a media storm that spanned publications such as the Wall Street Journal (e.g., Francis & Broughton, 2021), New York Times (e.g., Gelles, 2021), Reuters (e.g., Kerber, 2022), Seattle Times (e.g., Melin, 2021), and Miami Herald (e.g., Jean Kaiser, 2022). Del Rio stepped down as CEO on July 1, 2023, becoming a special consultant at NCLH (Kalosh, 2023).

5. Carnival Cruise Lines pandemic response

The response of CCL executives to the COVID-19 crisis mirrored managerial actions at NCLH. About 25% of CCL's U.K.-based employees were laid off (Jolly, 2020). CCL also laid off or furloughed about 45% of their Florida-based workforce, a total of 1,357 employees, with similar cuts in other areas of operation (Carnival to lay off hundreds, 2020). The remaining employees were given a 20% pay cut (Jolly, 2020).

CCL executives also accepted well-publicized salary cuts. In May 2020, at the same time managers announced workforce layoffs and pay cuts, CCL CEO Donald Arnold agreed to a 50% reduction in his salary, with other CCL executives taking a 25% cut (Jolly, 2020). However, as at NCLH, the image of shared sacrifice at CCL was inauthentic. CEO Arnold received nearly a 20% increase in total compensation, going from \$11.2 million in 2019 to \$13.3 million in 2020 (Lardner, 2021). Approximately \$5 million of that total came in the form of stock grants awarded as a retention incentive (Anderson, et al., 2021). Much of the remaining windfall was attributable to board-adjusted performance metrics (Lardner, 2021). Arnold's pay increase occurred despite the fact that CCL had just posted an annual loss of about \$10 billion, (Lardner, 2021), had recently accepted a \$6 billion low-cost financing bailout from the U.S. Federal Reserve (Anderson, et al., 2021), had just made sweeping lay-offs and cut pay across its remaining workforce (Carnival to lay off hundreds, 2020; Jolly, 2020), and was trailing Royal Caribbean in its efforts to resume operations (Mullaney, 2022).

The COVID-era raises that CCL executives received were criticized in The New Yorker (e.g., Lardner, 2021), the Miami Herald (e.g., Dolven & Wile, 2021) and numerous industry publications. As the only major cruise industry firm to lose a COVID-related lawsuit, CCL would earn still more critical COVID-related press coverage. In 2023, a judge in Australia ruled that CCL managers' decision to sail the Ruby Princess on March 9, 2020, was negligent (McGuirk, 2023). A total of 663 people

contracted COVID-19 on that voyage and 28 died (McGuirk, 2023). The judge asserted that CCL managers were likely aware of the risk and proceeded with the voyage anyway (McGuirk, 2023).

6. Royal Caribbean Cruise Lines Pandemic Response

Richard Fain served as CEO at RCL during the COVID-19 crisis. He was distinct from the chief executives at NCLH and CCL for having served as CEO for 33 years before stepping down in 2022 (Figure 3). RCL employees also suffered significant COVID-era hardships. In 2020, approximately 26% of RCL's shoreside staff were laid off (Royal Caribbean Provides, 2020).

Like the CEOs of other major cruise lines, Fain agreed to a 2020 salary reduction, accepting zero salary for several months. However, unlike the other cruise line CEOs, Fain's total compensation decreased by 17% during the pandemic, from \$14.4 million in 2019 to approximately \$12 million in 2020 (Mahe, 2020). Moreover, Fain's total 2020 compensation was relatively small compared with that of CEOs at CCL and NCLH. In 2020, Fain earned less than one-third of what NCLH's CEO earned and about \$1.3 million, or 10% less than CCL's CEO (Figure 3). This was true even though Fain had, by far, the highest seniority among the three major cruise lines (Figure 3) and dramatically surpassed industry rivals both in terms of share price performance (Figure 1) and progress returning to full operation (Mullaney, 2022).

By April 2025, RCL's market capitalization of \$57 billion far exceeded CCL's \$27 billion (Wall Street Journal, 2025a). This was in sharp contrast to the end of 2019, when CCL commanded a \$58 billion market cap, compared to RCL's \$28 billion. Like other cruise line CEOs, Fain received critical COVIDera press coverage highlighting the disparity between his total compensation and that of RCL employees (e.g., Towey, 2023). However, the frequency and scornfulness of the reporting was diminished compared with reporting aimed at NCLH and CCL. The Miami Herald condemned executive salary cuts at NCLH and CCL as "token and cynical gestures" (Dolven & Wile, 2021). The same story applauded Fain for being the only CEO of the major cruise lines to accept a genuine reduction in total compensation.

7. Discussion: Employee Motivation and Productivity

In 2020, at the height of the COVID-19 crisis, the CEOs of NCLH and CCL were awarded significant pay increases above their 2019 total compensation. Increased compensation was not a function of firm performance. It was manufactured by compliant boards of directors who adjusted pay metrics allowing executive compensation to diverge significantly from firm performance. The wealth of executives at NCLH and CCL ballooned despite the sinking fortunes of the firms they managed, and the extreme financial hardships and health and safety concerns their employees were experiencing.

We propose that this awkward juxtaposition of facts undermined managers' abilities to engage in authentic communication. Managers at CCL and NCLH repeatedly sent plainly inauthentic messages about their willingness to engage in shared sacrifice, their care about the preferences of shareholders, and their concerns about imminent bankruptcy and the associated need to cut payroll, among others. In each case of inauthentic communication, the aim appears to have been to distract or otherwise smooth over legitimate stakeholder concerns about arbitrary or excessive executive pay. If internal communication norms were consistent with external patterns, NCLH and CCL employees would have been exposed to a persistent chorus of inauthentic executive messaging. Employees in these organizations would also have likely read the inauthentic communications of their managers featured in the flurry of critical coverage of NCLH and CCL that proliferated among national media outlets during the COVID-19 crisis. Media coverage of opportunistic executive pay may be the most significant contributor to related declines in employee morale (Hendriks, et al.,

2023). Moreover, the existence of intensive and critical investigative media coverage raises questions about whether managers could adequately focus on firm strategy while simultaneously managing a challenging public relations crisis.

7.1. Employee Motivation and The Cost of Labor

Authentic communication is a cornerstone of AL (Jiang & Men, 2015). Conceptual findings from our analysis suggest that the boards of directors at NCLH and CCL made authentic communication nearly impossible by awarding excessive and arbitrary executive pay increases during the COVID-19 crisis. Scholars have established a link between AL and employee motivation (e.g., Maunz et al., 2024). Consistent with this research, we propose that failure to communicate authentically at NCLH and CCL may have undermined employee motivation. We further suggest that the post-COVID share price performance lag experienced by these firms was likely to have been at least partially attributable to declining employee motivation.

Support for this assertion can be found in the divergent cost of labor measures reported among the three major cruise lines (Figure 4). Utilizing firms' labor costs to understand employee motivation is a complex endeavor. It is possible that high labor costs could be caused by above-average wages, which could positively contribute to employee motivation (Didar & Mansourfar, 2023). However, employee productivity, which requires consideration of both inputs (e.g., cost of labor) and outputs (e.g., firm performance) in tandem (Zelenyuk, 2023), is positively related to employee motivation (Bun & Huberts, 2018; Kim & Jang, 2020; Zhang, et al., 2020).

Figure 4 shows that in the three-year period following the COVID-19 crisis, CCL and NCLH paid a much higher percentage of their total revenue than RCL did to cover direct labor costs. This represented a shift from before the pandemic when NCLH had the lowest cost of labor and CCL and RCL were closely matched. The COVID-19 emergency caused RCL's cost of labor to increase, but the change was moderate when compared with NCLH and CCL (Figure 4). NCLH went from having a significantly lower pre-pandemic cost of labor compared with rivals, to having by far the highest costs. The problem of inflated labor costs persisted through at least 2023 for both NCLH and CCL, well beyond the twilight of the COVID-19 crisis and the industry's full recovery. Using reported annual revenues (Wall Street Journal, 2025b) and the cost of goods sold (Statista 2024b; Statista 2024c; Statista 2024d), we determine that had NCLH achieved the same labor efficiency as RCL, their average gross margin from 2021-23 would have gone from 5% to 12%, or an increase in profit of \$983 million over three years. Given the same assumptions, CCL's gross margin would have gone from -3% to 1%, or an increase in profit of \$1.4 billion over the same three-year period.

NCLH and CCL experienced this disproportional increase in the cost of labor while simultaneously suffering diminished share price performance (Figure 1) and a delayed return to full operation (Mullaney, 2022). The combination of high labor cost inputs and low performance outcomes conforms with conditions that prior research (e.g., Bun & Huberts, 2018; Kim & Jang, 2020; Zhang, et al., 2020) suggests could be a sign of low employee motivation. Increased labor costs at NCLH and CCL persisted for years after the worst of the COVID-19 crisis had passed, and after RCL and the wider industry had fully recovered. This reality is consistent with prior research emphasizing how leadership practices can foster both supportive and unsupportive workplace cultures (e.g., Zhai et al., 2023). Cultural norms can persist long after the leaders who helped create them leave the organization (Ahn, 2018).

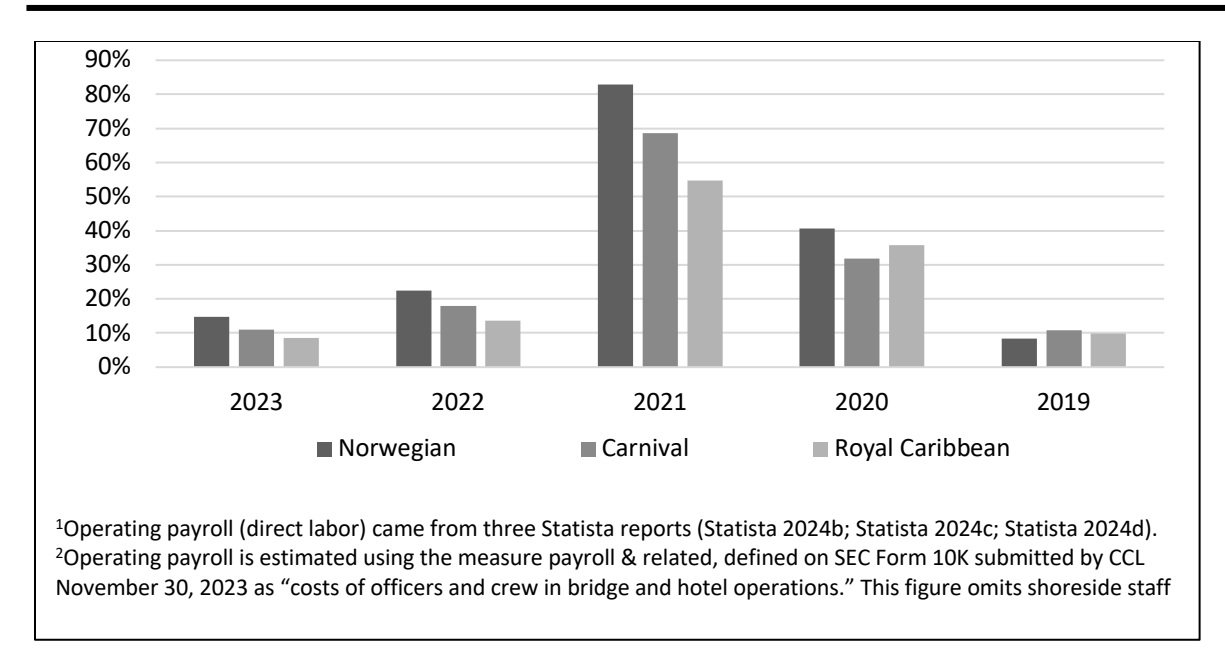


Figure 4. Cost of labor (operating payroll as a % of revenue)

7.2. Assessing motivations for COVID-era cruise line executive pay increases

The cruise line industry example highlighted in this analysis aligns with the rent extraction view of executive pay during crises. Public relations messages at NCLH and CCL, such as publicized salary cuts and other inauthentic communications, suggest executives recognized the firm performance implications of raising their own pay. Their requests for, and boards' approvals of, significant pay increases were probably made with the knowledge that these moves were likely to undermine shareholder interests. Further evidence of rent extraction includes the unprecedented shareholder opposition to NCLH CEO Del Rio's COVID-era compensation package. Approval of this package over the widespread objections of shareholders indicates managerial disregard for shareholder interests. Similarly, the proliferation of special advisor and consultant roles for departing executives while cruise lines were cutting payroll to avoid bankruptcy reflects rent extraction. Del Rio's son's appointment as President of Oceania Cruises also predictably complicated crisis management efforts, a further indication of rent extraction.

This inductive analysis provides only anecdotal support for the resource extraction view. However, executive pay adjustments were widespread during the COVID-19 pandemic. A Wall Street Journal analysis of compensation packages for more than 300 CEOs at major U.S. public companies found that 206 received raises in 2020, with a median increase of 15% (Francis & Broughton, 2021). Although the study did not evaluate the specific circumstances of these increases, the prevalence and scale of such adjustments suggest COVID-era rent extraction governance challenges may have been common.

While it is possible that executive compensation undermined managers' capacity for AL at NCLH and CCL, the causal path could also run in the opposite direction. Inauthentic leaders may achieve high pay by being opportunistic negotiators. From this perspective, an executive's negotiating position regarding pay may serve as a potent signal of leadership authenticity.

RCL CEO Fain managed a much larger firm than the far more highly paid CEO of NCLH. Fain also had much more seniority than CEOs at both NCLH and CCL (Figure 3). Given all this, and the fact that CEO influence over boards of directors increases with length of tenure (Graham, et al., 2020), it is

likely that Fain could have negotiated higher COVID-era compensation but chose not to. Fain's outstanding performance as CEO of RCL compared to industry rivals suggests that the signal sent by his compensation negotiating position may have been a meaningful indicator of managerial competency. The signals sent by the negotiating positions of the CEOs at NCLH and CCL may have been a sign of the opposite. Given the logical conclusion that Fain may have been able negotiate higher pay, but chose not to, and the observation that shareholder interests were neglected at NCLH and CCL, despite high and increasing pay, little evidence conforming with the efficient contracting view can be found in this study.

8. Conclusion

Crisis management can create unique leadership challenges. Overcoming these challenges requires employees to take actions that may not be mandatory according to established norms or contractual obligations. As was the case during the COVID-19 emergency, essential employee actions may entail an inherent risk to personal safety. Scholars use the words "citizenship behaviors" to describe discretionary employee actions that support the goals of the organization, and the words "intrinsic motivation" to describe the energy that induces employees to engage in citizenship behaviors. AL generates intrinsic motivation (Maunz et al., 2024), which in turn has a significant positive effect on the quantity and quality of citizenship behaviors (Rodriguez et al., 2024). Therefore, the absence of AL may depress intrinsic motivation and related citizenship behaviors that are critical for recovery from a crisis.

With the aim of capturing subjective and nuanced, but highly relevant, emotional, behavioral, and contextual elements, this study adopted an inductive analytical approach. Inductive analyses allow researchers to observe the practical significance of theoretical frameworks, potentially gaining insights that can inform other research methodologies. While potentially informative, inductive analyses do not generate the type of conclusive evidence that deductive statistical analyses can produce. A promising avenue for future research may be to employ deductive techniques by analyzing corporate reporting from a sample of firms and exploring any correlations between COVIDera executive pay increases and motivation or performance. Scholars may also consider administering employee surveys as a distinct approach for understanding employee motivation.

This study highlights tension in the literature around what motivates pay decisions during crises. Emergent themes suggest a possible causal relationship consistent with the rent extraction view. During periods of crisis, excessive or arbitrary executive compensation may depress managerial capacity for AL, which can undermine employee motivation, resulting in diminished firm performance. Support for the signaling view can also be found. It is also possible that cruise industry executives signaled their capacity for AL through their compensation negotiating positions. A promising avenue for future research may be to explore these contrasting, but possibly complimentary or cyclical causal paths. Although little evidence of efficient contracting can be found in this example, future research may consider whether there are predictable conditions, like crises, that may decrease the likelihood of efficient contracting. Since AL may exert heightened influence on motivation in service-intensive industries (Kvasić et al., 2021), future research may also consider whether themes from this analysis are consistent in other types of industries.

This study contributes to management scholarship by exploring the complex intersection of AL, executive compensation, employee motivation, and crisis management. This area has received little scholarly attention. Evidence from this analysis suggests that, particularly during crises, boards of directors should view the compensation negotiating positions of executives as potent signals of their commitment to AL and general managerial competence.

9. Disclaimer Statements

Funding: None

Conflict of Interest: None

10. References

- Aguilera, R. V., & Ruiz Castillo, M. (2025). Toward an updated corporate governance framework: Fundamentals, disruptions, and future research. Business Research Quarterly, 28(2), 336-348. https://doi.org/10.1177/23409444251320399
- Ahn, S.-Y. (2018). Founder Succession, The Imprint of Founders' Legacies, and Long-Term Corporate Survival. Sustainability, 10(5), 1485. https://doi.org/10.3390/su10051485
- Al-Faryan, M. A. S. (2024). Agency theory, corporate governance and corruption: an integrative literature review approach. Cogent Social Sciences, 10(1). https://doi.org/10.1080/23311886.2024.2337893
- Anderson, S., Pizzigati, S., & Wakamo, B. (May 10, 2021). Pandemic Pay Plunder. The Institute for Policy Studies 27. https://ips-dc.org/report-executive-excess-2021/
- Ashkanasy, N. M., & Daus, C. S. (2005). Rumors of the death of emotional intelligence in organizational behavior are vastly exaggerated. Journal of Organizational Behavior, 26(4), 441–452. https://doi.org/10.1002/job.320
- Bebchuk, L., & Grinstein, Y. (2005). The Growth of Executive Pay. Oxford Review of Economic Policy, 21(2), 283–303. https://doi.org/10.1093/oxrep/gri017
- Bebchuk, L., Cohen, A., & Spamann, H. (2010). The Wages of Failure: Executive Compensation at Bear Stearns and Lehman 2000-2008. Yale Journal on Regulation. 27, 257-282. https://ssrn.com/abstract=1513522
- Bradley, C., Greer, L., Trinh, E., & Sanchez-Burks, J. (2023). Responding to the Emotions of Others at Work: A Review and Integrative Theoretical Framework for the Effects of Emotion-Response Strategies on Work-Related Outcomes. Academy of Management Annals. 18(1). https://doi.org/10.5465/annals.2022.0044
- Buetow, S. (2025). Emotionally Sensitive Thematic Analysis. Qualitative Research in Psychology, 1–18. https://doi.org/10.1080/14780887.2025.2462919 Emotionally Sensitive Thematic Analysis. Qualitative Research in Psychology, 1–18. https://doi.org/10.1080/14780887.2025.2462919
- Bun, M., & Huberts, L. (2018). The Impact of Higher Fixed Pay and Lower Bonuses on Productivity. Journal of Labor Resources 39, 1–21. https://doi.org/10.1007/s12122-017-9260-9
- Carnival to lay off hundreds in Florida, other states. (May 14, 2020). Associated Press. <a href="https://apnews.com/general-news-domestic-new
- Carter, M, Lynch, L, & Peng, X. (2024). Covid-19 Motivated Changes to Executive Compensation. Journal of Management Accounting Research. https://ssrn.com/abstract=4839451
- Chully, A., Jose, J., & Luthufi, M. (2022). Authentic leadership in a pandemic world: an exploratory study in the Indian context. Journal of Management Development. 41(5) 301-316. https://doi.org/10.1108/JMD-10-2021-0281
- Code of Ethical Business Conduct. (n.d.). NCLH Cruise Line Holdings. https://www.ncl.com/sites/default/files/Code%20of%20Ethical%20Business%20Conduct.pdf
- Cruise Industry Worldwide. (June 10, 2024). Statista. https://www.statista.com/topics/1004/cruise-industry/#topicOverview
- Didar, H. & Mansourfar, G. (2023). The effect of total labor cost on the financial and non-financial reporting quality. Journal of Value and Behavioral Accounting. https://doi.org/10.61186/aapc.8.15.339
- Dolven, T. (2020, April 30). NCLH Cruise Line announces furloughs for 20% of staff. Miami Herald. https://www.miamiherald.com/news/business/tourism-cruises/article242412261.html
- Du, Y., Hasan, I., Lin, C., & Chien-Lin, L. (2025). CEO personality traits and compensation: evidence from investment efficiency. Review of Quantitative Finanance & Accounting. https://doi.org/10.1007/s11156-025-01391-8
- Edmans, A, Gosling, T, & Jenter, D. (2023). CEO compensation: Evidence from the field. Journal of Financial Economics. 150(3). https://doi.org/10.1016/j.jfineco.2023.103718.

- Els, B., & Jacobs, M. (2023). Unravelling the interplay of AL, EQ, cultural intelligence and psychological well-being. Journal of Industrial Psychology, 49(0). https://doi.org/10.4102/sajip.v49i0.2095
- Feuer, W. (2020, May 5). NCLH Cruise Line sees "substantial doubt" about its future, warns of possible bankruptcy as it seeks to raise \$2 billion. CNBC. https://www.cnbc.com/2020/05/05/NCLH-cruise-line-says-theres-substantial-doubt-about-its-ability-to-continue-as-a-going-concern.html
- Fisher, W. O. (2017). To Thine Own CEO Be True: Tailoring CEO Compensation to Individual Personality and Circumstances. Columbia Business Law Review, 2017(2), 599–696. https://doi.org/10.7916/cblr.v2017i2.1721
- Francis, T., & Broughton, K. (2021, Apr 11). CEO pay surged in a year of upheaval and leadership challenges. The Wall Street Journal. https://www.wsj.com/business/c-suite/covid-19-brought-the-economy-to-its-knees-but-ceo-pay-surged-11618142400
- Gabaix, X., Landier, A., & Sauvagnat, J. (2014). CEO Pay and Firm Size: An Update After the Crisis. The Economic Journal, 124: 40-59. https://doi.org/10.1111/ecoj.12084
- Gardner, W., Karam, E., Alvesson, M., & Einola, K. (2021). Authentic leadership theory: The case for and against. The Leadership Quarterly, 32(6). https://doi.org/10.1016/j.leaqua.2021.101495
- Gelles, D. (April 24, 2021). CEO pay remains stratospheric, even at companies battered by pandemic. New York Times. https://www.nytimes.com/2021/04/24/business/ceos-pandemic-compensation.html
- Graham, J.R., Kim, H. & Leary, M. (2020). CEO-board dynamics. Journal of Financial Economics. 137(3). 612-636. https://doi.org/10.1016/j.jfineco.2020.04.007
- Guo, L., Jalal, A. & Khaksari, S. Bank executive compensation structure, risk taking and the financial crisis. Rev Quant Finan Acc 45, 609–639 (2015). https://doi.org/10.1007/s11156-014-0449-1
- Hendriks, M., Burger, M. & Commandeur, H. (2023). The influence of CEO compensation on employee engagement. Review of Management Science 17, 607–633. https://doi.org/10.1007/s11846-022-00538-4
- Hill, C. W. L., & Phan, P. (2017). CEO Tenure as a Determinant of CEO Pay. Academy of Management Journal, 34(3), 707-717. https://doi.org/10.5465/256413
- Jean Kaiser, A. (2022, December 15). Miami-based NCLH Cruise Line lays off 9% of its shoreside workforce.

 Miami Herald. https://www.miamiherald.com/news/business/tourism-cruises/article270055727.html
- Jiang, H., & Men, R. L. (2015). Creating an Engaged Workforce: The Impact of Authentic Leadership, Transparent Organizational Communication, and Work-Life Enrichment. Communication Research, 44(2), 225-243. https://doi.org/10.1177/0093650215613137
- Jolly, J. (May 14, 2020). Cruise firm Carnival slashes jobs and pay in face of Covid-19 crisis. The Guardian. https://www.theguardian.com/business/2020/may/14/cruise-firm-carnival-slashes-jobs-and-pay-in-face-of-covid-19-crisis
- Kalosh, A. (2020, March 18). NCLH to dock shoreside pay 20%, move to four-day week. Seatrade Cruise News. https://www.seatrade-cruise.com/news/nclh-dock-shoreside-pay-20-move-four-day-week
- Kalosh, A. (2023, April 28). Del Rio's 2022 compensation at NCLH valued at \$21.2m. Seatrade Cruise News. https://www.seatrade-cruise.com/people-opinions/del-rios-2022-compensation-nclh-valued-212m
- Kerber, R. (2022, Febuary 24). Reuters. https://www.reuters.com/business/sustainable-business/rising-opposition-ceo-pay-tied-questionable-practices-report-says-2022-02-24/
- Kim, H. & Jang, S. (2020). The effect of increasing employee compensation on firm performance. International Journal of Hospitality Management. https://doi.org/10.1016/j.ijhm.2020.102513
- Kvasić, S., Nikolić, G., & Milojica, V. (2021). The impact of authentic leadership on employee psychological capital in the hospitality industry. Business Excellence, 15(1), 9-22. https://doi.org/10.22598/pibe/2021.15.1.9
- Lardner, J. (July 30, 2021). Inequality Has Soared During the Pandemic—and So Has C.E.O. Compensation. The New Yorker. https://www.newyorker.com/news/daily-comment/inequality-has-soared-during-the-pandemic-and-so-has-ceo-compensation.com
- Lewis, K. M. (2000). When leaders display emotion: How followers respond to negative emotional expression of male and female leaders. Journal of Organizational Behavior, 21, 221–234. https://doi.org/10.1002/(SICI)1099-1379(200003)21:2<221::AID-JOB36>3.0.CO;2-0

- Lopes, D. da S., Matos, J., de, Cardoso, T., & Zukowsky-Tavares, C. (2024). The authentic leader in times of crises: A portrait of the effects of authentic leadership on the well-being of its employees during the COVID-19 pandemic. International Journal of Scientific Management and Tourism, 10(2). https://doi.org/10.55905/ijsmtv10n2-045
- Lux AA, Lowe KB. Authentic leadership: 20-Year review editorial. Journal of Management & Organization. 2024;30(6):1634-1641. https://doi.org/10.1017/jmo.2024.59
- Mahe, S. (April 1, 2020). Royal Caribbean CEO forgoes salary as coronavirus hurts cruise lines. Business Insider. https://www.businessinsider.com/royal-caribbean-cruises-ceo-foregoes-salary-executive-pay-cuts-coronavirus-2020-4
- Maunz, L., Thal, S., & Glaser, J. (2024). Authentic leaders, energized employees? Indirect beneficial and adverse effects of authentic leadership on intrinsic motivation and exhaustion. Applied psychology, 73(4), 2224–2262. https://doi.org/10.1111/apps.12546
- McGuirk, R. (October 4, 2023). Carnival ruled negligent over cruise where 662 passengers got COVID-19 early in pandemic. The Associated Press. https://apnews.com/article/covid-cruise-negligent-carnival-ruby-princess-a396439081417fe7863e5f506e62e6ad
- Melin, A. (2021, May 11). CEO pandemic pay: 'Heads I win, tails I win almost as much'. Seattle Times. www.seattletimes.com/business/ceo-pandemic-pay-heads-i-win-tails-i-win-almost-as-much/
- Mullaney, T. (2022, July 7). The Highest Paid Cruise Industry CEOs. Skift. https://skift.com/2022/07/07/the-highest-paid-cruise-industry-ceos/
- NCLH Compensation History. (2025) ExecPay. https://www.execpay.org/company/norwegian-cruise-line-holdings-ltd-1355
- Perri, J. (2021). Cruise Lines Set Sail Toward Sales Recovery. Bloomberg Second Measure. https://secondmeasure.com/datapoints/cruise-lines-sales-recovery-norwegian-viking-royal-caribbean-carnival/
- Peterson, B. (2020, April 29). NCLH Cruise Line starts 3-month furloughs for corporate employees. Business Insider. https://www.businessinsider.com/norwegian-cruse-line-furloughs-employees-in-push-to-cut-costs-2020-4
- Reizer, A., Brender-Ilan, Y., & Sheaffer, Z. (2019). Employee motivation, emotions, and performance: a longitudinal diary study. Journal of Managerial Psychology. 34(6), 415-428. https://doi.org/10.1108/JMP-07-2018-0299
- Rodriguez, I., Indira, Jorge Muniz, J., & Munyon, T. (2024). "Authentic Leadership and Motivation as Moderators of the Organizational Politics–Knowledge Sharing Relationship: A Test amidst Crisis." Business research quarterly 27.1 (2024): 91–102. https://doi.org/10.1177/23409444231222504
- Royal Caribbean Group Provides Business Update. (May 8, 2020). PR Newswire. https://www.prnewswire.com/news-releases/royal-caribbean-group-provides-business-update-301055738.html
- Schuckert, M., Kim, T., Paek, S., & Lee, G. (2018). Motivate to innovate: How authentic and transformational leaders influence employees' psychological capital and service innovation behavior. International Journal of Contemporary Hospitality Management. 30. https://doi.org/10.1108/IJCHM-05-2016-0282
- Statista. (2024a). Number of ocean cruise passengers worldwide from 2009 to 2023. https://www-statista-com.ezproxy.csum.edu/statistics/385445/number-of-passengers-of-the-cruise-industry-worldwide/
- Statista. (2024b). Operating expenses of Royal Caribbean Cruises. https://www-statista-com.ezproxy.csum.edu/statistics/224281/royal-caribbean-cruises-operating-expenses/
- Statista. (2024c). Operating expenses of NCLH Cruise Line Holdings. https://www-statista-com.ezproxy.csum.edu/statistics/576987/NCLH-cruise-lines-operating-expenses/
- Statista. (2024d). Operating expenses of Carnival Corporation. https://www-statista-com.ezproxy.csum.edu/statistics/301613/cruise-operating-costs-of-carnival-corporation
- Towey, H. (April 27, 2023). Royal Caribbean CEO made \$10 million, 705-times the company's median worker. Business Insider. https://www.businessinsider.com/royal-caribbean-ceo-salary
- Wall Street Journal. (2025a). Stock chart for NCLH, CCL & RCL. https://www.wsj.com/market-data
- Wall Street Journal (2025b) Markets Section. https://www.wsj.com/finance
- Zelenyuk, V. (2023). Productivity analysis: roots, foundations, trends and perspectives. Journal of Productivity Analysis, 60. 229–247. https://doi.org/10.1007/s11123-023-00692-1

- Zhai, Y., Cai, S., Chen, X., Zhao, W., Yu, J., & Zhang, Y. (2023). The relationships between organizational culture and thriving at work among nurses: The mediating role of affective commitment and work engagement. Journal of Advanced Nursing, 79(1), 194–204. https://doi.org/10.1111/jan.15443
- Zhang, X., Liao, H., Li, N., & Colbert, A. E. (2020). Playing It Safe for My Family: Exploring the Dual Effects of Family Motivation on Employee Productivity and Creativity. Academy of Management Journal, 63(6), 1923–1950. https://doi-org.ezproxy.csum.edu/10.5465/amj.2018.0680

The Journal of Management and Engineering Integration (JMEI) © 2025 by AIEMS Inc., is licensed under CC BY 4.0. To view a copy of this license, visit https://creativecommons.org/licenses/by/4.0/

DOI: 10.62704/10057/31195

IMPLEMENTATION OF THE KANO MODEL IN HEALTHCARE SETTINGS: A NARRATIVE REVIEW

Mehrnoosh Saeyan 1

Ahmad Elshennawy 1

Elizabeth A. Cudney²

- ¹ University of Central Florida
- ² Maryville University

Mehrnoosh.saeyan@ucf.edu; Ahmad.Elshennawy@ucf.edu; ecudney@maryville.edu

Abstract

Healthcare quality is critical to patient satisfaction and the effectiveness of the healthcare system. Understanding patient perspectives and needs leads to higher patient satisfaction and client loyalty, and models, such as the Kano model, systematically evaluate client expectations. This literature review examines the application of the Kano model in healthcare settings and analyzes studies conducted from 2017 to 2025. The findings confirm its effectiveness in assessing patient expectations, especially when integrated with other methodologies, such as the balanced scorecard and the SERVQUAL dimensions. However, there are still challenges that need to be overcome. The successful implementation of this model depends on an appropriate sample size, rigorous procedures, and attention to cultural differences.

Keywords: Kano Model, Healthcare, Patient Satisfaction, Service Quality

1. Introduction

Healthcare is a cornerstone of societal well-being, shaping economic growth, political stability, and cultural development with broad implications (Javed et al., 2019). This sector is facing rising pressure to meet evolving patient needs, and patient satisfaction is a vital measure of service quality and system effectiveness (Asamrew et al., 2020; Howsawi et al., 2020). As costs rise and complexity increases, it is crucial to consider the patient perspective while designing and implementing healthcare practices (Cudney et al., 2023).

Healthcare providers strive to enhance their services; therefore, they are increasingly turning to models borrowed from other industries to better understand and meet patient needs. One such model is the Kano model, a concept related to product development, developed by Professor Noriaki Kano in the 1980s (Kano et al., 1984) to understand customer needs. The Kano model is a systematic approach employed to collect, assess, and evaluate consumer feedback, which provides a more valuable understanding of customer expectations than conventional choice-based conjoint surveys (Cudney et al., 2023). The Kano model is an appropriate methodology that can be employed to increase the level of customer satisfaction in any industry, including healthcare (Chen et al., 2019; Materla, Cudney, & Antony, 2019; Materla, Cudney, & Hopen, 2019). Utilizing the Kano model in healthcare settings, such as clinics and hospitals, helps to analyze quality attributes that influence patient satisfaction and identify key areas for improvement (de Vasconcelos et al., 2023; Materla, Cudney, & Antony, 2019).

Submitted: April 30, 2025 Revised: September 8, 2025 Despite its growing use, the Kano model's application in healthcare is still in the preliminary stages. This requires more attention from scholars and a thorough examination of the current body of literature on the subject. Materla, Cudney, and Antony (2019) provided a systematic review of studies from 2002 to 2016. Their study laid a robust foundation and offered comprehensive information on the implementation and integration of the Kano model along with other quality approaches and methodologies to acquire client expectations and enhance the quality of services received in healthcare centers (Materla, Cudney, & Antony, 2019). Building on their prior study, this narrative review examines the literature to assess the current state of knowledge and build upon their work by focusing on studies published from 2017 onward. This study aims to explore how the Kano model has been implemented through pure and integrated approaches in various global regions, evaluate its effectiveness in boosting patient satisfaction and service quality, identify challenges, and propose novel research directions.

2. The Kano Model: Theoretical Foundations

The Kano model, introduced by Kano et al. (1984), explains the interactions between various quality attributes and customer satisfaction. It classifies quality elements based on their impact on customer satisfaction (Mikulić & Prebežac, 2011). Moreover, the Kano model categorizes quality attributes according to the degree of achievement (projected on the horizontal axis) and customer satisfaction (projected on the vertical axis). The model identifies five core categories of quality attributes, which include must-be one-dimensional, attractive, indifferent, and reverse (Jin et al., 2022; Kano et al., 1984). The sixth category, questionable, has been added in recent studies to account for inconsistent customer responses (Barrios-Ipenza et al., 2021; Wachinger et al., 2023).

Customers expect must-be attributes: their absence causes frustration, but their presence does not increase satisfaction (Yao et al., 2024). One-dimensional attributes exhibit a linear relationship with satisfaction, improving it as performance increases and decreasing it when performance is lacking. Attractive attributes delight customers when present but do not cause dissatisfaction when absent. Indifferent attributes have no impact on satisfaction, whereas reverse attributes bring dissatisfaction when present and satisfaction when absent. The questionable category addresses ambiguity in customer perceptions (Deng et al., 2023; Materla, Cudney, & Hopen, 2019). Table 1 and Figure 1 explain each attribute and schematically represent these quality levels.

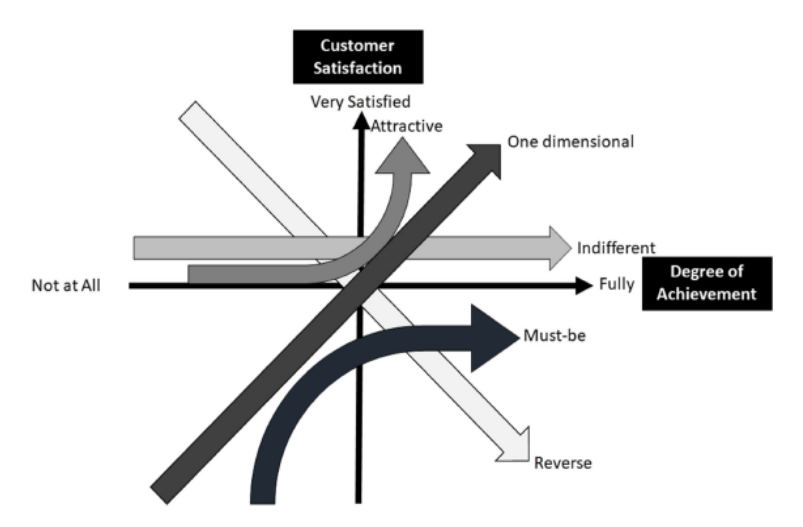


Figure 1. The Kano Model (Cudney et al., 2023)

Table 1. Components of the Kano Model

Quality	Description
Attributes	
One-	Refer to the characteristics that are linearly linked to satisfaction, meaning that when
dimensional	present, they increase satisfaction, and their absence brings dissatisfaction. These
	characteristics are often referred to as performance quality, satisfiers, and attributes
	that enhance satisfaction as they increase.
Must-be	Refer to characteristics that lead to dissatisfaction when absent or malfunctioning,
	but do not enhance satisfaction. Therefore, customers or users typically assume that
	must-be attributes are already included in the product or service. These
	characteristics are often referred to as essential features and must-have.
Attractive	Refer to characteristics that lead to a prominent level of satisfaction when present,
	while their absence does not elicit any dissatisfaction. These characteristics are often
	referred to as delighters and exciters.
Indifferent	Refer to characteristics that do not have any influence on either satisfaction or
	dissatisfaction. These are neutral features.
Reverse	Refer to characteristics that increase satisfaction when absent and dissatisfaction
	when present.
Questionable	Refer to characteristics where the user's perception is inconsistent.

3. Methodology

This study adapted the framework for writing a narrative review introduced by Ferrari (2015) to structure the research. This narrative review searched among peer-reviewed studies from 2017 to March 2025, sourced from PubMed, Web of Science, IEEE Xplore, and Google Scholar, using keywords such as "Kano Model," "healthcare," "patient satisfaction," and "service quality." After reviewing the abstracts, 14 original research articles were selected based on their application of the Kano model in healthcare. The data were qualitatively analyzed to identify trends, applications, and gaps, with findings organized by methodology and region to highlight both methodology innovation and contextual nuances.

4. Applications of the Kano Model in Healthcare

The Kano model has been employed in the healthcare setting to determine quality elements and features that contribute to patient satisfaction and enhance the quality of healthcare service (Myszewski & Sinha, 2020). This review explores these applications through two primary lenses: Pure Kano, in which the model is used independently to classify attributes, and combined approaches, which are used and integrated with other frameworks.

4.1 Using the Pure Kano Model

The application of the Kano model in healthcare settings, in its pure form, relies on the Kano questionnaire to categorize attributes based on their impact on patient satisfaction. This provides a clear and accessible method for providers to prioritize improvements. Table 2 summarizes the studies that used the pure Kano model, detailing their purpose, location, sample size, key findings, and limitations.

In India, Harijith and Naduthodi (2017) investigated healthcare quality attributes at the Government Medical College. Using the Kano model, they classified the 30 attributes. They categorized four one-dimensional attributes, including prompt reply to patients' complaints, employee friendliness, and respectfulness. They also found nine attractive attributes, such as hospital parking and clear directions for each department. The findings revealed that patients considered well-maintained medical devices, easy access facilities, thoroughly cleaned restrooms, skilled nurses in emergencies, hospital sanitation, no medication side effects, recovery after treatment, and hot and fresh water availability very important. This approach offered valuable insights into resource allocation. However, the study lacked a reported sample size, which restricts its generalizability.

In another study in India, Santhoshkumar et al. (2022) determined and categorized the quality characteristics of Pandian Hospital using the Kano model to create a patient satisfaction matrix. They gathered 200 surveys from ambulatory patients. To ensure the content validity of the scale, they conducted a preliminary assessment involving 15 outpatients and interviews with the hospital's administrator and managing director. Among the 25 attributes, six were classified as attractive, including prompt performance of all services and clear directions for each department, and six were one-dimensional, such as the right services at the beginning. The study identified and ranked 10 key characteristics for implementation to reduce the gap between patients and healthcare providers and enhance patient satisfaction and loyalty. This study categorized the table of quality attributes into five groups that appear to align with the SERVQUAL dimensions; however, it did not explicitly mention using this methodology in either the abstract or main body. Therefore, this study was classified as the Pure Kano section.

In the Middle East, Howsawi et al. (2020) conducted research to identify quality attributes of healthcare in Saudi Arabia's primary healthcare centers. They distributed a cross-sectional survey among 243 adult patients from 10 primary healthcare centers under the Ministry of Health. Using the Kano model, they assessed 18 attributes and categorized 14 as one-dimensional. The study highlighted that doctors' care and attention, laboratory staff and nurses' friendliness, and receptionist friendliness and respectfulness were found to be the most important factors. This multisite study offered valuable insights for improving care quality and supporting privatization efforts. However, convenience sampling was employed, which may have introduced bias.

In China, Deng et al. (2023) investigated the efficacy and significance of assessing the requirements of hospital signage systems. The researchers surveyed 300 participants from three hospitals in Guangzhou to analyze 32 key performance indicators of hospital signage systems. The study revealed that four attributes were one-dimensional, and danger indication was ranked as the most important attribute. The study found 12 as attractive, including route guides, floor guides, and harmonization with the environment. This study also highlighted the role of hospital signage design in promoting sustainability within healthcare services. The authors recommend using penalty-reward contrast analysis (PRCA) in future research to examine the relationship between the quality features of hospital signage systems and patient satisfaction.

Chen et al. (2024) surveyed 101 patients at a teaching clinic at Yangzhou University Hospital. This study introduced a sixth category, termed the "mixed" category, in addition to the five standard Kano categories. The mixed category included services where classification was ambiguous, with the second-highest category score nearly equal to the highest. The study calculated total strength (TS) and category strength (CS) to determine the overall importance and classification strength of each service item, identifying those that could evolve into must-be attributes over time. Five attributes were categorized under the mixed category. For example, a comfortable clinic environment was

identified as a mixed attribute, which probably transforms from an attractive to a must-be attribute over time. The study results showed that patients generally viewed teaching clinics positively, highlighting their potential to improve service quality and enhance patient experiences in general practice.

In another 2024 study in China, Zhang et al. (2024) used the Kano model to investigate healthcare service demands among breast cancer survivors at a specialized care hospital in Nanjing. The research classified services according to their impact on patient satisfaction. The data were collected from a cross-sectional survey of 296 survivors. Among the 30 attributes, 13 were identified as one-dimensional and three as attractive. The better-worse analysis calculated the satisfaction index (SI) and dissatisfaction index (DSI) to quantify how each service affects satisfaction when present or absent, underscoring that prioritizing must-be and one-dimensional attributes is essential for improving care quality. Future research should prioritize longitudinal studies to track changing needs as survivors progress through treatment stages and include more diverse populations to explore demand variations across contexts and cultures.

Yao et al. (2024) applied the Kano model to assess patient service demands in an emergency observation unit (EOU) at Guizhou Provincial People's Hospital in China, proposing strategic improvements to enhance emergency care quality. This study identified 11 key service demands as one-dimensional, including nurse behavior and professionalism in pain relief. Based on this study, future research was recommended to prioritize multicenter studies to enhance generalizability, longitudinal assessments to monitor evolving patient demands, and integration with Al-driven systems to improve real-time responsiveness. Additionally, combining the Kano model with Lean Six Sigma could offer further optimization strategies for emergency healthcare services. The study underscores the importance of patient-centered improvements in emergency care and suggests that addressing these prioritized service demands could significantly enhance patient satisfaction and healthcare quality.

Materla, Cudney, and Hopen (2019) applied the Kano model to classify 21 service attributes at the Student Health Services Center at the Missouri University of Science and Technology in the United States. They identified 16 one-dimensional attributes, such as delivering correct care on the first attempt and providing patient-friendly facilities. The findings revealed that students valued the availability of trained healthcare providers within 10 minutes of arrival and the option of after-hours services as attractive attributes. The study emphasized the importance of advocating for continuous monitoring of patient needs to sustain service quality. The research demonstrates that the Kano model can support ongoing quality improvement and enhance patient satisfaction.

In another study, Cudney et al. (2023) investigated patient satisfaction during wound care treatments in a rural facility in the United States, using the Kano model to identify key elements influencing service quality. In this study, correct care was provided the first time, and rooms that allow for privacy were among the one-dimensional attributes that have a direct correlation between their presence and patient satisfaction. Another key attribute critical to enhancing customer satisfaction included essential caregiving supplies, employment of skilled and qualified medical personnel, and confidence in the quality of care provided. The findings emphasized the value of prioritizing patients' needs and expectations, especially in underserved areas, and suggested that involving patients in decision-making positively impacts satisfaction.

Barrios-Ipenza et al. (2021) evaluated the quality of medical services in two public-private partnership hospitals in Peru. A total of 250 patients participated in this study and were asked to assess 31 attributes. The study considered four main dimensions and initially categorized the service attributes based on these dimensions. Their questionnaire classified 27 attributes as one-

dimensional, including healthcare personnel's professionalism and hygiene standards of the facilities. These findings spanned dimensions such as health staff and infrastructure, illustrating how individualized services enhance patient satisfaction and loyalty. However, the study's focus on a single country limits its broader applicability.

Table 2. Summary of Reviewed Articles That Used the Pure Kano Model

Study	Purpose / Objective	Location	Sample Size	Key Findings	Limitations
(Harijith & Naduthodi, 2017)	Identify and rank healthcare quality characteristics to improve design choices and service quality in the medical industry	India	Not Specified	M: 8 A: 9 O: 4 I: 9	 Limited generalizability of findings No indication of the sample size
(Materla, Cudney, & Hopen, 2019)	Find the healthcare requirements of students and enhance service quality to maintain health within the entire campus	USA	138	A:2 O: 16 I: 3	 Respondents are young The expectations of student health services may be different from those of primary care physicians and other healthcare units
(Howsawi et al., 2020)	Specify quality attributes of patient care at primary healthcare facilities	Saudi Arabia	243	A: 3 O: 14 I: 1	Convenient sample selection based on availability and accessibility
(Barrios- Ipenza et al., 2021)	Examine health services quality, customer satisfaction, and key attributes impacting service quality in two hospitals	Peru	250	M: 3 O: 27 R:1 (Inverse)	 Limited generalizability of findings (due to different cultural, sociodemographic, and hospital management characteristics)
(Santhoshkum ar et al., 2022)	Categorize healthcare attributes, assess patient satisfaction, and enhance consumer loyalty	India	200	M: 1 A: 6 O: 6 I: 12	Single-cite focus
(Cudney et al., 2023)	Obtain the main factors of patient service quality in a rural wound care center	USA	40	O: 14 Intermina ble: 3	Limited generalizability of findingsSmall sample sizeSingle-cite focus
(Deng et al., 2023)	Analyze users' usage needs and understanding of hospital signage systems to improve the quality of healthcare services.	China	300	M: 4 A: 12 O: 4 I: 12	 Limited generalizability of findings due to different cultural, sociodemographic, and hospital management characteristics Limited sample size

Study	Purpose / Objective	Location	Sample Size	Key Findings	Limitations
(Chen et al., 2024)	Enhance the service quality of teaching clinics and advance the field of general practice by defining service demand.	China	101	M: 1 A: 2 O: 4 I: 2 Mixed attribute: 5	 Limited duration of teaching outpatient service Single-cite focus
(Zhang et al., 2024)	Investigate healthcare service demands for breast cancer survivors	China	296	M: 1 A: 3 O: 13 I: 11	 Limited generalizability of findings due to specific regional, cultural, and time constraints
(Yao et al., 2024)	Assess the needs of emergency observation patients to prioritize unit improvements and enhance patient satisfaction	China	100	M: 1 A: 1 O: 11	 Limited generalizability of findings due to convenience sampling Potential bias due to self-reported data Lack of causal inferences due to cross-sectional design. Time restriction

^{*}Must-be M, Attractive: A, One-Dimensional: O, Indifferent: I, Reverse: R

4.2 Using Kano Model with Other Methodologies

Some researchers have integrated the Kano model with other approaches to increase service quality. In Asia, Tufail et al. (2021) combined quality tools to improve healthcare services in a Pakistani hospital during the COVID-19 pandemic. The study employed Lean Six Sigma's DMAIC process, incorporating the Kano model via a structured questionnaire distributed to 147 respondents, including patients, their attendants, and staff. This approach assessed patient satisfaction with healthcare services during the pandemic and passive immunization periods. The findings identified general facilities, long wait times, and high patient volume as critical factors influencing hospital process optimization.

In another study, Wang et al. (2025) utilized the Kano model to enhance satisfaction and optimize healthcare delivery. The research analyzed 151 outpatients who underwent thyroid fine needle aspiration at Shanghai General Hospital. The Delphi method was used to establish the key indicators of the nursing service needs questionnaire. This integrated approach enabled comprehensive identification and prioritization of patient needs. Out of the six main dimensions, all the attributes under the service attitude dimension were attractive, and all the items under precautions for medical visits were one-dimensional. The authors suggest adopting an internationally recognized scale for broader applicability.

In Latin America, Lacerda (2022) evaluated the service quality of basic health units in Recife, Brazil, using an online survey that integrated the Kano and SERVQUAL models. The study collected 120 responses via social media, assessing five categories, tangibility, reliability, responsiveness, assurance, and empathy, across 22 attributes. The results classified all attributes as one-dimensional, indicating that service improvements directly enhanced patient satisfaction. Key factors such as a hygienic and welcoming atmosphere, timely service, and courteous staff interactions were identified as significant contributors to service quality improvement.

De Vasconcelos et al. (2023) conducted a strategic and comprehensive study at Oswaldo Cruz University Hospital, a public hospital in Brazil, recognized for its specialized medical services and quality programs. This research aimed to strengthen strategic planning and better understand patient priorities by combining the Kano model with the balanced scorecard. A probabilistic sample of 35 patients from the tuberculosis control program was selected, and 20 service attributes were evaluated across four main areas: outpatient services, facility environment, laboratory testing, and pharmacy. All the items in the pharmacy category were classified as one-dimensional, indicating a direct link between performance and satisfaction.

Table 3 summarizes studies that integrate the Kano model with another technique and provides their purpose, location, sample size, key findings, and limitations.

Table 3. Summary of Reviewed Articles That Integrated the Kano Model with Another Technique

Study	Purpose / Objective	Location	Sample Size	Methodology	Key Findings	Limitations
(Tufail et al., 2021)	Enhance healthcare service quality during the COVID-19 pandemic	Pakistan	147	Used the Kano model as part of a Lean Six Sigma project at a hospital system	The number of categorized attributes is not explicitly mentioned	The paper does not discuss the limitations
(Lacerda et al., 2022)	Assess the service quality of the Basic Health Unit to identify important characteristics for improving user satisfaction and quality of services	Brazil	120	The Kano model and SERVQUAL dimensions	0: 22	 Sampling Bias Respondents are young (mostly 18 to 25) Lack of generalization due to demographic presentation (gender, sample group's age, and educational levels)
(de Vasconce los et al., 2023)	Propose an integrated approach to enhance patient satisfaction and improve the quality of healthcare services in public hospitals	Brazil	35	The Kano model and balanced scorecard	M: 4 O: 15	 Limited generalizability of findings due to small sample size Some patients' unwillingness to participate (due to the length of the questionnaire, level of literacy, and privacy concerns)
(Wang et al., 2025)	Investigate the service needs of outpatients undergoing thyroid	China	151	The Kano Model and Delphi method	M: 9 O: 10 A: 12 I: 1	Single-cite focusLimited to the outpatient environment

Study	Purpose / Objective	Location	Sample Size	Methodology	Key Findings	Limitations
	fine needle					• Limited
	aspiration biopsy,					generalizability of
	enhance patient					findings due to
	satisfaction, and					the lack of
	improve healthcare					subgroup analysis
	service delivery by					in the sample and
	identifying key					the self-designed
	nursing service					questionnaire
	attributes					

5. Discussion / Effectiveness, Challenges, and Future Directions

The Kano model has been widely used in healthcare facilities, and its effectiveness varies based on the study location, patient demographics, and healthcare infrastructure. Its strength lies in its ability to pinpoint attributes that shape patient satisfaction (Materla, Cudney, & Hopen, 2019), whether applied independently or integrated with other tools. Pure applications of the Kano model are particularly effective for identifying service quality attributes. Must-be categories, such as sanitation in India (Harijith & Naduthodi, 2017) or streamlined healthcare delivery in China (Yao et al., 2024), help prevent dissatisfaction when met. One-dimensional, such as the clinic receptionist's courteous and welcoming demeanor in Saudi Arabia (Howsawi et al., 2020), nurses and healthcare personnel's professionalism (Barrios-Ipenza et al., 2021; Yao et al., 2024), or delivering correct care on the first attempt (Cudney et al., 2023; Materla, Cudney, & Hopen, 2019; Santhoshkumar et al., 2022) directly correlate with patients' satisfaction. Attractive attributes include after-hours services in a student health center in the U.S. (Materla, Cudney, & Hopen, 2019) or effective color contrast in the hospital signage system in China not only enhances patients' experience but also provides competitive differentiation by delighting patients without being expected, fostering loyalty, which is a key advantage in privatized systems (Deng et al., 2023).

While the pure application of the Kano model effectively categorizes patients' expectations, integrated approaches strengthen its impact by combining it with other methodologies that optimize processes, improve strategic decision-making, and refine service quality assessments. For example, Lacerda et al. (2022) used the SERVQUAL dimensions with the Kano model to provide a structured framework of quality dimensions that enriched the Kano model in classifying and prioritizing patient satisfaction attributes within Brazil's Unified Health System. Similarly, the balanced scorecard framework used by de Vasconcelos et al. (2023) in Brazil, to align Kano-based service improvements with hospital-wide performance metrics. These integrations help optimize resource allocation and ensure that quality enhancements are both data-driven and strategically aligned.

Despite these benefits, challenges exist across both approaches. One is the small sample size, such as the 35 participants in the study by de Vasconcelos et al. (2023) in Brazil, or 40 in a study in the U.S. by Cudney et al. (2023), which limits the statistical power and generalizability. Infrastructural and cultural differences may pose another hurdle for the generalizability of the study results. For example, cleanliness and hygiene standards in the healthcare setting were categorized as a must-be attribute in a Government Medical College in India (Harijith & Naduthodi, 2017), whereas they were found to be one-dimensional in other health settings in Latin America (Barrios-Ipenza et al., 2021; Lacerda et al., 2022). These differences underscore the need for tailored and culturally sensitive frameworks. Another methodological concern is the lack of a longitudinal perspective. Some of the

studies are cross-sectional, representing only a snapshot of patients' preferences and missing the opportunity to view how satisfaction attributes change over time. Additionally, integrated approaches often demand greater resources and technical knowledge. For example, integrating the Kano model with the Delphi method, as overseen in Wang et al. (2025), requires coordinated expert input and multiple validation rounds. Moreover, some integrated approaches need elements that may not be available in under-resourced healthcare settings.

To address these challenges, future research should focus on the following three directions. First, a longitudinal study design can give the researchers insight into attribute shifts, such as attractive to must-be, as patient expectations evolve (Chen et al., 2024), or in dynamic environments such as emergency care. Second, Al-enhanced text analysis tools can extract patient viewpoints from large datasets, such as online reviews, patient feedback in hospital systems, or health forums, and help classify healthcare service attributes according to the Kano model. Lastly, future research could explore how demographic factors such as education level or socioeconomic status influence the perception of healthcare service attributes. By comparing how different patient groups classify attributes, researchers can identify variations in expectations across public and private hospitals or between urban and underserved areas. Such insights would support more targeted service design, which would help the healthcare system provide services that patients require and ensure the correct investment of resources.

6. Conclusion

This review studies how the Kano model has been used in different healthcare settings to better understand patient satisfaction and identify areas for service improvement. Studies conducted in hospitals, clinics, and university health centers worldwide have shown that the model effectively classifies healthcare service quality features. While using the Kano model in its pure form has been effective, combining it with other methods such as SERVQUAL or the balanced scorecard gave researchers a deeper and more strategic view of what matters to patients. This review also highlights several challenges. Many studies had small sample sizes, some relied only on cross-sectional surveys, and the classification of attributes was not always consistent. Cultural and contextual differences also make it hard to generalize results across settings. Moreover, though insightful, integrated approaches often require more time, training, and resources, which may not apply to every healthcare system.

Future research could use longitudinal designs and AI-enhanced tools to gather insights from large amounts of patient feedback and explore how different groups of patients perceive service quality to improve the application of the Kano model in healthcare settings. These approaches could help healthcare services to be more responsive, targeted, and truly centered on patients' needs.

7. Disclaimer statements

Funding: None

Conflict of Interest: None

8. References

Asamrew, N., Endris, A. A., & Tadesse, M. (2020). Level of Patient Satisfaction with Inpatient Services and Its Determinants: A Study of a Specialized Hospital in Ethiopia. *Journal of Environmental and Public Health*, 2020, 2473469. https://doi.org/10.1155/2020/2473469

- Barrios-Ipenza, F., Calvo-Mora, A., Criado-García, F., & Curioso, W. H. (2021). Quality Evaluation of Health Services Using the Kano Model in Two Hospitals in Peru. *International journal of environmental research and public health*, 18(11), 6159. https://doi.org/10.3390/ijerph18116159
- Chen, M.-C., Hsu, C.-L., & Lee, L.-H. (2019). Service Quality and Customer Satisfaction in Pharmaceutical Logistics: An Analysis Based on Kano Model and Importance-Satisfaction Model. *International Journal of Environmental Research and Public Health*, 16(21). https://doi.org/10.3390/ijerph16214091
- Chen, Z., Yin, A., & Wang, Y. (2024). Demand analysis of general practice patients for teaching clinic based on Kano model. *Frontiers in public health*, *12*, 1336683–1336683. https://doi.org/10.3389/fpubh.2024.1336683
- Cudney, E. A., Reynolds Kueny, C., & Murray, S. L. (2023). Analyzing patient satisfaction in a rural wound care center. *The TQM Journal, ahead-of-print*(ahead-of-print). https://doi.org/10.1108/TQM-08-2022-0273
- de Vasconcelos, C. R., de Carvalho, R. S. M. C., de Melo, F. J. C., & de Medeiros, D. D. (2023). Improving Quality in Public Health Service: An Integrated Approach to the Kano Model and the Balanced Scorecard. *Journal of Nonprofit & Public Sector Marketing*, 35(2), 215–241. https://doi.org/10.1080/10495142.2022.2066598
- Deng, L., Romainoor, N. H., & Zhang, B. (2023). Evaluation of the Usage Requirements of Hospital Signage Systems Based on the Kano Model. *Sustainability*, 4972 (4918 pp.). https://doi.org/10.3390/su15064972 (Sustainability (Switzerland))
- Ferrari, R. (2015). Writing narrative style literature reviews. *Medical writing (Leeds), 24*(4), 230–235. https://doi.org/10.1179/2047480615Z.000000000329
- Harijith, R. G., & Naduthodi, H. (2017). Kano model customer satisfaction analysis of medical services. *International Research Journal of Engineering and Technology*, *4*(6), 1426–1429.
- Howsawi, A. A., Althageel, M. F., Mohaideen, N. K., Khan, M. S., Alzahrani, A. S., Alkhadir, M. A., Alaqeel, S. M., Alkathiri, M. A., & Hawsawi, R. A. (2020). Application of the Kano model to determine quality attributes of patient's care at the primary healthcare centers of the Ministry of Health in Saudi Arabia, 2019. *J Family Community Med*, *27*(3), 178–185. https://doi.org/10.4103/jfcm.JFCM 92 20
- Javed, S. A., Liu, S., Mahmoudi, A., & Nawaz, M. (2019). Patients' satisfaction and public and private sectors' health care service quality in Pakistan: Application of grey decision analysis approaches. *Int J Health Plann Manage*, *34*(1), e168–e182. https://doi.org/10.1002/hpm.2629
- Jin, J., Jia, D., & Chen, K. (2022). Mining online reviews with a Kansei-integrated Kano model for innovative product design. *International Journal of Production Research*, 60(22), 6708–6727. https://doi.org/10.1080/00207543.2021.1949641
- Kano, N., Seraku, N., Takahashi, F., & Tsuji, S.-i. (1984). Attractive Quality and Must-Be Quality. *Journal of The Japanese Society for Quality Control*, 14(2), 147–156. https://doi.org/10.20684/quality.14.2 147
- Lacerda, A. B., Souza, A. S. d. S., Da Silva, G. K. L., Azevedo, E. H. M. D., & Melo, F. J. C. D. (2022). Basic Health Units services quality assessment through Kano and SERVQUAL models. *Benchmarking: An International Journal*, 29(9), 2858–2880. https://doi.org/10.1108/BIJ-06-2021-0351
- Materla, T., Cudney, E. A., & Antony, J. (2019). The application of Kano model in the healthcare industry: a systematic literature review. *Total Quality Management & Business Excellence*, *30*(5-6), 660–681. https://doi.org/10.1080/14783363.2017.1328980
- Materla, T., Cudney, E. A., & Hopen, D. (2019). Evaluating factors affecting patient satisfaction using the Kano model. *International Journal of Health Care Quality Assurance*, 32(1), 137–151. https://doi.org/10.1108/IJHCQA-02-2018-0056
- Mikulić, J., & Prebežac, D. (2011). A critical review of techniques for classifying quality attributes in the Kano model. *Managing Service Quality: An International Journal*, 21(1), 46–66. https://doi.org/10.1108/09604521111100243
- Myszewski, J. M., & Sinha, M. (2020). A model for determining the value of patient satisfaction in healthcare. Business Process Management Journal, 26(3), 798–815. https://doi.org/10.1108/BPMJ-03-2019-0123
- Santhoshkumar, F., Ttr, J., & Kumar, S. (2022). Kano's model for customer satisfaction analysis of a hospital. International journal of health sciences. https://doi.org/10.53730/ijhs.v6nS1.7654

- Tufail, M. M. B., Shakeel, M., Sheikh, F., & Anjum, N. (2021). Implementation of lean Six-Sigma project in enhancing health care service quality during COVID-19 pandemic. *AIMS Public Health*, 8(4), 704–719. https://doi.org/10.3934/publichealth.2021056
- Wachinger, J., Reñosa, M. D. C., Guevarra, J. R., Landicho-Guevarra, J., Demonteverde, M. P., Silvestre, C., Endoma, V., Landicho, J., Aligato, M. F., Bravo, T. A., Chase, R. P., & McMahon, S. A. (2023). Keeping the Customer Satisfied: Applying a Kano Model to Improve Vaccine Promotion in the Philippines. *Global health science and practice*, *11*(6), e2300199. https://doi.org/10.9745/GHSP-D-23-00199
- Wang, X. Q., Pei, C. F., Liang, H. M., Wang, X., Pei, C., Jia, C., Liu, L., & Liang, H. (2025). Analysis of the service needs of outpatients undergoing thyroid fine needle aspiration biopsy based on the Kano model. *BMC nursing.*, 24(1). https://doi.org/10.1186/s12912-024-02674-6
- Yao, H., Guo, P., Du, W., Zhang, Y., Li, T., & Xiao, G. (2024). Service demand analysis and optimization strategy construction of emergency observation patients based on the Kano model. *Heliyon*, 10(16), e36323. https://doi.org/10.1016/j.heliyon.2024.e36323
- Zhang, M. M., Zhang, L. L., Wang, Y., Zhang, M., Zhang, L., Zhi, X., Cheng, F., Yao, Y., Deng, R., Liu, C., & Wang, Y. (2024). Demand analysis of health care services for community-dwelling breast cancer survivors based on the Kano model: A cross-sectional study. *International journal of nursing sciences.*, 11(2), 171–178. https://doi.org/10.1016/j.ijnss.2024.03.015

The Journal of Management and Engineering Integration (JMEI) © 2025 by AIEMS Inc., is licensed under CC BY 4.0. To view a copy of this license, visit https://creativecommons.org/licenses/by/4.0/

DOI: 10.62704/10057/31196

REAL-TIME GRASPING FORCE ESTIMATION AND STABILITY IN INDUSTRIAL ROBOTIC GRIPPER

Yimesker Yihun¹

Yi Sheng Tan²

Safeh Clinton Mawah¹

Amanuel Tereda¹

Hongsheng He³

- ¹ North Carolina A&T State University
- ² Lk Architecture- MEP Engineering Department

yyihun@ncat.edu; Ytan@IK-architecture.com; scmawah@aggies.ncat.edu; aatereda@aggies.ncat.edu; hongsheng.he@ua.edu

Abstract

In this study, a four-fingered robotic gripper was custom-designed and integrated with a UR5 robot arm to enable adaptive, real-time grasping of objects with varying shapes, sizes, and weights. Dynamic and static analyses were performed to validate the structural integrity, force distribution, and load-handling capacity of the gripper. The mechanical design incorporated lightweight honeycomb structures to maximize the strength-to-weight ratio, while under actuation minimized actuator complexity. Following structural validation, a closed-loop control algorithm was implemented using Force Sensing Resistor (FSR) feedback to regulate grasping force in real time. The system estimates object weight dynamically and adjusts the force threshold iteratively to ensure stability without exceeding the structural limits or causing object damage. Experimental validation using cylindrical, spherical, and rectangular objects demonstrated that tactile sensing significantly reduced excessive gripping force and improved stability, as quantified by a force reduction metric. The gripper achieved reliable handling of objects ranging from 0.025 to 5kg, enhancing the URS robot's dexterity and versatility for industrial applications. Results suggest that incorporating tactile feedback and adaptive force control mechanisms greatly improve the performance and safety of robotic gripping systems. Future work will explore machine learning-based adaptive control strategies to extend the gripper's capabilities to a broader range of materials and surface textures. This approach offers a cost-effective, customizable solution for enhancing autonomous robotic manipulation in dynamic, unpredictable environments.

Keywords: Industrial Gripper, Real-time Weight Learning, UR5 Robot Integration

1. Introduction

Industrial grippers face significant challenges when adapting to objects of varying shapes, sizes, weights, and material properties while maintaining stable and secure handling (Elfferich, Dodou, & Della Santina, 2022). Addressing this diversity requires the integration of advanced mechanisms and materials, including compliant structures, modular designs, and dynamic adjustment capabilities

Submitted: April 30, 2025 Revised: September 5, 2025

³The University of Alabama

(Blanco, Navas, Emmi, & Fernandez, 2024). Real-time feedback from force sensors has become critical to enhance stability and precision, allowing grippers to adjust the applied force to prevent damage while securing the object during manipulation tasks (Xu, Zhang, Yuan, & Liang, 2021). Achieving reliable, adaptive grasping necessitates a deep understanding of both the mechanical behavior of grippers and the physical properties of the objects they handle (Oliveira, Moreira, & Silva, 2021), along with extensive experimental validation across diverse scenarios (Hussain et al., 2021).

Conventional gripper systems often rely on pre-set force parameters and static designs, limiting their adaptability in highly variable environments where object properties change frequently (Liu et al., 2024). While progress has been made, such as closed-loop grip force control using tactile sensors (Khamis, Xia, & Redmond, 2021), proximity sensing for stability assessment (Suzuki, Yoshida, Tsuji, Nishimura, & Watanabe, 2022), hybrid force control in stiff grippers (Zuo, Song, & Chen, 2021), and real-time object classification using energy-efficient tactile systems (Amin, Gianoglio, & Valle, 2023). Existing solutions generally remain constrained by design limitations. Many systems are restricted to specific object types, lack dynamic force adjustment, or are optimized for limited gripping scenarios. To overcome these limitations, this study presents a novel four-fingered robotic gripper integrated with a UR5 robotic arm, designed to dynamically adjust its grip strength and ensure stable manipulation across a wide range of object shapes, sizes, and weights. The proposed system incorporates real-time feedback from integrated FSR sensors to estimate object weight and iteratively adjust gripping thresholds, enabling adaptive force control during operation. Compared to prior works, our design emphasizes broad adaptability, minimizing manual intervention and improving versatility in unpredictable industrial environments. By combining lightweight, costeffective mechanical design with adaptive, sensor-based force regulation, this gripper advances the development of flexible robotic systems capable of autonomous operation.

2. Methods

The development of the adaptive robotic gripper followed a systematic sequence, beginning with the design and simulation of the gripper structure to ensure strength, range of motion, and compatibility with the UR5 robotic arm as shown in Fig. 1. After confirming the mechanical integrity through dynamic and static analysis, the gripper was fabricated and mechanically validated for fitment and load capacity. Subsequently, an adaptive control system was integrated using FSR sensors, allowing real-time feedback-based adjustment of grasping force. The control algorithm continuously monitored applied forces and dynamically tuned motor input to maintain grip stability while preventing excessive loading. Validation experiments were conducted to assess gripping performance across diverse object shapes and weights, completing the methodology.

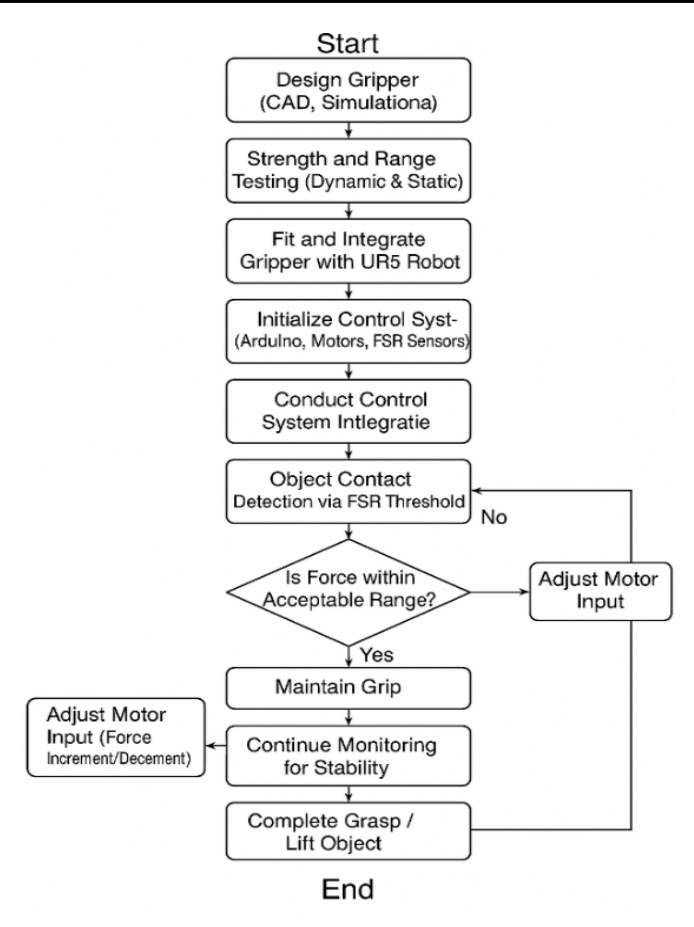


Figure 1. Methodology Flowchart

2.1 Design and Simulation of the Gripper

The initial development phase focused on designing a cost-effective and adaptable four-fingered robotic gripper tailored to the UR5 robotic arm's end-effector specifications. The gripper was modeled using Fusion360 and dynamically simulated in Adams software to evaluate its mechanical behavior, load distribution, and range of motion across various grasping scenarios.

To enhance structural resilience while minimizing weight, a honeycomb architecture was incorporated into the gripper design, achieving an optimal strength-to-weight ratio (Kaur & Kim, 2019). A four-bar linkage system was utilized for each finger to provide underactuated motion, simplifying the actuation system while maintaining effective adaptability to diverse object shapes. The width of the gripper was set at 128mm, enabling it to accommodate a wide range of object sizes

Static and dynamic analyses were performed to assess grasp force capability, stress distribution, and overall structural integrity. These simulations verified that the gripper could reliably handle loads ranging from 0.04kg up to the UR5 robot's maximum payload of 5kg. Additionally, safety factors were evaluated to ensure the gripper remained within mechanical limits during operation.

The final numerical model provided comprehensive insights into the gripping mechanics, load paths, and stability under various loading conditions, including the effects of tactile forces during real object interaction. The validated design was then fabricated for physical integration with the UR5 platform. An exploded view and multiple perspectives of the gripper assembly are shown in Fig. 2, providing a detailed visualization of the mechanical structure.

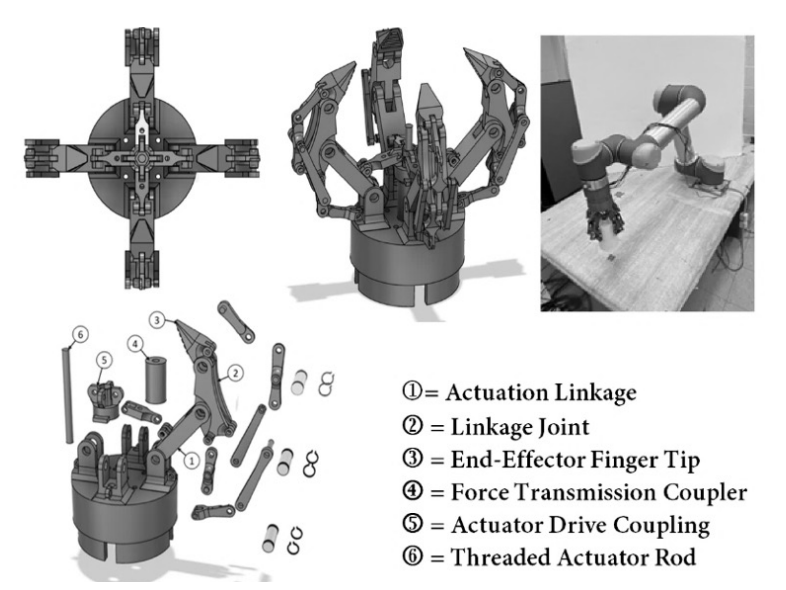


Figure 2. Overall View of The Four-Finger Robotic Gripper Assembly

2.2 Structural Strength Analysis

The dynamic performance of the developed gripper was initially evaluated through simulation, focusing on its ability to grasp and stabilize a spherical object of specified mass. As depicted in Fig. 3, the gripper's motion, driven by motor torque, was analyzed to characterize the transient behavior during grasp acquisition. The simulation validated the virtual prototype's functional capability across the gripping cycle, revealing smooth actuation and secure object capture dynamics. A transient external force of 50N was applied at the fingertip to determine the maximum achievable grasping force, with the motor operating at 15rpm and powered by a 9V supply. The gripper successfully demonstrated the ability to sustain objects weighing up to 17kg. The localized contact area at the gripper tip was measured to be $2.24cm^2$, resulting in a calculated contact pressure of $0.762MPa~(76.2M/cm^2)$.

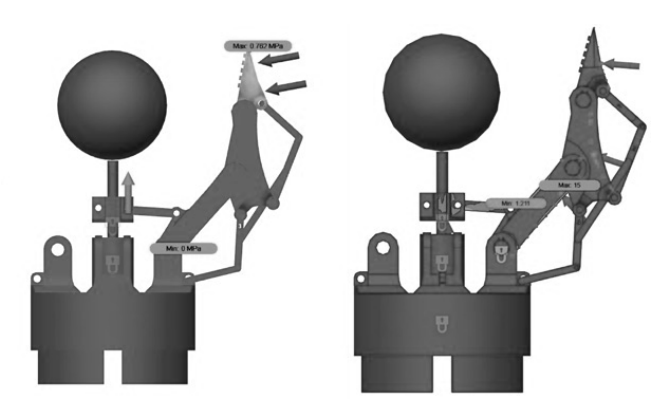


Figure 3. Gripper Motion and Grasping Force Analysis

Subsequent static analysis was conducted to assess the structural robustness and stress distribution under maximum loading conditions. Static simulations applied forces at multiple contact points along the gripper fingers, providing a detailed depiction of load transmission paths and stress concentrations during the gripping operation. The maximum grasping force obtained from dynamic

analysis 170N was uniformly applied across the system to validate the mechanical strength and to determine the factor of safety inherent in the design. The resulting stress fields confirmed that the gripper structure maintained sufficient margins against yielding and deformation, thereby ensuring reliability under operational conditions. These results affirm that the gripper is mechanically capable of executing grasping tasks across a wide range of load scenarios with structural integrity and dynamic stability. The main structure of the gripper was produced using 3D printing, specifically utilizing a polylactic acid (PLA) filament. PLA was selected for its balance between durability and reduced brittleness when compared to resin filament (Azadi et al., 2021).

2.3 Hardware for Control Systems

For the control system, an Arduino Uno microcontroller was used to coordinate the complex movements of the gripper. To achieve a grasp load capacity of 5kg, a bipolar step motor was chosen for its ability to deliver the required torque for reliable operation. To mitigate the vibrations commonly associated with bipolar step motors, a motor driver was employed. This motor driver is designed to regulate both pulse and ampere parameters, ensuring optimal motor performance. To further enhance the gripper's functionality, friction-enhancing rubber padding was applied to the surface of each finger. This addition increased the contact area between the fingertips and the objects being manipulated, providing greater grip stability. Additionally, Force-Sensing Resistor (FSR) sensors were integrated into the fingertips to improve tactile feedback. These sensors not only refined data acquisition but also played a vital role in incorporating tactile force feedback within the microcontroller-operated system, ensuring precise control during operation.

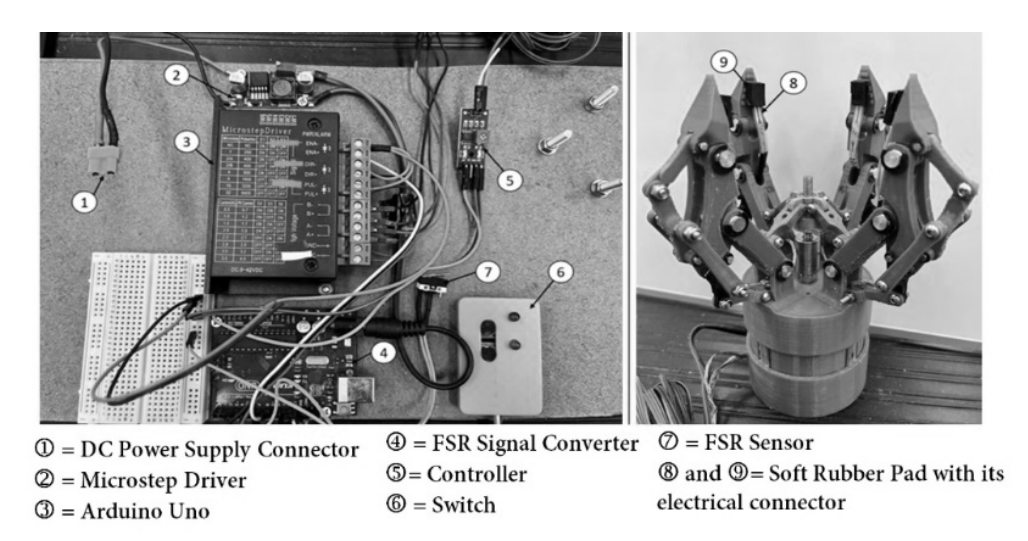


Figure 4. Assembly and Configuration of the Gripper Prototype

3. Grasping, Lifting Load Learning and Analysis

The gripper operation initiates with system initialization, followed by object contact detection via thresholding the Force Sensing Resistor (FSR) signals. Upon establishing contact, a minimal grasping force is applied to prevent premature slippage, and the normal force exerted at the fingertips is continuously monitored in real time. Figure 5 illustrates the closed-loop feedback control architecture employed for dynamic force adjustment.

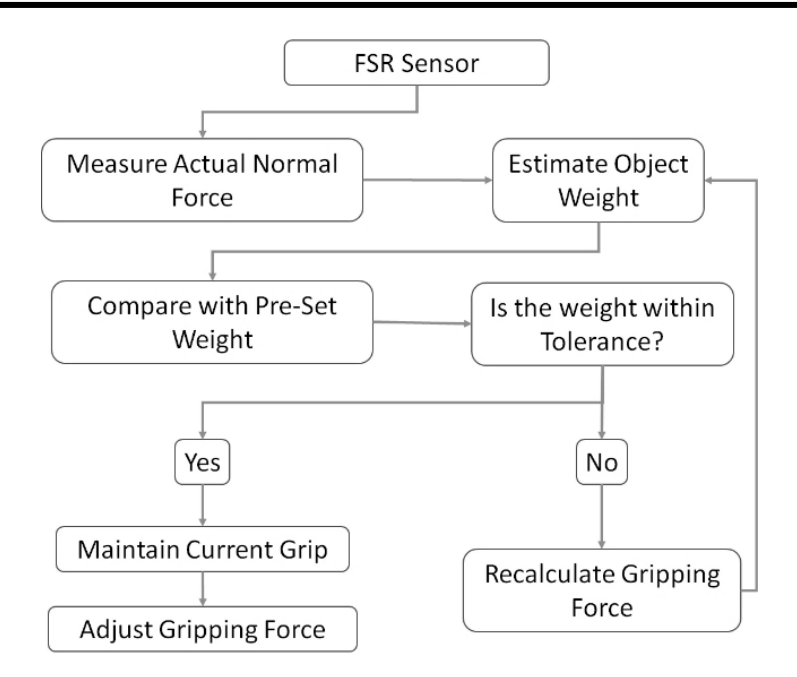


Figure 5. Real-Time Gripping Force Adjustment Using FSR Feedback Loop

Grasp slippage is primarily initiated when the applied tangential force due to object weight or manipulation exceeds the maximum frictional force available at the contact interface (Bicchi & Kumar, 2000). To avoid slippage, the normal force F_N applied by the gripper must satisfy the following inequality: $F_T \leq \mu F_N$, where F_T is the tangential (load-induced) force, and μ is the coefficient of friction at the contact interface. As the object is lifted, the tangential force F_T effectively corresponds to the object's weight W under gravity, i.e., $F_T = W = mg$, where m is the object's mass and g is the gravitational acceleration.

The FSR sensors measure the normal pressure P_N at the fingertip contact regions. Given the contact area A_c , the applied normal force F_N can be approximated as: $F_N = P_N A_c$. Combining the two expressions yields a critical condition for secure lifting without slippage: $mg \leq \mu P_N A_c$. From the FSR-measured normal pressure P_N , and known contact area A_c , the object's weight can be indirectly estimated, and the necessary adjustments to gripping force can be dynamically regulated to maintain grip stability.

The real-time control loop compares the estimated 'mg' against pre-set stability thresholds and adjusts the motor inputs to increase or decrease the grasping force, accordingly, ensuring that slippage margins are maintained throughout lifting and manipulation tasks.

The experimental methodology encompasses three primary stages:

- **System Identification**: Establish the calibration curve between applied normal forces and FSR output signals using standardized weights and contact scenarios.
- Validation Testing: Evaluate the real-time control system under dynamic lifting conditions, assessing the ability to adaptively regulate gripping force based on live FSR feedback.
- Signal Integration: Embed the FSR-based normal force monitoring into the Arduinocontrolled closed-loop system, enabling continuous force adjustment during robotic manipulation.

The gripper's grasp stability and load-handling were tested through simulation and experiments. The Arduino Integrated Development Environment (IDE) interfaced IDE with FSR sensors, modeled and monitored the gripper's force in real time. The finger mechanism's dynamics during grasping were analyzed to prevent slippage. Prototype tests verified the simulation results, confirming the system's ability to handle various loads and improving the design and control strategies.

3.1 Grasping, Lifting Load Learning, and Analysis

During the validation test, three distinct object shapes: cylindrical, spherical, and rectangular were used to evaluate the gripper's performance and gather data on its grasping capabilities. For each object, two experiments were conducted: Measuring the actual force required to lift the object within a predetermined force limit and calculating the integrated force through tactile force analysis.

To ensure a secure and stable grip, a tactile force was applied, and an equation incorporating the coefficient of friction was utilized to minimize slippage while maximizing the overall grasp strength without causing damage to the object. The coefficient of friction (μ), ranging from 0.2 to 0.6, was selected based on the material properties and surface texture of the object. This approach optimized the gripping force while also increasing the consistency and reliability of the grasp, enabling the gripper to handle objects of different shapes and materials. Figure 6 demonstrates the gripper's ability to grasp and lift objects of different shapes, along with force vs. time graphs that compare the results with and without tactile force analysis during the validation experiment for each object.

3.2 Validation and Result Discussion

Figure 6 presents a force vs. time graph, demonstrating that a gripper lacking tactile feedback exerts a higher and more variable force, while a gripper with tactile sensors consistently applies a lower and steadier force over time. This encompasses the results for various objects, both with and without tactile sensors. The findings indicate that tactile sensing is vital for enhancing the adaptability and effectiveness of robotic manipulation.

To evaluate the impact of tactile sensing, a performance metric, denoted as 'u', is used. This metric quantifies the reduction in excessive force when tactile feedback is incorporated. A higher 'u' value indicates a more significant improvement in force regulation. It is calculated using the following equation:

$$u = \frac{Maxforce(withoutTactileForce) - Maxforce(withTactileForce)}{Maxforce(withTactileForce)}$$

Table 1 summarizes the maximum forces applied by the robotic gripper with and without tactile sensing for different object shapes:

Object Shape	Max Force Without Tactile (N)	Max Force with Tactile (N)	Reduction Ratio (u)
Cylindrical	2.19	1.79	0.452
Spherical	2.24	1.46	0.534
Rectangular	3.02	2.08	0.223

Table 1: Maximum Gripper Forces with And Without Tactile Sensing for Different Object Shapes

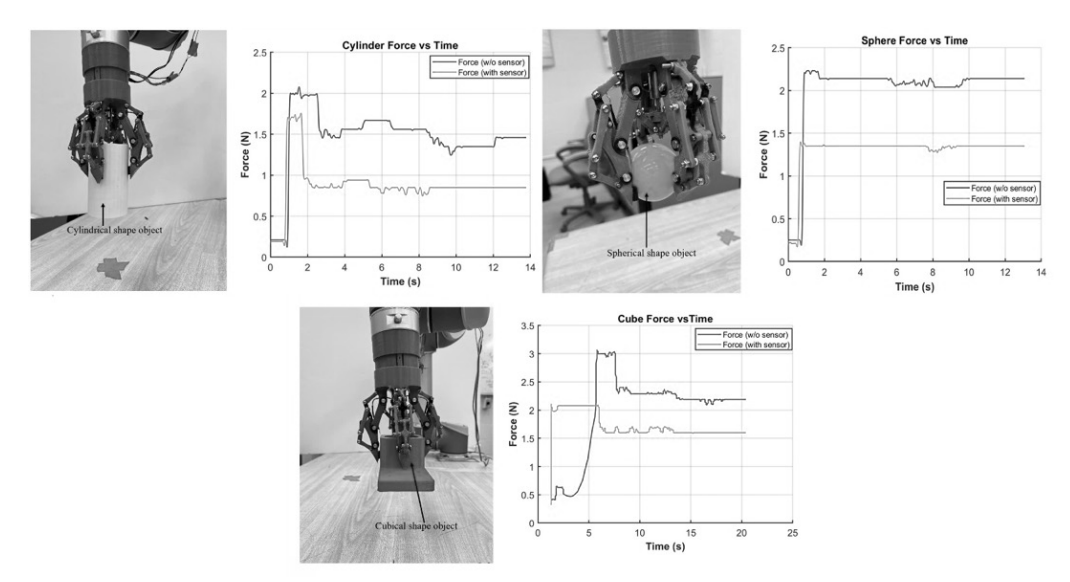


Figure 6. Results for Various Objects With/Without Tactile Sensor

For the cylindrical object, the maximum force without tactile sensing is 2.19N, while with tactile sensors it is reduced to 1.79N. This results in a force reduction factor of u=0.452, meaning that the tactile-enabled gripper applies approximately 45.2% less force than its non-tactile counterpart. Similarly, for the spherical object, the force decreases from 2.24N to 1.46N, resulting in a higher reduction factor of u=0.534, indicating that tactile sensing provides even greater force optimization. The rectangular object, with a force reduction from 3.02N to 2.08N, has a smaller reduction factor of u=0.223, suggesting that force control varies depending on the geometry of the object.

To complement the physical experiments, we conducted additional analyses in simulation and clarified the rationale behind the chosen test objects. The gripper was evaluated using CAD and dynamic simulations in MSC Adams to model contact forces and grasp stability across a wider set of object sizes (20–120 mm span) and weights (0.025–5 kg). These simulations confirmed that the underactuated four-bar linkage distributes contact forces passively and maintains stable grasping without exceeding finger stress limits under the tested range. The results suggest that the control approach remains effective across objects beyond those physically tested.

The three objects selected for experimental evaluation—cylindrical, spherical, and rectangular—represent canonical primitives in robotic grasping. Cylinders challenge the system with rolling stability, spheres provide minimal contact area (representing worst-case slippage conditions), and rectangles introduce edge-constrained grasping dynamics. Together, these shapes span the fundamental constraints associated with grasping rigid industrial components and offer a representative benchmark for evaluating gripper adaptability. While current physical validation is limited to these object types, supporting simulations suggest broader applicability. However, simulations cannot fully substitute empirical evaluation. Future work will extend physical testing to include deformable, irregular, and textured geometries to rigorously validate the gripper's robustness and generalizability.

4. Conclusion

This work presented a four-fingered adaptive gripper integrated with the UR5 robot and real-time FSR-based force control. The system demonstrated precise, stable grasping of diverse object types, handling loads from 0.025 kg to 5 kg. Tactile feedback enabled minimal force application, reducing slippage and improving grip reliability. Structural and experimental validations confirmed the gripper's robustness for industrial use. Future efforts will enhance adaptability using learning-based control,

expand tactile sensing resolution, and adopt lighter materials for improved efficiency. These developments aim to advance intelligent, modular grippers for dynamic, real-world automation tasks.

5. Disclaimer Statements

Funding: None

Conflict of Interest: None

6. References

- Amin, Y., Gianoglio, C., & Valle, M. (2023). Embedded real-time objects' hardness classification for robotic grippers. *Future Generation Computer Systems*, *148*, 211-224. https://doi.org/10.1016/j.future.2023.06.002
- Azadi, M., Dadashi, A., Dezianian, S., Kianifar, M., Torkaman, S., & Chiyani, M. (2021). High-cycle bending fatigue properties of additive-manufactured ABS and PLA polymers fabricated by fused deposition modeling 3D-printing. *Forces in Mechanics, 3,* 100016. https://doi.org/10.1016/j.finmec.2021.100016
- Bicchi, A., & Kumar, V. (2000). *Robotic grasping and contact: A review*. Paper presented at the Proceedings 2000 ICRA. Millennium conference. IEEE international conference on robotics and automation. Symposia proceedings (Cat. No. 00CH37065). doi: 10.1109/ROBOT.2000.844081
- Blanco, K., Navas, E., Emmi, L., & Fernandez, R. (2024). Manufacturing of 3D printed soft grippers: a review. *Ieee Access*, *12*, 30434-30451.doi: 10.1109/ACCESS.2024.3369493
- Elfferich, J. F., Dodou, D., & Della Santina, C. (2022). Soft robotic grippers for crop handling or harvesting: A review. *leee Access*, 10, 75428-75443. doi: 10.1109/ACCESS.2022.3190863
- Hussain, I., Malvezzi, M., Gan, D., Iqbal, Z., Seneviratne, L., Prattichizzo, D., & Renda, F. (2021). Compliant gripper design, prototyping, and modeling using screw theory formulation. *The International Journal of Robotics Research*, 40(1), 55-71. https://doi.org/10.1177/0278364920947818
- Kaur, M., & Kim, W. S. (2019). Toward a smart compliant robotic gripper equipped with 3D-designed cellular fingers. *Advanced intelligent systems*, 1(3), 1900019. https://doi.org/10.1002/aisy.201900019
- Khamis, H., Xia, B., & Redmond, S. J. (2021). *Real-time friction estimation for grip force control.* Paper presented at the 2021 IEEE International Conference on Robotics and Automation (ICRA). doi: 10.1109/ICRA48506.2021.9561640.
- Liu, Y., Zhang, J., Lou, Y., Zhang, B., Zhou, J., & Chen, J. (2024). Soft bionic gripper with tactile sensing and slip detection for damage-free grasping of fragile fruits and vegetables. *Computers and Electronics in Agriculture*, 220, 108904. https://doi.org/10.1016/j.compag.2024.108904
- Oliveira, L. F., Moreira, A. P., & Silva, M. F. (2021). Advances in agriculture robotics: A state-of-the-art review and challenges ahead. *Robotics*, 10(2), 52. doi:10.5281/zenodo.14001929
- Suzuki, Y., Yoshida, R., Tsuji, T., Nishimura, T., & Watanabe, T. (2022). Grasping strategy for unknown objects based on real-time grasp-stability evaluation using proximity sensing. *IEEE Robotics and Automation Letters*, 7(4), 8643-8650. doi:10.1109/LRA.2022.3188885
- Xu, W., Zhang, H., Yuan, H., & Liang, B. (2021). A compliant adaptive gripper and its intrinsic force sensing method. *IEEE Transactions on Robotics*, *37*(5), 1584-1603. doi:10.1109/TRO.2021.3060971
- Zuo, W., Song, G., & Chen, Z. (2021). Grasping force control of robotic gripper with high stiffness. *IEEE/ASME Transactions on Mechatronics, 27*(2), 1105-1116. doi:10.1109/TMECH.2021.3081377

The Journal of Management and Engineering Integration (JMEI) © 2025 by AIEMS Inc., is licensed under CC BY 4.0. To view a copy of this license, visit https://creativecommons.org/licenses/by/4.0/

DOI: 10.62704/10057/31197

APPLYING LEAN ASSESSMENTS TO OPTIMIZE MACHINE EFFICIENCY AND MINIMIZE WASTE

Ashlynn Clark ¹
Ridge Towner ¹
Adam Carlton Lynch ¹
¹ Wichita State University

acclark1@shockers.wichita.edu

Abstract

This project investigated the impact of Total Productive Maintenance (TPM) on a Bavius 5-axis CNC machine used in aircraft floor beam production. In Fall 2024, students partnered with Spirit AeroSystems to assess and improve maintenance using 5S, OEE, and value stream mapping. This study identifies inefficiencies, evaluates process effectiveness, and offers recommendations. Early results show mixed outcomes, providing key insights into TPM's role in boosting operational efficiency.

Keywords: OEE, TPM, Value Stream Map.

1. Introduction

1.1 Background

To remain competitive, companies are turning to real-time data and faster decision making to improve equipment efficiency and productivity. Many are using Industry 4.0 technologies like AI, IoT, big data, and blockchain to automate processes, lower costs, and boost security. These tools help businesses share data smoothly across operations, leading to better productivity and quality, while reducing manual work [1]. Advanced manufacturing with tools such as CAD, CIM, CNC machines, and robotics helps companies produce high-quality products at competitive prices while maintaining flexibility. These technologies allow businesses to adjust to changes in demand, reduce costs, and easily customize [2].

This project examines a five-axis CNC machine, which is used for drilling and milling parts, such as floor beams for commercial aircraft. The machine could move in multiple directions, making it highly flexible and precise. A laser tool setter is also used to ensure that the tools are properly calibrated. Metrology is key to ensuring that the parts are made accurately. The CNC machine used in this study uses a ruby-tipped probe to check the alignment of the part before it starts its production. It also has features that account for temperature changes and ensure precise measurements during the process [3].

1.2 Literature Review

1.2.1 Active Learning Techniques

Active learning encourages student engagement through activities such as working together with a small group, working through applicable case studies, or role-playing scenarios [4]. In short, active learning seeks to stray from some of the more traditional strategies for learning

Submitted: April 30, 2025 Revised: September 9, 2025 to give students a more active role in their own path towards course outcomes.

1.2.2. Problem Based Learning

Problem-Based Learning (PBL) is a learning style that promotes critical thinking and problem-solving using discipline-specific problems as the trigger. There needs to be a resolution and courses that use problem-based learning as the leading learning strategy to give students the opportunity to problem-solve with their peers in a team setting, as well as grow their own self-learning through the problems and scenarios given [5]. Learners gain knowledge from the observation and analysis of the scenario and apply that knowledge to the overarching problem.

1.2.3 Project Based Learning

Project Based Learning uses real-world problems to emphasize the learning objectives of a course rather than traditional methods such as lecturing or note-taking. By structuring a course around a project, students can see the results of the information that they are gaining in real time instead of taking a test or quiz to gauge their understanding [6]. Students who learn through a project can boost their creativity, equip them with applicable skills, and help improve their collaboration with their classmates. Project Based Learning also teaches how important it is to plan work ahead of time to accomplish everything in a timely manner [7]. Project-based learning is also an active learning technique, as mentioned above, and is the technique that this study and project is based upon.

1.2.4 Lean Six Sigma

The five principles lean are value, value stream, flow, pull system, and perfection. Lean focuses on reducing waste by simplifying processes and removing non-value-added activities, whereas Six Sigma aims to reduce defects and process variability. Lean Six Sigma is a combination of well-known waste elimination and process improvement techniques, Lean Manufacturing and Six Sigma [5]. Lean Six Sigma is a powerful structure for the continuous improvement of manufacturing environments.

1.2.5 DMAIC vs. DMADV

Six Sigma employs two planning processes: DMAIC (Define, Measure, Analyze, Improve, Control) and DMADV (Define, Measure, Analyze, Design, Verify). DMAIC is used for process improvements in existing products or systems, focusing on reducing variability and improving quality through data-driven decisions. It is applicable in a wide range of scenarios in which the ongoing performance needs to be enhanced. By contrast, DMADV is applied when developing new products or processes, focusing on the design and verification of products that meet customer needs. The last two steps of DMADV, design and verification, involve refining the product design and ensuring that it aligns with customer expectations and requirements through testing and feedback [8].

1.2.6 DMAIC Tools by Phase

As explained above, DMAIC is a Six Sigma tool used for process planning and improvement in a variety of applications. The Define Phase focuses on clearly stating the problem and forming a team critical to the project's success. Along with a problem statement and team charters, process mapping can be used to create a visual representation of the processes involved [8]. The Measure Phase is dedicated to collecting accurate data relevant to the project [12]. In the Analyze Phase, this data is evaluated to identify issues and develop solutions using tools such as cause-and-effect diagrams, root cause analysis, or Pareto charts [8]. The Improve Phase

implements solutions developed in the Analyze Phase, with tools chosen carefully to fit the project's needs. Finally, the Control Phase focuses on establishing standard work, training boards, and operating procedures to ensure consistent implementation and measurable improvements.

1.2.7 Lean Flow Tools

5S is a workplace organization method that aims to improve efficiency and employee habits. It involves sorting (removing unnecessary items), setting in order (organizing tools for easy access), shine (regular cleaning to detect issues), standardization (creating standards for workflow), and sustainability (repeating the process to establish a culture of organization) [9].

Overall Equipment Effectiveness (OEE) is a key performance indicator developed as part of Total Productive Maintenance (TPM) to measure equipment productivity in manufacturing systems [11]. Total Productive Maintenance (TPM), introduced by Nakajima (1988), covers the full lifecycle of equipment across all divisions, including planning, manufacturing, and maintenance [10]. Single-minute Exchange of Die (SMED) focuses on reducing production batch sizes and minimizing downtime by streamlining the tool and machine changeover processes [9].

1.3 Problem Statement

This study applies lean practices, such as TPM, OEE, 5S, and value stream mapping, to standardize work for a CNC machine at Spirit AeroSystems. The focus is on improving standard work practices, organizing the workspace, and implementing TPM to enhance equipment effectiveness through preventative maintenance. By reducing downtime, breakdowns, and inefficiencies, the goal is to optimize productivity while ensuring safe, organized, and streamlined operation.

1.3.1 Research Question

RQ1: How to effectively improve the machine space by using Lean 5S, OEE and TPM?

1.3.2 Contribution of the Study

This study examined the effectiveness of lean methods and TPM in enhancing equipment and worker productivity. By identifying inefficiencies and applying techniques such as value stream mapping, OEE, 5S, and process flow mapping, this study provides insight into operational bottlenecks and improvements. TPM implementation has helped increase equipment effectiveness by minimizing downtime, reducing breakdowns, and optimizing the manufacturing process for near-error-free operation.

1.4 Structure of the Study

The study also covers the Methods & Materials (Section 2.0), Results & Analysis (Section 3.0), and Interpretation, Implications, Limitations, Future Research, and Conclusions (Section 4.0).

2. Methodology

This project focuses on creating a standardized Total Productive Maintenance (TPM) plan for a 5-axis CNC machine at Spirit AeroSystems. In Fall 2024, the team worked with the company sponsor to observe operations, identify challenges, and develop proactive maintenance strategies. Key tools included Overall Equipment Effectiveness (OEE) calculations, process time studies, and Voice of Employee (VOE) feedback. The goal is to use these insights to improve machine reliability and provide operators with a repeatable framework for future iterations of the Beam Drilling Line.

2.1 Materials

This project focuses on the Bavius CNC machine, its tools, and materials. Key items included red tags to mark unnecessary components, a label printer for organized storage, and colored tape for visual coolant and oil level indicators. Customer-provided tool list samples will help create a standardized, easy-to-follow tool system for operators. The most critical resource is the current operating procedures, which will be reviewed to determine whether a new Standard Operating Procedure (SOP) is needed.

2.1.1 Lean Assessment

After defining the project scope, a lean manufacturing assessment identified areas for improvement, focusing on Total Productive Maintenance (TPM), Overall Equipment Effectiveness (OEE), and 5S for productivity and organization. Key aspects include material flow analysis, machine availability, and workplace cleanliness, emphasizing waste reduction. Several methodologies guided the assessment: an SIPOC diagram mapped inputs and outputs, FMEA identified potential failure modes, and a Pareto chart highlighted critical issues. A fishbone diagram traced root causes, while value stream mapping analyzed current workflows and outlined a more efficient future state. These tools collectively enhance the process flow, machine effectiveness, and maintenance strategies while reinforcing 5S principles.

2.1.2 Development of Lean Strategy

A lean manufacturing strategy should align with the project scope to optimize the machine work area. The first step is to identify waste through value stream analysis, considering the company's constraints. After updating the value stream map, the focus shifts to improving equipment reliability and productivity through OEE, TPM, and a standard operating procedure (SOP) to provide clear, step-by-step instructions for consistent and efficient tasks, ensuring quality, safety, and compliance.

2.1.3 Implementation of Lean tools and Solution Deployment

The Machine's Total Productive Maintenance (TPM) solution should utilize different lean manufacturing tools. The LEAN tools must be implemented effectively to eliminate waste, boost productivity, and create standard work processes. After using the tools, subsequent action should be taken to ensure the improvements are implemented. Additionally, a systematic process should be established to monitor key improvement metrics and identify further improvement opportunities.

2.2 Method/Approach

Data collection is crucial for implementing and improving workflow. The team uses methods such as process flow charts, time studies, and employee feedback to gather valuable insights. These data were then analyzed to assess the current state and develop recommendations for future improvements.

2.2.1 Process Flowchart

The flowchart illustrates the workflow involved in the completion of a drilled part. Flowcharts visually represent the tasks of a process, identifying areas for improvement at specific steps. In this project, the flowchart serves as a tool for the team to discuss and generate ideas for process improvement.

2.2.2 Time Studying

The team will observe the process to identify what "states" the process is in during available work time. The states will be recorded on different expectations, including value-add and non-value-add. Value-add time is defined by the time in which the product is having value added to it. Non-value-add time is the time that does not directly add value to the product (e.g., Machine Setup of a part).

2.2.3 Voice of Employee (VOE)

The Voice of the Employee (VOE) provided direct feedback from operators, helping identify issues and potential solutions for the project. The drilling machine operates in two shifts: 6 AM to 2:30 PM and 3 PM to 11 PM. During Gemba walks, the team questions operators to understand the process steps. VOE is a critical tool for this project as it helps identify essential steps and highlight bottlenecks and inefficiencies. It also provides insight into potential improvements that would benefit the operator and optimize the layout to make production more efficient.

2.2.4 Overall Equipment Effectiveness (OEE)

Overall Equipment Effectiveness (OEE) measures a machine's productivity by assessing three key factors: availability (A), performance efficiency (P), and quality rate (Q). This calculation helps define the productivity of the production process with multiple metrics for diagnosing inefficiencies.

$OEE = A \times P \times Q$

Availability (A) - (Operating Time / Net Available Time) × 100%

Operating Time = Total Time – Downtime

Total Time = Workday – Planned Downtime

Performance Efficiency (P) = (Ideal Cycle Time × Total Part Run / Real time) × 100%

Quality Rate (Q) = (Total Part Run – Total Defects) / Total Part Run

3. Results

3.1 Results for RQ1

Lean 5S is a core strategy for optimizing machine space and boosting efficiency. It starts with Sort to remove unnecessary items, followed by Set in Order to organize tools for easy access. Shine maintains cleanliness and helps detect issues early, while Standardize creates consistency through clear procedures. Sustain ensures these improvements last over time. Overall Equipment Effectiveness (OEE) supports 5S by measuring availability, performance, and quality to identify bottlenecks and improve workflow. Total Productive Maintenance (TPM) further reduces downtime through proactive maintenance and operator training, improving machine reliability and space utilization.

3.2 Results from OEE and 5S

3.2.1 OEE

The Overall Equipment Effectiveness (OEE) offers a detailed view of production efficiency by tracking equipment use, labor, and material flow. It categorizes machine idle time (e.g., setup, breaks, and cleaning) to highlight waste. While some downtime is necessary, OEE helps identify and reduce excessive delays, thereby supporting lean operations. OEE helps assess the daily machine performance, as shown in the figure below.

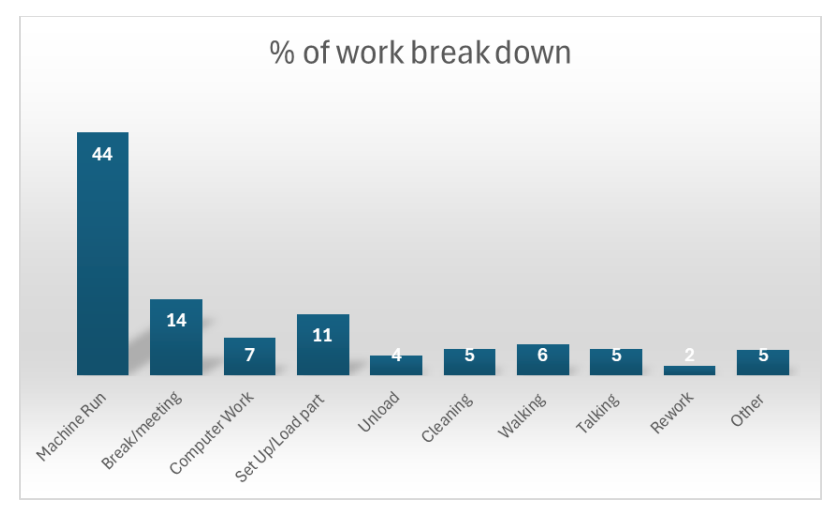


Figure 1. Observed Bar chart

The time study showed the machine ran 44% of the time and was idle 56%, largely due to maintenance needs. Out of 168 weekly hours, removing 48 weekend hours left with 120 available hours. This was further reduced by planned and unplanned downtime, changeovers, reduced speed, and rework, resulting in only 71 productive hours per week.

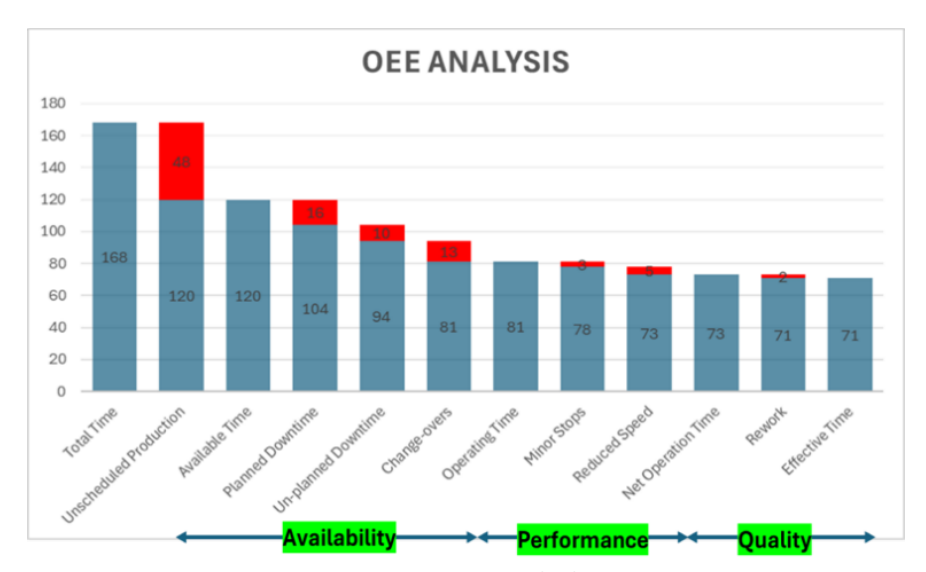


Figure 2. Time Loss Calculation

OEE1 = Effective time/Total Time = 71/168 = 41%

OEE2 = Effective time/Available time = 71/120 = 59%

Based on the Overall Equipment Effectiveness (OEE) calculation, time losses were categorized into availability, performance, and quality losses, as shown in Figure 2. The machine's OEE was measured at only 41%, indicating major inefficiencies and clear opportunities for improvement. A key focus is implementing a standardized operating procedure (SOP) and structured tool change system to track tool lifespan, prevent breakage, and reduce downtime. This approach ensures timely tool replacement, improves reliability, and supports consistent production efficiency.

3.2.2 5S Application

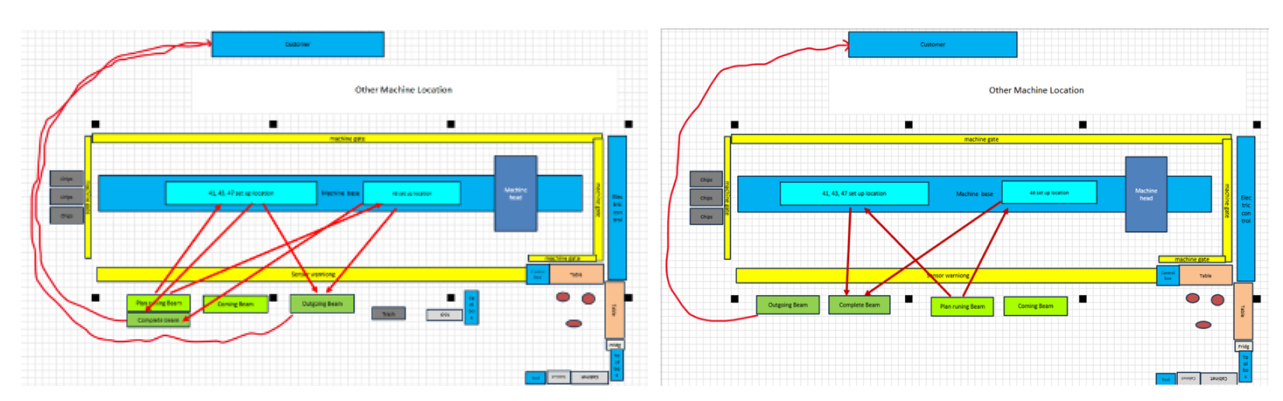


Figure 3. Current vs. Future State

As shown in the above images, the current layout involves excessive non-value-added movement, with operators constantly traveling to different areas to retrieve the materials for the CNC machine. The layout lacks a consistent process, and there are no designated areas for the incoming, queued, or outgoing beams. In the future, materials will be positioned closer to the operator to reduce walking, and specific spaces will be assigned to each material type. This streamlines the workflow, minimizes unnecessary movements, and allows operators to access materials more efficiently, therefore enhancing productivity.

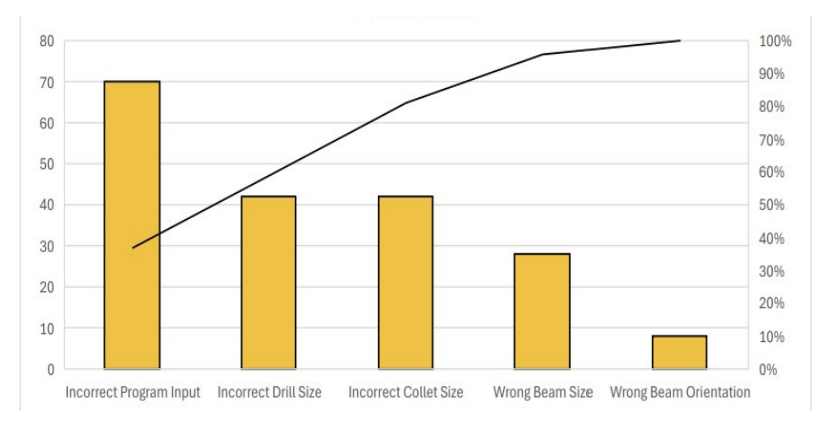
3.3 Lean Assessment Results

3.3.1 Failure Mode Effects and Analysis (FMEA) Results

Using an FMEA chart helped identify potential defects in the SIPOC results by assessing the Severity, Occurrence, and Detectability, allowing us to prioritize areas requiring intervention. It was found that most issues stemmed from the machining process, which was the primary cause of the scrapped parts.

3.3.2 Pareto Chart Results

Based on the data received from the FMEA table, five key failures were identified: Incorrect Collet Size, Wrong Beam Orientation, Incorrect Drill Size, Incorrect Program Input, and Wrong Beam Size, caused 87% of the defects that can cause scrap and rework.



Category Total
Incorrect Drill Size 42
Wrong Beam Size 28
Wrong Beam Orientation 8
Incorrect Program Input 70
Incorrect Collet Size 42

Figure 4: Pareto Chart of Defects

4. Discussion

4.1 Interpretation of Results

The three proposed solutions are (1) conducting a red tag event to remove unnecessary tools and equipment; (2) implementing a labeling system with labeled drawers, tool-holder pots, and a standardized tool list visible to all operators; and (3) creating a standard operating procedure (SOP) to provide detailed, step-by-step instructions for performing tasks consistently, ensuring quality, safety, and compliance.

4.2 Implications

4.2.1 For Academia (Teaching and Research)

This study highlights the use of lean tools, such as 5S, OEE, and TPM, demonstrating their practical applications in industry. The integration of SIPOC diagrams, FMEA charts, and Root Cause Analysis enhances students' understanding of lean methodologies for real-world implementations.

4.2.2 Industry Practice

The 5S methodology (Sort, Set-in-Order, and Shine) improves workplace organization, while TPM and OEE calculations illustrate data-driven approaches to manufacturing efficiency and maintenance.

4.3 Limitations and Biases

During study, the operators, stakeholders, and researchers may have been biased about what should have been prioritized in our project scope. Below are examples of the research conducted.

4.3.1 Confirmation Bias

Confirmation bias occurred when the researchers focused on assumptions rather than data or alternative perspectives. This limited our understanding by disregarding input from others.

4.3.2 Measurement Bias

Measurement bias can occur if the data are incorrectly or inconsistently measured. Based on the limitations that were placed on the collection of data, the researchers had to use some averages and information found on the machine website.

4.3.3 Performance Bias

Performance bias may arise if operators alter their work pace when observing and skew data on standard operations. Additionally, researchers observing the entire cycle without a specific focus may prioritize different aspects, potentially overlooking critical information.

4.4 Suggestions for Future Research

Future TPM research should follow a structured approach, integrating routine maintenance for reliability, operator-assigned upkeep for efficiency, and proactive scheduling to minimize downtime. Predictive analytics can further optimize resources by anticipating failures. Applying the Plan-Do-Check-Act (PDCA) cycle ensures continuous improvement, data-driven decisions, and customer feedback integration to refine TPM strategies.

4.5 Conclusion

This study focused on implementing TPM and OEE strategies for the Bavius machine to improve

efficiency and reduce waste. Key recommendations include standardized maintenance schedules, improved operator workflows, and 5S practices to enhance organization and reduce downtime. Additional improvements involve optimizing workspace ergonomics and tool accessibility. The insights gained will support Spirit AeroSystems in enhancing machine performance through Lean methodologies.

5. Disclaimer Statements

Funding: None

Conflict of Interest: None

6. References

- [1] Hayat, Ahatsham & Shahare, Vivek & Sharma, Ashish & Arora, Nitin. (2023). Introduction to Industry 4.0. 10.1007/978-981-19-8730-4 2.
- [2] Gunawardana, Kennedy. (2010). Introduction of Advanced Manufacturing Technology: a literature review. Sabaragamuwa University Journal. 6. 10.4038/suslj.v6i1.1694.
- [3] Moru, Desmond & Agholor, Darlington & Imouokhome, Francis. (2021). Machine Vision and Metrology Systems: An Overview. International Journal of Data Science. 2. 77-84. 10.18517/ijods.2.2.77-84.2021.
- [4] Walker S. E. (2003). Active learning strategies to promote critical thinking. Journal of athletic training, 38(3), 263–267.
- [5] Elaine H.J. Yew, Karen Goh, Problem-Based Learning: An Overview of its Process and Impact on Learning, Health Professions Education, Volume 2, Issue 2, 2016, Pages 75-79, ISSN 2452-3011, https://doi.org/10.1016/j.hpe.2016.01.004.
- [6] Zhang, Q., Irfan, M., Khattak, M. A. O., Zhu, X., & Hassan, M. (2012). Lean Six Sigma: a literature review. Interdisciplinary Journal of Contemporary research in business, 3(10), 599-605
- [7] Condliffe, B. (2017). Project-Based Learning: A Literature Review. Working Paper. MDRC.
- [8] Cronemyr, P. (2007). DMAIC and DMADV-differences, similarities, and synergies. International Journal of Six Sigma and Competitive Advantage, 3(3), 193-209.
- [9] García-Alcaraz, J. L., Diaz Reza, J. R., Sanchez Ramirez, C., Limon Romero, J., Jimenez Macias, E., Lardies, C. J., & Rodriguez Medina, M. A. (2021). Lean manufacturing tools applied to material flow and their impact on economic sustainability. Sustainability, 13(19), 10599
- [10] Chan, F. T. S., Lau, H. C. W., Ip, R. W. L., Chan, H. K., & Kong, S. (2005). Implementation of total productive maintenance: A case study. International journal of production economics, 95(1), 71-94.
- [11] Ng Corrales, L. D. C., Lambán, M. P., Hernandez Korner, M. E., & Royo, J. (2020). Overall equipment effectiveness: Systematic literature review and overview of different approaches. Applied sciences, 10(18), 6469.
- [12] Stephen, P. (2004). Application of DMAIC to integrate lean manufacturing and six sigma (Doctoral dissertation, Virginia Tech).

The Journal of Management and Engineering Integration (JMEI) © 2025 by AIEMS Inc., is licensed under CC BY 4.0. To view a copy of this license, visit https://creativecommons.org/licenses/by/4.0/

DOI: 10.62704/10057/31198

ANALYSIS OF WILDLIFE STRIKES USING CONTROL CHARTS

Saleh Ateiwi¹
Hamzah Mousa¹
Gamal Weheba¹

¹ Wichita State University

sxateiwi@shockers.wichita.edu

Abstract

Strikes between wildlife and aircraft pose many risks to aviators, aircraft, and passengers. Data on reported strikes in the US within the past twenty-five years is available from the Federal Aviation Administration (FAA) Wildlife Strike Database. Employing appropriate control charts for analyzing such data can expose temporal patterns and contributing factors, providing insights for effective mitigation strategies. This paper presents control charting techniques suited for the data reported, aiming to inform policy decisions and enhance air travel safety.

Keywords: Wildlife Strikes, Data Stratification, Control Charts, Multi-Stream Processes.

1. Introduction

Beyond the safety implications, wildlife strikes carry substantial economic costs due to aircraft repairs, flight delays, and wildlife management expenses. The combination of high incident frequency and potential severity makes wildlife strike analysis a critical area of study for aviation safety management. Just like any process, air travel is subject to variation over time. As noted by Montgomery (2019), control charts have been successfully used to monitor process variation over time. These charts help differentiate between causes of variation. In any process, variation can be attributed to random or assignable causes. Assignable causes signify the presence of external factors affecting the process. Random causes are inherent in the process and are difficult to track.

This research was inspired by the analysis presented by Alharbi et al. (2024). They considered Wildlife Strikes in the U.S. from 2013-2022. The analysis was aimed at understanding the wildlife strike risks by assessing how often strikes result in varying degrees of damage. They performed a one-way analysis of variance and Tukey's test to determine if there were any differences in the mean rate of wildlife strikes by damage category. They reported that in all five damage categories, there was a decrease in reports during 2020, which they attributed to the decrease in the number of operations during the COVID-19 pandemic. The following section presents a brief review of related studies. An overview of the wildlife strike data is presented in Section 3. Statistical analysis and control charts are included in Sections 4 and 5. Most of the statistical analyses were performed using the STATGRAPHICS software (Statpoint Technologies Inc., Centurion version 19.6, 2024). Section 6 presents a discussion while concluding remarks with suggestions for future research are presented in Section 7.

Submitted: June 21, 2025 Revised: September 4, 2025

2. Literature Review

Since 1990, the FAA initiated a Database containing records of reported wildlife strikes to better understand the scope and nature of the problem. It is claimed that wildlife strikes with aircraft are increasing in the United States and elsewhere. There appears to be an increasing interest in collecting and analyzing wildlife strike data. These strikes were found to be triggered by animal migration patterns, environmental changes, and administrative mandates. Dolbeer et al. (2000) provided a statistical study showing a ranking of 21 wildlife species or species groups based on actual wildlife strike data from the FAA's National Wildlife Strike Database (1991-1998). Their findings show that deer, vultures, and geese posed the highest risk to aviation, while smaller birds like swallows and sparrows were the least hazardous. A related study by Mendonca et al. (2024) employed a descriptive data analysis to offer an intuitive and comprehensive overview of wildlife strikes at the 30 busiest airports in the U.S. from 2020 to 2022. Their findings support the normalization of strike data using flight volume (Wildlife Strike Index). They also observed increased strike severity during and after the COVID-19 period. Crain (2015) analyzed carnivore incidents with U.S. civil aircraft using data from the FAA's National Wildlife Strike Database (1990-2012). He employed simple linear regression to assess annual trends and chi-square tests to compare incidents by month, time of day, and flight phase. His results revealed a 13.1% annual increase in carnivore strikes, with coyotes (Canis latrans) as the most frequently struck species. Landing roll and takeoff run were found to be the most hazardous flight phases. Most incidents occurred at night during the autumn (August-November), highlighting seasonal variations in strike risks. Despite \$7 million in estimated damage to aircraft, most incidents resulted in no structural harm.

Ferra et al. (2021) analyzed the wildlife strike data from 2015-2019 across five U.S. regions and found significant geographical variation in strike frequency, with the highest rates in the western mountainous region and Texas. They utilized an analysis of variance (ANOVA) procedure and regional comparison to highlight how local environmental factors can shape strike exposure. De Tella and Mendonca (2022) investigated Part 139 Airports in Florida's wildlife strikes and damaging strikes from 2011 through 2020. They reported that most accidents occurred during the arrival phase. They divided the year into seasons (winter, spring, summer, fall) that have start dates and durations, then ran a non-parametric (Kruskal-Wallis H) test to examine differences between each season. They reported that 2019 shows the highest number of wildlife strikes and that it was likely to be higher in summer and fall. Ochs and Mendonca (2022) utilized a cloud-based mapping platform (ArcGIS) to analyze wildlife strike risks at Florida's 26 Part 139 airports (2012-2021). They created an interactive map that categorized airports by the percentage of damaging strikes (3-38%). The study found that most strikes occurred during the approach phase and below 500 ft. Orlando International recorded the highest volume (1,641 strikes) but Vero Beach (37% damaging) and Naples (34%) posed the greatest relative risk. By visualizing regional risk factors, the results complemented their national wildlife strike analyses.

Parsons et al. (2022) employed interrupted time series analysis with an Autoregressive Integrated Moving Average (ARIMA) model to assess the impact of COVID-19 on wildlife strike rates in the U.S. from 2014 to 2020. Using pre-pandemic data (2014–2019), they forecasted expected strike rates and compared them to actual rates during the pandemic (March–December 2020). The results revealed that wildlife strike rates exceeded the model's 95% confidence interval in 5 out of 10 months analyzed, particularly during spring and summer 2020. They concluded that the COVID-19 pandemic coincided with the adverse deviation in wildlife strike rates, validating industry warnings about increased risks during reduced air traffic.

Altringer et al. (2023) used fixed-effects negative binomial regression to analyze wildlife strike

data during the COVID-19 pandemic. They found that although total air traffic and the absolute number of strikes declined, the wildlife strike rate increased significantly from May to September 2020, particularly in June. This rise was linked to reduced air traffic volume, which likely made airport environments more attractive to wildlife. Their findings highlighted that lower human activity can unintentionally increase collision risk, especially during seasons of high wildlife activity. Alhumaidi et al. (2023) employed a one-way ANOVA and Tukey's pairwise comparison tests to analyze wildlife strike reports by phase of flight in the U.S. from 2010 to 2019. The results revealed a statistically significant difference in strike frequency across flight phases, with the approach phase having the highest mean strikes and parked aircraft the lowest. They stated that "The approach phase was different from all other phases (p-value < 0.001)".

3. Wildlife Strike Data

Wildlife strike data was downloaded from the FAA (2024) Database for all strikes in the US from 2000 to 2024. Since strike reporting is voluntary, the data represents only the information submitted by professionals such as pilots, airport operations, and maintenance personnel. Strike data is recorded in chronological order with indications of the strike date and time, airport, airline, aircraft, engine type, damage, and species. The Database includes 285,576 reported wildlife strikes from 2000 to 2024. The resulting aircraft damage is reported in one of four categories: destroyed, substantial, minor, and undetermined. The annual pattern is shown in Figure 1. As shown, starting in 2016, there are more annual wildlife strikes reported in the undetermined damage category in the Database. In addition, initial analysis of data revealed that in a total of 285,576 reported strikes, only 4,392 included the cost of repair. In this research, only the subset including repair costs is considered.

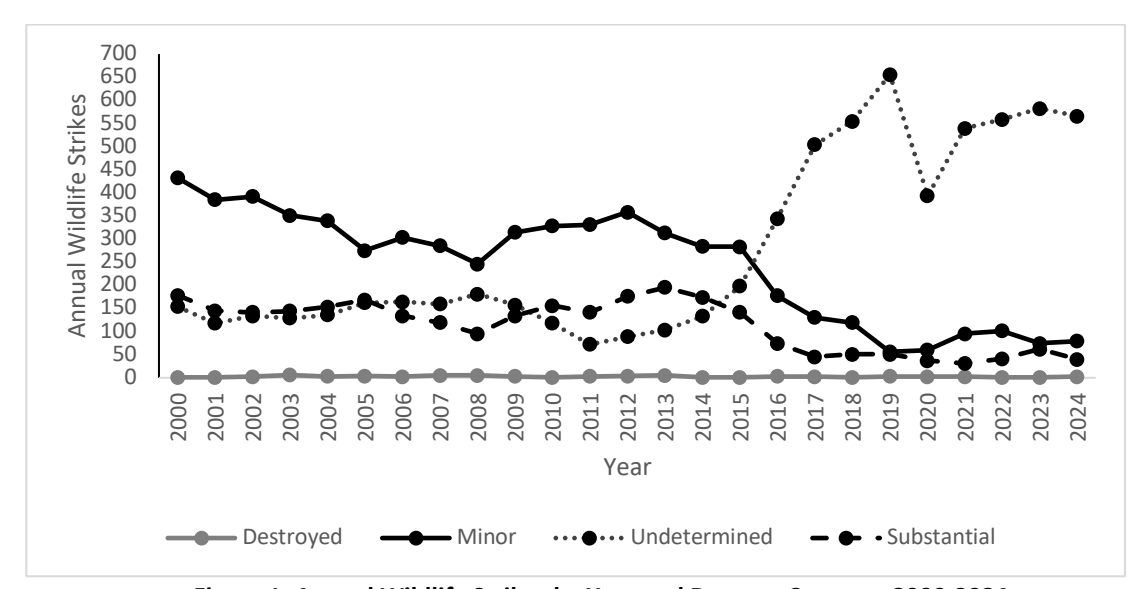


Figure 1: Annual Wildlife Strikes by Year and Damage Category 2000-2024

An examination of the number of strikes with reported repair costs reveals a clear cyclic monthly pattern with high levels of correlation as shown in Figure 2. This is a typical behavior of a multi-stream process. Due to the wildlife migration pattern, each month will be considered as a stream.

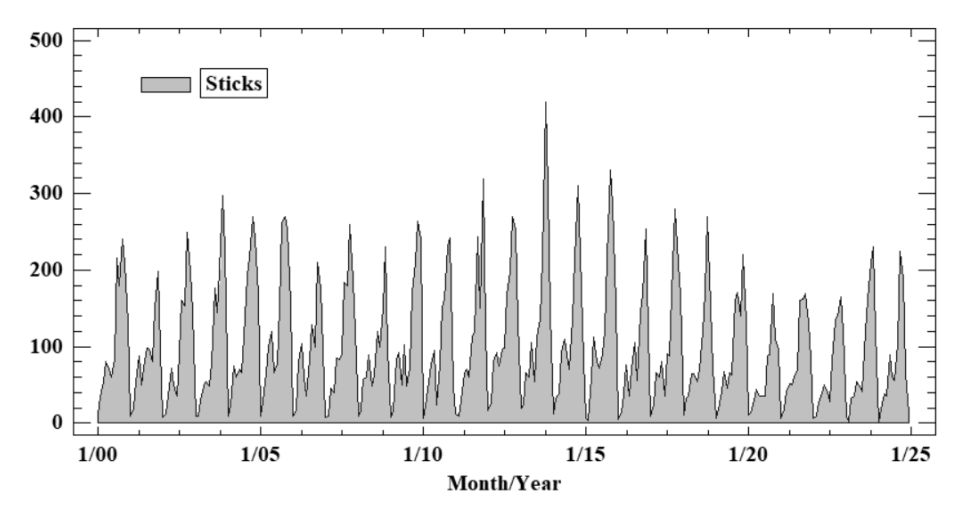


Figure 2: Wildlife Strikes with Reported Repair Cost by Month (2000-2024)

4. Analysis Of the Number of Strikes

In meeting the underlying assumptions of control charts discussed in Ott and Snee (1973), Nelson (1986), Wheeler and Chambers (2010), monthly data can be analyzed using separate charts. With each month representing an area of opportunity (inspection unit), control charts for the number of strikes recorded were constructed. As an example, Figure 3 depicts the c-chart for the number of strikes reported during the month of January. As shown, the chart suggested a significant increase in the number of reported strikes in 2013. This type of change signals the presence of an assignable cause and should be investigated. However, the overall pattern suggests a reduction in the average count following 2015. Figure 4 presents the reported counts with two sets of limits. The data appears well within their respective limits, indicating a reduction in the average from 10.3 to 7.5 strikes following 2015. Changes in relevant factors leading to such a reduction need to be identified.

To account for the variability in the number of flights affected (sample size), a chart for the average number of strikes per aircraft (u-chart) was used. The u-chart for the reported strikes in January is shown in Figure 5. Here, the averages are calculated based on the reported number of flights resulting in variable width control limits. Once again, pattern analysis confirms a significant reduction in the average after January 2015. Changes leading to such a significant decrease in reported strikes need to be identified and credited for improving air travel safety within the U.S.

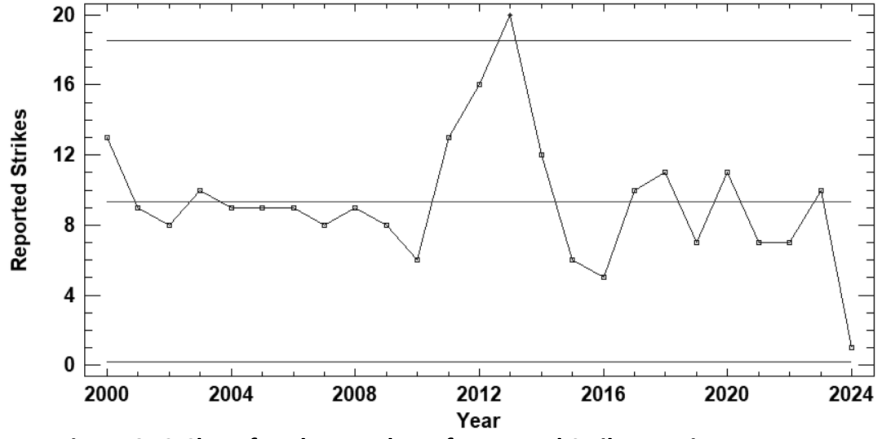


Figure 3: C-Chart for The Number of Reported Strikes During January

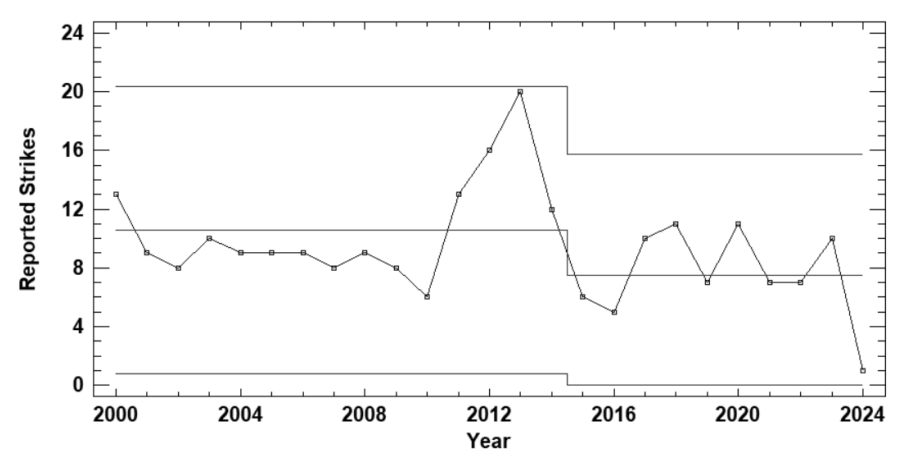


Figure 4: C-Chart for The Number of Reported Strikes with Two Sets of Limits.

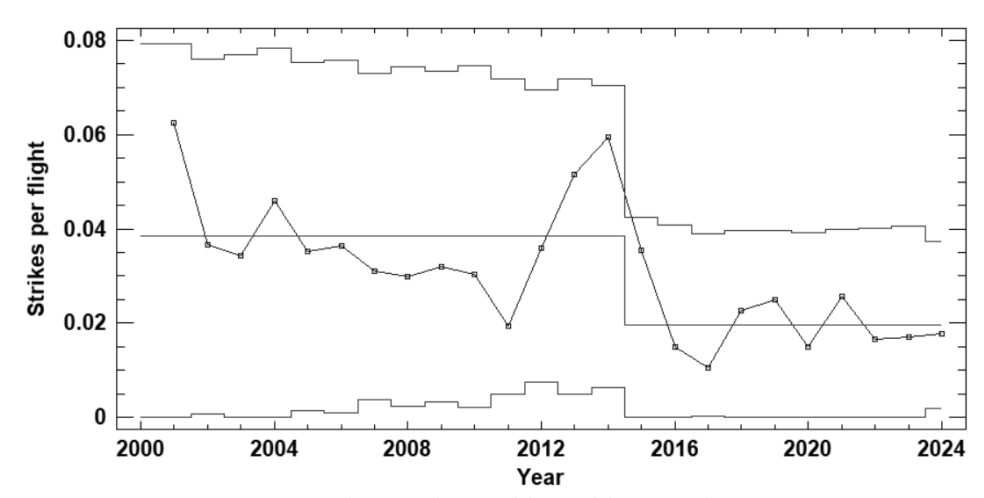


Figure 5: U-Chart with Variable Width Control Limits.

Since reported strikes have different consequences, monthly data can be analyzed using a demerit value chart [Montgomery (2019)]. Here, the A-E classification shown in Table 1 was utilized. This classification is used in mishap investigation [DOD (2020)]. Depending on the reported repair cost, each strike was classified, and a corresponding weight was assigned to each. An example of the chart for January is shown in Figure 6. This chart was constructed using Microsoft Excel. Variable width control limits were used to account for the variability in the number of flights. As shown, the demerit value calculated for 2011 exceeds the upper control limit. This can be attributed to a relatively large number of reported counts with classes A and B.

Table 1: Mishap Classification and Weights

Mishap Class	Total damage	Weight
Α	\$2,500,000 or more and/or aircraft destroyed	100
В	\$600,000 or more but less than \$2,500,000	50
С	\$60,000 or more but less than \$600,000	20
D	\$25,000 or more but less than \$60,000	5
Е	\$1 or more but less than \$24,999	1

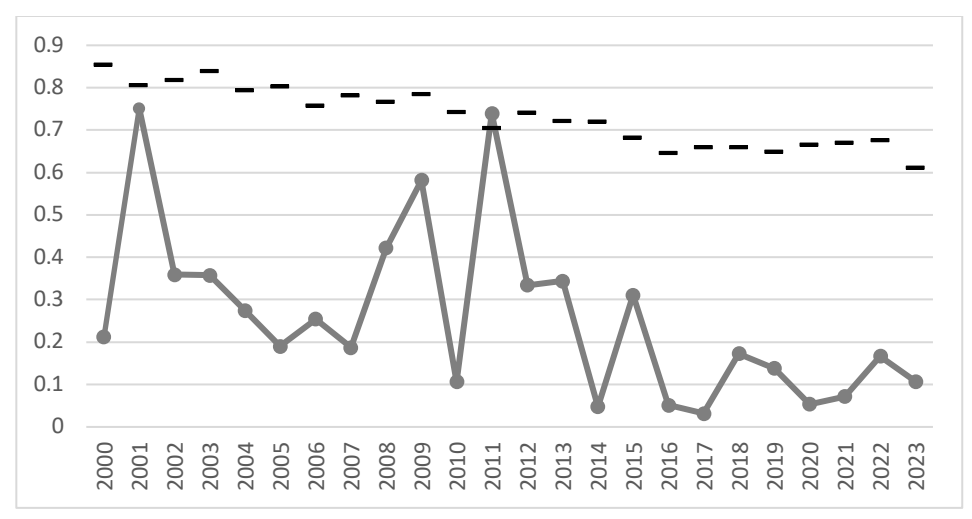


Figure 6. Demerit Value Chart for January.

5. Analysis of Repair Costs

Reported repair costs can be analyzed using control charts for variables [Montgomery (2019)]. A plot of the reported costs over time did not indicate cycles or trends. As such, a control chart for individual measurements was considered. However, an examination of the data indicated that the reported costs are not normally distributed. This is evident from the normal probability plot shown in Figure 7. Utilizing the distribution fitting function in Statgraphics, the cost data were found to follow a lognormal distribution with 3 parameters (p-value = 0.93). Estimated parameters of the fitted distribution are shown in Table 2.

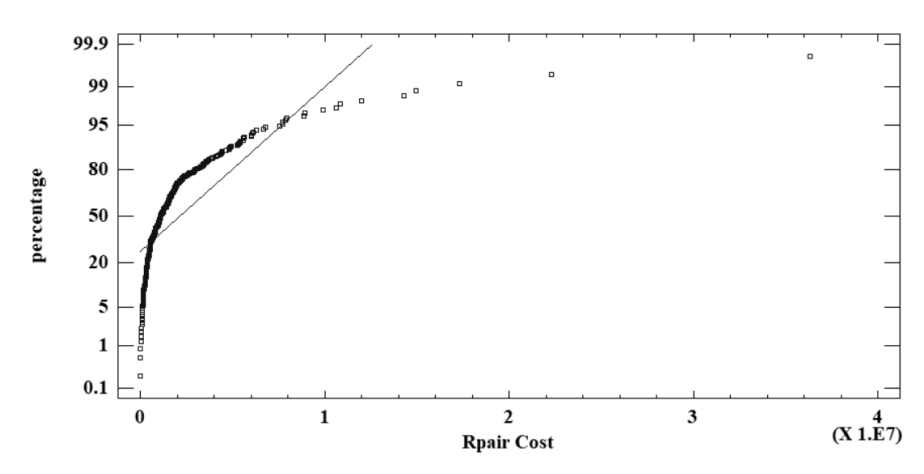


Figure 7. Normal Probability Plot of Reported Repair Costs

Table 2. Estimated parameters of the fitted distributio	n
---	---

Parameter	Estimate	Stnd. Error	Lower 95% CL	Upper 95% CL
Mean	2.21E+06	198685	1.82E+06	2.60E+06
Std. Dev.	3.79E+06	603744	2.78E+06	5.18E+06
Threshold	-27431.1	19278	-65215.4	10353.3
*Location	13.9431	0.075129	13.7959	14.0904
*Scale	1.16401	0.0620588	1.04851	1.29222

* Alternative parameterization

Values of 0.135 and 99.865 percentiles were obtained from the fitted model as \$7,153 and \$37,296,500. These values include 99.73% of the fitted distribution and hence were used as probability limits on the chart shown in Figure 8. As shown, the reported repair costs appear to be stable at an average of \$2,209,470 per month over the study period.

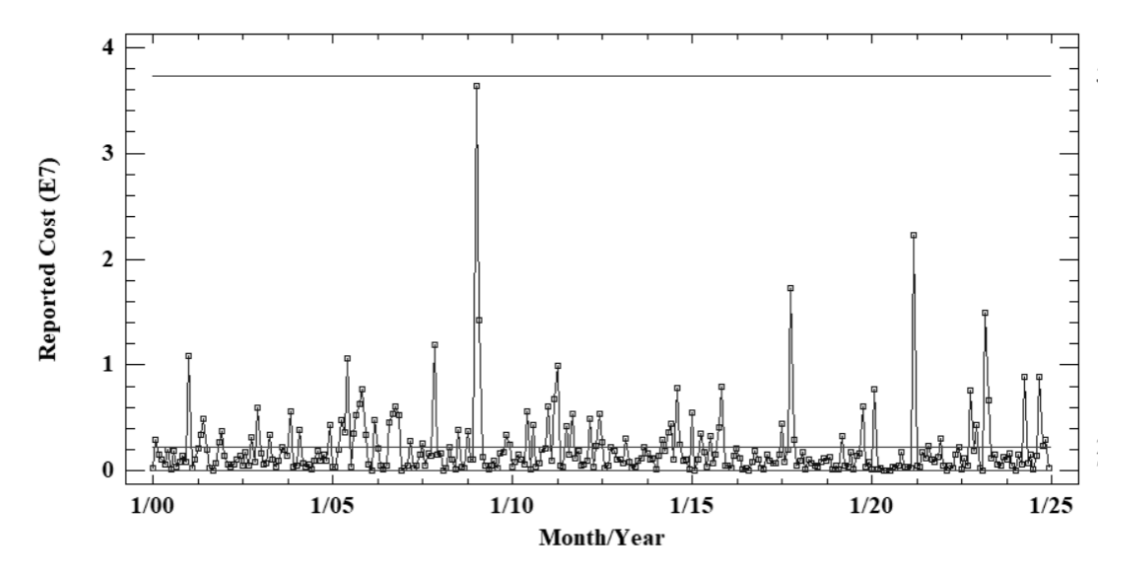


Figure 8. Control Chart for Reported Repair Costs

6. Discussion

The efforts made by the FAA to allow pilots, airport officials, and others to report wildlife strikes have motivated researchers to study the mutual interactions between air travel activities and the risk of wildlife strikes. However, the data is not complete and represents a sample of the population of all the wildlife strikes that have occurred. A significant proportion of strikes were reported with undetermined damage. This is the only count that appears to be increasing. This research focused on complete data that provides the associated repair costs. It should be noted that when the charts for attributes presented in Section 4 are used, values below the lower control limits may not represent a real reduction in the number of strikes. These may simply result from a lack of reporting. However, consistent trends and/or shifts in the average would suggest an increase or decrease in the reported strikes.

The statistical analyses presented in Section 5 have led to a better characterization of the distribution of repair costs. Based on the chart in Figure 8, a reliable estimate of the average reported repair cost was obtained. Another possible approach for constructing the chart would require transforming (x) the repair cost data. A power transformation in the form $y = x^0.1$ would allow the construction of a control chart for values of y without violating the normality assumption. However, working with the chart for x in Figure 8 is more convenient as it allows researchers to plot the actual reported costs over future periods.

7. Conclusions

Control charts are more suited for analyzing wildlife strike data than the descriptive methods

commonly used in related studies. This paper presented a few examples to demonstrate the ability of control charts to distinguish between apparent and real differences. Control charts help identify reports that warrant further investigation to provide a better understanding and quantification of the risks involved. One of the advantages of utilizing control charts is to help researchers identify real changes and ask the correct questions. As was pointed out in Section 4, only one point on the demerit value chart in Figure 6 needs to be investigated. A study of the pattern identified in Figures 4 and 5 may result in a better understanding of the factors affecting the risk of strikes. This can be confirmed as more data becomes available. Based on the statistical analysis of the subset of the wildlife strikes considered, there is an indication of a substantial decrease in the average number of strikes following 2015. The average repair costs appeared to remain at \$2,209,470 per month over the study period. The analysis does not support claims of significant changes during the COVID-19 pandemic (2020-2021). These authors are working on the development of a modified version of group control charts (GCC) originally proposed by Boyd (1950). A single GCC may be utilized to monitor the reported counts over the 12 months (streams). Only values of the maximum and minimum counts would be plotted on this type of control chart. As was discussed by Ribas and Weheba (2024), the control limits need to be corrected to account for the number of streams and the level of correlation between them. Similar studies of wildlife-vehicle collision data will be presented. It is hoped that this work will draw the attention of researchers to the ability of control charts to analyze data with due consideration of the sequence by which the data were reported.

8. Disclaimer Statements

Funding: None

Conflict of interest: None

9. References

- Alharbi, M., Meechan, C., Sharma, V. and Wheeler, B., (2024). Wildlife Strikes by Damage Category in the U.S. from 2013-2022. Proceedings of the IEMS 2024 Conference, pp. 63-70, DOI: 10.62704/10057/28723
- Alhumaidi, S. H., Alruwaili, I. Y., and Wheeler, B. E. (2023). U.S. Wildlife Strikes by Phase of Flight. The Journal of Management and Engineering Integration, Vol. 16, No 1, pp. 48-56. DOI: 10.62704/10057/25980
- Altringer, L., SC, M., Kougher, J., Begier, M., and S. S. (2023). The impact of the COVID-19 pandemic on wildlife—aircraft collisions at US airports. Sci Rep, Vol. 13, No. 1, pp. 1-11, DOI: 10.1038/s41598-023-38451-9
- Boyd, D. (1950). Applying the Group Control Chart for x and R. Industrial Quality Control, Vol. 3, pp. 22-25 Craina, A. R., Belantb, J. L., and DeVault, T. L. (2015). Carnivore Incidents with U.S. Civil Aircraft. Transportation Research Part D, pp. 160-166, DOI: 10.1016/j.trd.2014.12.001
- De Tella, T. D., and Mendonca, F. A. (2022). Safety Management of Wildlife Hazards to Aviation: An Analysis of Wildlife Strikes in Part 139 Airports in Florida 2011–2020. Journal of Aviation Technology and Engineering, Vol. 11, No 2, pp. 18-29, DOI: 10.7771/2159-6670.1257
- DOD (2020), Current Mishap Definitions, https://navalsafetycommand.navy.mil/Reporting-lnvestigations/Current-Mishap-Definitions, visited March 6, 2025.
- Dolbeer, R. A., Wright, S. E., and Cleary, E. C. (2000). Ranking the hazard level of wildlife species to aviation. Wildlife Society Bulletin, Vol. 28, No. 2, pp. 372-378, https://www.jstor.org/stable/3783694
- FAA (2024). Wildlife Strike Database. Federal Aviation Administration. Retrieved February 15, 2025, from https://wildlife.faa.gov/search
- Ferra, G., Alghamdi, H., Wheeler, B. E., and Li, T. (2021). Comparing the Frequency of Reported Wildlife Strikes by Region in the United States. The Journal of Management and Engineering Integration, Vol. 14, No. 1, pp. 37-45, DOI: 10.62704/10057/24767
- Mendonca, F. A., Huang, C., Keller, J., and Anderson, C. (2024). Trends in Wildlife Strikes to Aircraft in Brazil.

- Journal of Aviation Technology and Engineering, Vol. 13, No. 2, pp. 22-49, DOI: $\underline{10.7771/2159-6670.1321}$
- Montgomery, D. C. (2019), Introduction to Statistical Quality Control, 7th edition, John Wiley & Sons, Inc., New York, NY
- Nelson, L. S. (1986), "Control chart for multiple stream processes", Journal of Quality Technology, Vol. 18, No. 4, pp. 255-256. DOI: 10.1080/00224065.1986.11979024
- Ochs, L. P., and Mendonca, F. A. (2022). High-Risk Wildlife Strike Regions: An In-depth Visual High-Risk Wildlife Strike Regions at and Around Part 139 Airports in Florida. Beyond, Vol. 6, No. 1, pp. 1-8, https://commons.erau.edu/beyond/vol6/iss1/7
- Ott, E. R., and Snee, R. D. (1973), "Identifying useful differences in a multiple-head machine", Journal of Quality Technology, Vol. 5, No. 2, pp. 47-57, DOI: 10.1080/00224065.1973.11980575
- Parsons, D., Malouf, M., and Martin, W. (2022). The impact of COVID-19 on wildlife strike rates in the United States. Human-Wildlife Interactions, Vol. 16, No. 3, pp. 433-441, DOI: 10.26077/c36e-1bfd
- Ribas, C., and Weheba, G. (2024), Control Limits for Monitoring the Average of Correlated Streams, Proceedings of the 6th International Conference on Quality Engineering and Management, pp. 798-813, https://hdl.handle.net/10057/27962
- Wheeler, D. J., and Chambers, D. S. (2010). Understanding Statistical Process Control, 3rd edition, SPC Press, Knoxville, TN.

The Journal of Management and Engineering Integration (JMEI) © 2025 by AIEMS Inc., is licensed under CC BY 4.0. To view a copy of this license, visit https://creativecommons.org/licenses/by/4.0/

A SOFT ACTOR-CRITIC APPROACH FOR ENERGY-CONSCIOUS FLEXIBLE JOB SHOP SCHEDULING INCORPORATING MACHINE USAGE CONSTRAINTS AND JOB RELEASE TIMES

Saurabh Sanjay Singh ¹
Deepak Gupta ¹
¹ Wichita State University
sxsingh28@shockers.wichita.edu

Abstract

According to the International Energy Agency, manufacturing accounts for 30% of global energy consumption, making job shop scheduling a critical lever for reducing energy consumption. In the flexible job-shop scheduling problem (FJSP), each job consists of a sequence of operations, each of which can be processed on one of several eligible machines, and the scheduler must decide both which machine to assign to each operation and the order in which operations are processed on each machine. The Energy-Conscious Flexible Job-Shop Scheduling Problem with Release Times and Machine Usage constraints (EC-FJSP-RTMU) extends the traditional FJSP by (1) embedding a detailed multi-component energy model that quantifies the energy consumption of processing, setup, idle time, transportation, machine startup, and common facility operations, and (2) explicitly enforcing job release times and machine-usage constraints. We address this enriched scheduling problem using the Soft Actor-Critic (SAC) reinforcement learning algorithm, which learns policies to minimize total energy consumption subject to all timing and usage constraints. The SAC agent is trained in a workshop simulation featuring parallel-machine slots, shutdown policies and machine warm-up/cool-down thermal dynamics. Benchmark experiments on eighteen instances show that the SAC agent consistently produces constraint-compliant feasible schedules in under 0.42 seconds.

Keywords: Flexible Job-Shop Scheduling, Energy-Conscious Scheduling, Soft Actor-Critic; Reinforcement Learning, Job Release Times, Machine Usage Constraints

1. Introduction

Manufacturing accounts for roughly 30% of global final energy use, the single largest end-use sector and thus even small gains in efficiency can yield substantial cost and emissions reductions (Fernando et al., 2021; Nurdiawati & Urban, 2021; Sechi et al., 2022). Although high-efficiency machines help, many small and medium enterprises cannot finance major capital outlays. Therefore, job-routing and sequencing optimization offers a more accessible lever. Careful scheduling can lower idle power, smooth peak demand charges, and cut total kilowatt-hours without changing physical assets, making it an appealing path to better energy performance.

Building on this opportunity, several studies have demonstrated the impact of smarter scheduling under time-of-use tariffs. For example, Park and Ham (2022) achieved a 6.9% reduction in job-shop electricity costs using integer and constraint-programming models. Meanwhile, Rakovitis et al. (2022) reported energy savings of 13.5% compared to recent benchmarks, and up to 43.1% versus a gene-expression heuristic. Other approaches also show promise: Meng et al. (2019)

Submitted: June 18, 2025 Revised: September 5, 2025 developed mixed-integer formulations and Wei et al. (2022) proposed multi-objective heuristics that adjust machining speed and blend particle-swarm with genetic algorithms. Most of these studies assume that every job is ready at time zero and impose no limits on daily machine hours, which may limit their applicability in real-world shop floors.

To capture both machine assignment and sequencing in one framework, flexible job-shop scheduling problem (FJSP) generalizes the classical job-shop model by allowing each operation to run on any eligible machine. Even though the classical job-shop is NP-hard, the flexible version inherits that difficulty and becomes more challenging owing to routing freedom (Fattahi et al., 2007; Jiang et al., 2023). Every instance therefore couples a routing choice that assigns a machine to each operation with a sequencing choice that orders jobs over various machines, and this combined decision space grows exponentially with the numbers of jobs, operations, and machines (Dauzère-Pérès et al., 2023). Exact optimization works only for very small instances, so larger cases rely on heuristic or meta-heuristic methods.

Practical plants add two further realities. First, Jobs need to be started at different times throughout the day because each order has a specific release time, which is the earliest point when raw materials or upstream parts become available, and no operation can begin before that time. Second, many factories impose daily limits on machine run-time to respect labor shifts, preventive maintenance, and/or operational contracts. Recent studies address parts of this picture: simulation work explores dispatch rules that consider job release information (Thenarasu et al., 2022), and several algorithms that incorporate machine-availability windows address total energy consumption under variable processing times (Zhu & Zhou 2020; Shao et al., 2024a; Wang et al., 2022). Yet few investigations treat energy consumption together with both job release times and explicit daily machine usage ceilings.

This study contributes in two ways:

- 1. Problem formulation: Introduces the Energy-Conscious Flexible Job-Shop Scheduling Problem with Job Release Times and Machine Usage Constraints (EC-FJSP-RTMU), an enriched FJSP variant that minimizes total energy consumption while respecting job release times and daily machine usage limits.
- 2. Solution and evidence: Benchmark experiments show that a Soft Actor-Critic solver generates feasible schedules in under one second that satisfy all release-time and usage constraints.

The rest of the paper is organized as follows. Section 2 reviews related work on energy-aware flexible job-shop scheduling. Section 3 develops our soft actor-critic—based scheduling methodology. Section 4 reports computational results on standard benchmarks and outlines future research directions.

2. Literature Review

Early studies that sought to minimize energy in the flexible job-shops relied on mixed-integer formulations. A multi-objective mixed-integer program for a flexible assembly environment exactly models total flow time, defined as the sum of the durations from each job's release to its completion, together with energy consumption; however, solution times rise sharply once the instance exceeds a moderate size, so the model is usually embedded in a metaheuristic rather than solved directly (Hu et al., 2024). A two-stage model that adds robustness for machine breakdowns and job insertions confirms the same pattern: exact optimization yields precise schedules but must eventually hand control to advanced heuristics when disruptions enlarge the search space (Zhao et

al., 2024). These findings establish both the expressive power of mixed-integer programming for flexible job-shops and its central limitation when the job-shop or its energy constraints lead to a relatively much larger solution space.

In response, researchers adopted hybrid and population-based research to preserve modelling richness while relaxing the requirement for guaranteed optimality. An evolutionary algorithm coupled with integer-programming neighborhoods was shown to succeed across thirty-three flexible job-shop benchmarks by trading exhaustive enumeration for guided exploration (Zhang et al., 2024a). A memetic framework extended this idea to distributed shops with breakdowns and machine-load balancing, maintaining quality across sixty instances that an exact solver could not tackle within practical time limits (Zhang et al., 2024b). Adaptive operator schemes in hybrid genetic search also yield improvements (Hao et al., 2025). In addition, reinforcement-guided parameter tuning cuts delay penalties and energy use in an industrial glass line production (Cui & Yuan, 2024). Swarm-based hybrids such as quantum particle swarm fused with variable-neighborhood search provide faster convergence and stable results in FJSP settings yet still depend on careful parameter calibration to reach their best performance (Xu et al., 2024).

Deep reinforcement learning now offers a data-driven alternative that learns dispatching directly from interaction with the shop environment. Value-based agents employing dueling double deep Qnetworks (DDQN) reduce overestimation bias and outperform rule-based benchmarks in dynamic flexible production lines (Yang et al., 2024). Actor-critic and proximal policy optimization (PPO) methods generalize these gains to distributed shops with transfers, consistently surpassing classical heuristics (Lei et al., 2024; Maharjan et al., 2024). End-to-end deterministic policy gradients enable mapping job-operation-machine tuples without handcrafted encoding (Shao et al., 2024b). Graph neural network embeddings further strengthen scalability, allowing multi-agent systems to coordinate resources in previously unseen shop sizes while respecting energy budgets (Huang et al., 2024; Pu et al., 2024). These agents embed release times, machine usage ceilings, and stochastic arrivals within the state representation or through invalid action masking, and they routinely narrow optimality gaps while reacting in real time to unexpected events (Wu et al., 2024; Yuan et al., 2025).

The search for scalable scheduling has therefore progressed from exact formulations through carefully tuned metaheuristics to reinforcement learning. Within the current generation of learning methods, the Soft Actor-Critic (SAC) algorithm stands out as a particularly well-suited engine for an energy-conscious flexible job shop. Its entropy regularized objective encourages broad exploration while maintaining learning stability, which has translated into faster convergence and superior control quality in other high dimensional dispatch and energy management tasks (Dong et al., 2024; Sun et al., 2025; Zhang et al., 2024c). SAC's continuous action space can represent start time offsets, machine usage constraints and load shifting decisions directly, avoiding the discretization that limits many earlier job shop agents. Comparative studies report that SAC adapts more readily than deep Q-networks (DQN) or PPO when environmental dynamics change, for example during traffic surges in autonomous-navigation benchmarks or sudden demand shifts in integrated-energy systems (Elallid et al., 2024; Dong et al., 2024). Consequently, SAC provides a natural foundation for an energy-aware FJSP scheduler that unifies release time feasibility, machine usage constraints, and energy minimization within a single learning framework.

3. Methodology

3.1 Operational Constraints of The Energy-Conscious Flexible Job Shop

The Energy-Conscious Flexible Job Shop Scheduling Problem with Job Release Times and Machine Usage constraints (EC-FJSP-RTMU) involves completing a finite set of independent jobs on a shop

floor with several machines. Each job is a sequence of operations, and each operation may run on any machine in its eligibility list. Every machine provides multiple slots, which are distinct resource units that let it execute operations in parallel, boosting throughput and flexibility.

Each operation may involve three sequential sub-tasks:

- Transportation, the time to move the job between machines.
- Setup, the time to configure the machine for that operation.
- Processing, the actual operation execution time.

The scheduler selects the machine and slot for each operation and schedules its start time, while meeting the following constraints:

- Precedence and sequencing: Each operation must adhere to its position in the job sequence, be assigned to exactly one machine and slot, and start only after its predecessor's setup and processing are complete; if it moves to a different machine, the required transport time must first elapse.
- Exclusive machine usage: A machine slot cannot host more than one setup or processing task simultaneously.
- Order of activities on machine change: Whenever an operation moves to a different machine, transport must occur first, then setup, and only after that may processing begin.
- Job release times: No operation may start before its job's specified release time.
- Machine usage limits: Each machine can be used for at most a fixed number of operations over the entire scheduling horizon.
- Idle time shutdowns: If a machine remains idle past a specified breakeven interval, it must be powered off and each machine has a fixed cap on how many shutdowns it can undergo during the scheduling horizon.
- Thermal transitions: Powering a machine on triggers a warm-up phase; powering it off triggers a cool-down phase.

We make the following assumptions about the system and resources: all machines are ready at time zero; an infinite fleet of identical transporters (each carrying one job at a time without interruption) is on hand; operations are non-preemptive (once started, they run to completion on their assigned machine and slot); and the scheduler has perfect information about every job and machine state at all times, with no machine breakdowns.

3.2 Energy Consumption Factors Considered for The Energy-Conscious Flexible Job Shop

Energy consumption is divided into six components:

- Setup energy consumption: energy consumed per unit time during reconfiguration activities (for example, tool changes or fixture adjustments) required before an operation can begin.
- Processing energy consumption: energy consumed per unit time while a machine is processing an operation.
- Transportation energy consumption: energy consumed per unit time when transferring operations between machines.
- Idle energy consumption: energy drawn by a machine that is switched on but not actively processing or setting up an operation.
- Turn-on energy consumption: one-time energy consumption each time a machine is switched on.
- · Common facility energy consumption: baseline energy overhead consumed per unit of

total makespan, representing the cost of keeping the job shop operational.

3.3 Proposed Scheduling Framework

Soft Actor-Critic (SAC) algorithm, adapted for the EC-FJSP-RTMU, is defined by the following components:

- Agent: Samples job to machine assignments to minimize energy usage and meet scheduling constraints.
- Action: Selects which operations to schedule on each machine slot at every decision step.
- Environment: Simulates job execution and machine behavior, updating states based on actions, constraints, and time progression.
- Reward: Provides feedback by penalizing energy consumption, machine inefficiency, and long job completion times.
- Observation: Returns the current system state, including remaining operation times, machine usage, and job progress.

A detailed breakdown of the agent's role in scheduling appears in Algorithm 1, and all notations and variables are listed in Table 1.

Table 1. Notations and Decision Variables

Notation	Description		
$\mathcal{M},\mathcal{J};\mathcal{K}_{j}$	Machines, jobs; operations per job		
\mathcal{S},\mathcal{F}	Schedule, completed operations		
τ, Δτ	Current time, time increment		
τ^{start} , τ^{end} , τ^{ready}	Operation timing		
h_i , d_i	warm-up, cool-down durations		
$ au_i^{idle}$	Idle duration start time		
η_i	State ∈ {off, heating, on, cooling}		
U_i, γ_i	Usage count and limit		
T_i^{on} , $ au_i^{max}$	Turn-on count and limit		
c_i^{on}	Turn-on energy consumption		
c_i^i, c_i^p, c_i^s	Idle, Processing, Setup Energy consumption		
c ^{trans} , c ^{facility}	Transportation, Common Facility Energy consumption		
p_{ijk}, s_{ijk}	Processing, Setup times		
$t_{i'i}$	Transportation times between machines		
r_{j}	Job Release times		
C_{jk}	Operation completion time		

Algorithm 1 SAC Agent driven scheduling framework

```
1: Initialize:
 2: Load trained policy \pi_{\theta}, \tau \leftarrow 0, \mathcal{E} \leftarrow 0
 3: \forall i \in \mathcal{M} : \eta_i \leftarrow \text{off}, U_i \leftarrow 0, T_i^{on} \leftarrow 0, h_i^{rem} \leftarrow 0, d_i^{rem} \leftarrow 0, \tau_i^{idle} \leftarrow \text{null}
 4: S \leftarrow \emptyset, F \leftarrow \emptyset
                                      Schedule and completed operations
 5: while \exists j \in \mathcal{J}, k \in \mathcal{K}_j : (j,k) \notin \mathcal{F} do
            Agent Decision:
            s \leftarrow (\eta, U, \mathcal{F}, \tau, \mathcal{E}, \mathsf{all}\ r_i)

⊳ Full state observation

 7:
            (i^*, s^*, j^*, k^*) \leftarrow \pi_{\theta}(s)
                                                             8:
            Machine State Management:
            if \eta_{i^*} = \text{off and } T_{i^*}^{on} < \tau_{i^*}^{max} then
10:
                 \mathcal{E} \leftarrow \mathcal{E} + c_{i^*}^{on}
                                                                                                              11:
                 \eta_{i^*} \leftarrow \text{heating, } h_{i^*}^{rem} \leftarrow h_{i^*}, T_{i^*}^{on} \leftarrow T_{i^*}^{on} + 1
12:
            else if \eta_{i^*}= on and \tau-\tau_{i^*}^{idle}>\frac{c_{i^*}^{on}}{c_{i^*}^2} then
13:
                 \mathcal{E} \leftarrow \mathcal{E} + (\tau - \tau_{i^*}^{idle})c_{i^*}^i
14:

    b Idle energy

                  \eta_{i^*} \leftarrow \text{cooling}, d_{i^*}^{rem} \leftarrow d_{i^*}
15:
            end if
16:
            Operation Scheduling:
17:
            if \eta_{i^*} = on and U_{i^*} < \gamma_{i^*} and slot s^* available then
18:
                  i' \leftarrow \mathsf{prev}(j^*)
                                                                                                     ▷ Previous machine
19:
                 t_{trans} \leftarrow I_{i^* \neq i'} \cdot t_{i'i^*}
                                                          Transport time if machine changed
20:
                  \tau^{ready} \leftarrow \max(C_{j^*,k^*-1},r_{j^*})
                                                                                    ▷ Precedence & release time
21:
                 \tau^{start} \leftarrow \max(\tau^{ready} + t_{trans}, \text{slot available time})
22:
                  if 	au^{start} valid then
23:
                       \tau^{end} \leftarrow \tau^{start} + s_{i^*j^*k^*} + p_{i^*j^*k^*}
24:
                       \mathcal{S}.\mathsf{append}([j^*,k^*,i^*,s^*,\tau^{start},\tau^{end}])
25:
                       \mathcal{E} \leftarrow \mathcal{E} + \underbrace{t_{trans}c^{trans}}_{\text{transport}} + \underbrace{s_{i^*j^*k^*}c_{i^*}^s}_{\text{setup}} + \underbrace{p_{i^*j^*k^*}c_{i^*}^p}_{\text{processing}}
U_{i^*} \leftarrow U_{i^*} + 1, \, \mathcal{F} \leftarrow \mathcal{F} \cup \{(j^*, k^*)\}
26:
27:
                  end if
28:
29:
            end if
            Time Advancement:
30:
            \Delta \tau \leftarrow \min(\text{operation completions}, h_i^{rem}, d_i^{rem})
31:
            \tau \leftarrow \tau + \Delta \tau
            Update \eta_i,\,h_i^{rem},\,d_i^{rem},\,\tau_i^{idle} for all machines
33:
34: end while
35: \mathcal{E} \leftarrow \mathcal{E} + \tau \cdot c^{facility}
                                                                                           Common facility energy
36: return S, \mathcal{E}, \tau
```

Algorithm 1. Scheduling Framework

4. Computational Results

To evaluate the SAC over the EC-FJSP-RTMU, we tested 18 benchmark instances from Dauzère-Pérès and Paulli (2025). We extended each instance to include energy related parameters:

processing energy consumption (EC) of up to 8 units/time, setup EC of up to 3.6 units/time ($1.2 \times idle$), transporter EC of 3 units/time, common facility EC of 10 units/time, machine turn-on EC of 60 units, machine idle EC of 3 units/time, breakeven time of 20 time units, heat-up and cooldown times of 16 time units each, a turn-off limit of 3/machine, and 2 slots per machine.

We enforce the machine usage constraint as:

$$Machine_usage_constraint = \left[\frac{Total\ Operations\ Count}{Machine\ Count} \times Usage\ Slack\ \right]; Usage\ Slack = 1.5$$

and we assign job release times by sampling each release time independently from the uniform distribution over $[0, W_{\text{max}}]$:

$$t_i \sim \mathcal{U}(0, W_{max}), \quad i = 1, \dots, N_{job}$$

where N_{job} is the number of jobs, and

$$W_{max} = \max_{J} \sum_{O \in O_{J}} \min_{m} P_{J,o,m}$$

is the maximum, over all jobs J, of the sum of each operation's minimum processing time on any machine.

The benchmark sets consist of instances of size 10×5 , 15×8 , and 20×10 (number of jobs × machines). They were chosen because these moderate yet varied dimensions where each job has more operations than machines, forcing sequential routing and heterogeneous machine eligibility and processing-time variation make for a reproducible but challenging suite. Our SAC-based agent produced feasible schedules for every instance (adhering to energy, machine-usage, and job-release-time constraints) in under 0.42 seconds per run. The complete results are in Table 2.

CPU **Total Energy** Instance Consumption (Seconds) 01a 169,600 0.1130 02a 171,689 0.2177 03a 164,214 0.0998 164,899 04a 0.0999 05a 159,892 0.1228 164,497 06a 0.0880 07a 220,327 0.1948 08a 206,473 0.1570 230,228 0.1509 09a

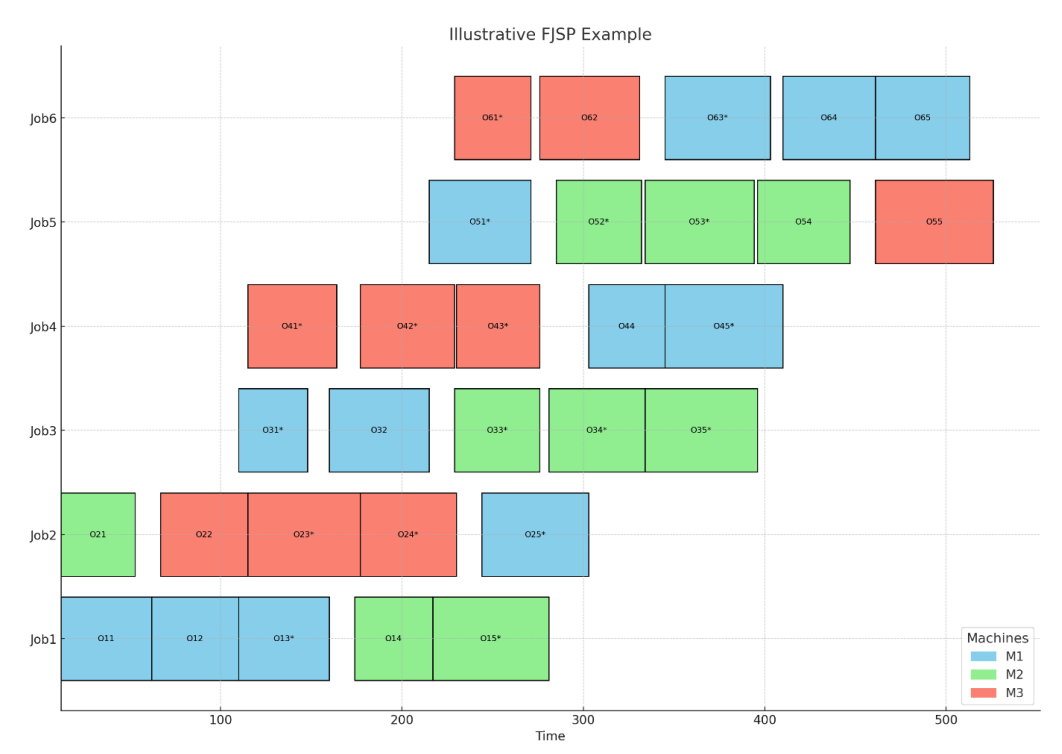
Table 2. Benchmark Instance Results

Instance	Total Energy	CPU	
ilistance	Consumption	(Seconds)	
10a 208,462		0.1878	
11a	212,702	0.1439	
12a	219,030	0.1534	
13a	258,387	0.2953	
14a	248,869	0.2284	
15a	264,704	0.2145	
16a	248,310	0.4117	
17a	238,622	0.2487	
18a	265,704	0.2078	

To complement the benchmark results and offer a more intuitive understanding of our approach to action, we present a focused example on a custom FJSP instance. This scenario is designed to illustrate the system's scheduling behavior in a controlled yet representative setting.

This illustrative example features a custom FJSP instance with 8 jobs and 3 machines, each job comprising 5 operations with durations ranging from 7 to 26 time units. The resulting schedule, shown in the Gantt chart in Figure 1, satisfies all energy, machine usage, and job release time constraints. The solution completes all jobs in 526 time units, demonstrating a responsive and

energy-aware scheduling strategy. Jobs begin processing promptly upon release, while machine usage remains within allowed limits. Energy consumption is distributed across six categories: 2,544 units for setup through consolidated preparations, 2,520 units for processing via efficient machine loading, and 336 units for transportation through optimized routing. Idle energy is minimized to 158 units via controlled machine states, with 90 units attributed to turn-on events and 5,260 units to facility-wide baseline consumption. The result reflects a well-balanced production plan that meets operational goals while managing energy consumption effectively.



*The Schedule Adheres to All Energy, Machine Usage, And Job Release Time Constraints.

Figure 1. Gantt Chart for The Illustrative Instance With 8 Jobs And 3 Machines.

Future research could extend our SAC-based EC-FJSP-RTMU to a multi-objective framework that simultaneously minimizes energy consumption and makespan, learning Pareto-optimal policies. Hybrid methods combining reinforcement learning with metaheuristics (example, tabu search or grey wolf optimization) may improve scalability and solution quality on large and diverse instances. Developing robust, online adaptive policies to handle dynamic job arrivals and machine breakdowns would further bridge the gap to real-world shop-floor conditions. Finally, leveraging transfer learning across benchmark families and embedding the scheduler within digital-twin environments could enable seamless, continuous optimization in smart manufacturing.

5. Disclaimer Statements

Funding: This work was funded in part by the U.S. Department of Energy (DOE) Office of Energy Efficiency and Renewable Energy's Advanced Manufacturing Office (AMO) through the Industrial Training and Assessment Center (ITAC) program.

Conflict of Interest: None

6. References

- Elallid, B. B., Benamar, N., Bagaa, M., & Hadjadj-Aoul, Y. (2024). Enhancing Autonomous Driving Navigation Using Soft Actor-Critic. Future Internet, 16(7), 238. https://doi.org/10.3390/fi16070238
- Cui, W., & Yuan, B. (2024). A hybrid genetic algorithm based on reinforcement learning for the energy-aware production scheduling in the photovoltaic glass industry. Computers & Operations Research, 163, 106521. https://doi.org/10.1016/j.cor.2023.106521
- Dauzère-Pérès, S, & J Paulli. (2025). Solving the General Multiprocessor Job-shop Scheduling Problem.

 Erasmus University Rotterdam. https://pure.eur.nl/en/publications/solving-the-general-multiprocessor-job-shop-scheduling-problem
- Dauzère-Pérès, S., Ding, J., Shen, L., & Tamssaouet, K. (2023). The flexible job shop scheduling problem: A review. European Journal of Operational Research. https://doi.org/10.1016/j.ejor.2023.05.017
- Dong, Y., Zhang, H., Wang, C., & Zhou, X. (2023). Soft actor-critic DRL algorithm for interval optimal dispatch of integrated energy systems with uncertainty in demand response and renewable energy. Engineering Applications of Artificial Intelligence, 127, 107230. https://doi.org/10.1016/j.engappai.2023.107230
- Fattahi, P., Saidi Mehrabad, M., & Jolai, F. (2007). Mathematical modeling and heuristic approaches to flexible job shop scheduling problems. Journal of Intelligent Manufacturing, 18(3), 331–342. https://doi.org/10.1007/s10845-007-0026-8
- Fernando, W. L. R., Karunathilake, H. P., & Gamage, J. R. (2021). Strategies to reduce energy and metalworking fluid consumption for the sustainability of turning operation: A review. Cleaner Engineering and Technology, 3, 100100. https://doi.org/10.1016/j.clet.2021.100100
- Hao, L., Zou, Z., & Liang, X. (2025). Solving multi-objective energy-saving flexible job shop scheduling problem by hybrid search genetic algorithm. Computers & Industrial Engineering, 110829–110829. https://doi.org/10.1016/j.cie.2024.110829
- Hu, Y., Zhang, L., Zhang, Z., Li, Z., & Tang, Q. (2024). Matheuristic and learning-oriented multi-objective artificial bee colony algorithm for energy-aware flexible assembly job shop scheduling problem. Engineering Applications of Artificial Intelligence, 133, 108634–108634. https://doi.org/10.1016/j.engappai.2024.108634
- Huang, D., Zhao, H., Zhang, L., & Chen, K. (2024). Learning to Dispatch for Flexible Job Shop Scheduling based on Deep Reinforcement Learning via Graph Gated Channel Transformation. IEEE Access, 1–1. https://doi.org/10.1109/access.2024.3384923
- Jiang, B., Ma, Y., Chen, L., Huang, B., Huang, Y., & Guan, L. (2023). A Review on Intelligent Scheduling and Optimization for Flexible Job Shop. International Journal of Control Automation and Systems, 21(10), 3127–3150. https://doi.org/10.1007/s12555-023-0578-1
- Lei, Y., Deng, Q., Liao, M., & Gao, S. (2024). Deep reinforcement learning for dynamic distributed job shop scheduling problem with transfers. Expert Systems with Applications, 251, 123970. https://doi.org/10.1016/j.eswa.2024.123970
- Maharjan, R., Andersen, P.-A., & Jiao, L. (2024). Exploring Efficient Job Shop Scheduling Using Deep Reinforcement Learning. Lecture Notes in Computer Science, 251–257. https://doi.org/10.1007/978-3-031-77918-3 20
- Meng, L., Zhang, C., Shao, X., & Ren, Y. (2019). MILP models for energy-aware flexible job shop scheduling problem. Journal of Cleaner Production, 210, 710–723. https://doi.org/10.1016/j.jclepro.2018.11.021
- Nurdiawati, A., & Urban, F. (2021). Towards Deep Decarbonisation of Energy-Intensive Industries: A Review of Current Status, Technologies and Policies. Energies, 14(9), 2408. https://doi.org/10.3390/en14092408
- Park, M.-J., & Ham, A. (2022). Energy-aware flexible job shop scheduling under time-of-use pricing. International Journal of Production Economics, 248, 108507. https://doi.org/10.1016/j.ijpe.2022.108507
- Pu, Y., Li, F., & Shahin Rahimifard. (2024). Multi-Agent Reinforcement Learning for Job Shop Scheduling in Dynamic Environments. Sustainability, 16(8), 3234–3234. https://doi.org/10.3390/su16083234
- Rakovitis, N., Li, D., Zhang, N., Li, J., Zhang, L., & Xiao, X. (2022). Novel approach to energy-efficient flexible job-shop scheduling problems. Energy, 238, 121773. https://doi.org/10.1016/j.energy.2021.121773

- Sechi, S., Giarola, S., & Leone, P. (2022). Taxonomy for Industrial Cluster Decarbonization: An Analysis for the Italian Hard-to-Abate Industry. Energies, 15(22), 8586. https://doi.org/10.3390/en15228586
- Shao, C., Yu, Z., Ding, H., & Cao, G. (2024b). A Deep Reinforcement Learning Method for Flexible Job-Shop Scheduling Problem. 184–188. https://doi.org/10.1109/icecai62591.2024.10675292
- Shao, X., Fuladi Shubhendu Kshitij, & Chang Soo Kim. (2024a). GAILS: an effective multi-object job shop scheduler based on genetic algorithm and iterative local search. Scientific Reports, 14(1). https://doi.org/10.1038/s41598-024-51778-1
- Sun, H., Hu, Y., Luo, J., Guo, Q., & Zhao, J. (2025). Enhancing HVAC Control Systems Using a Steady Soft Actor—Critic Deep Reinforcement Learning Approach. Buildings, 15(4), 644–644. https://doi.org/10.3390/buildings15040644
- Thenarasu, M., Rameshkumar, K., Rousseau, J., & Anbuudayasankar, S. P. (2022). Development and analysis of priority decision rules using MCDM approach for a flexible job shop scheduling: A simulation study. Simulation Modelling Practice and Theory, 114, 102416. https://doi.org/10.1016/j.simpat.2021.102416
- Wang, G.-G., Gao, D., & Pedrycz, W. (2022). Solving Multi-Objective Fuzzy Job-shop Scheduling Problem by a Hybrid Adaptive Differential Evolution Algorithm. IEEE Transactions on Industrial Informatics, 1–1. https://doi.org/10.1109/tii.2022.3165636
- Wei, Z., Liao, W., & Zhang, L. (2022). Hybrid energy-efficient scheduling measures for flexible job-shop problem with variable machining speeds. Expert Systems with Applications, 197, 116785. https://doi.org/10.1016/j.eswa.2022.116785
- Wu, X., Yan, X., Guan, D., & Wei, M. (2024). A deep reinforcement learning model for dynamic job-shop scheduling problem with uncertain processing time. Engineering Applications of Artificial Intelligence, 131, 107790–107790. https://doi.org/10.1016/j.engappai.2023.107790
- Xu, Y., Zhang, M., Yang, M., & Wang, D. (2024). Hybrid quantum particle swarm optimization and variable neighborhood search for flexible job-shop scheduling problem. Journal of Manufacturing Systems, 73, 334–348. https://doi.org/10.1016/j.jmsy.2024.02.007
- Yang, D., Shu, X., Yu, Z., Lu, G., Ji, S., Wang, J., & He, K. (2024). Dynamic flexible job shop scheduling based on deep reinforcement learning. Proceedings of the Institution of Mechanical Engineers Part B Journal of Engineering Manufacture. https://doi.org/10.1177/09544054241272855
- Yuan, E., Wang, L., Song, S., Cheng, S., & Fan, W. (2025). Dynamic scheduling for multi-objective flexible job shop via deep reinforcement learning. Applied Soft Computing, 171, 112787–112787. https://doi.org/10.1016/j.asoc.2025.112787
- Zhang, G., Yan, S., Song, X., Zhang, D., & Guo, S. (2024a). Evolutionary algorithm incorporating reinforcement learning for energy-conscious flexible job-shop scheduling problem with transportation and setup times. Engineering Applications of Artificial Intelligence, 133, 107974–107974. https://doi.org/10.1016/j.engappai.2024.107974
- Zhang, H., Qin, C., Xu, G., Chen, Y., & Gao, Z. (2024b). An energy-saving distributed flexible job shop scheduling with machine breakdowns. Applied Soft Computing, 112276–112276. https://doi.org/10.1016/j.asoc.2024.112276
- Zhang, W., Zhuang, M., Tang, H., Li, X., & Guo, S. (2024c). A hybrid particle swarm optimisation for flexible casting job shop scheduling problem with batch processing machine. IET Collaborative Intelligent Manufacturing, 6(4). https://doi.org/10.1049/cim2.12117
- Zhao, S., Zhou, H., Zhao, Y., & Wang, D. (2024). DQL-assisted competitive evolutionary algorithm for energy-aware robust flexible job shop scheduling under unexpected disruptions. Swarm and Evolutionary Computation, 91, 101750–101750. https://doi.org/10.1016/j.swevo.2024.101750
- Zhu, Z., & Zhou, X. (2020). An efficient evolutionary grey wolf optimizer for multi-objective flexible job shop scheduling problem with hierarchical job precedence constraints. Computers & Industrial Engineering, 140, 106280. https://doi.org/10.1016/j.cie.2020.106280

The Journal of Management and Engineering Integration (JMEI) © 2025 by AIEMS Inc., is licensed under CC BY 4.0. To view a copy of this license, visit https://creativecommons.org/licenses/by/4.0/

DOI: 10.62704/10057/31200

INNOVATIONS IN POWDER MATERIALS FOR BINDER JETTING

Abdelhakim A. Al Turk ¹
Gamal Weheba ¹

¹ Wichita State University

<u>Aalturk3@kent.edu</u>

Abstract

Additive manufacturing has evolved from a prototyping tool to a primary method for producing functional, end-use products. Binder jetting, in particular, has gained significant attention in the construction industry. This paper reviews innovative powder material mixes used in binder jetting techniques. These materials, combined with modifications to printing parameters such as layer thickness and binder saturation level, offer improvements in mechanical strength, dimensional accuracy, and the sustainability of 3D-printed objects. The review highlights recent experimental studies that investigate the effects of powder composition, binder saturation, and post-processing techniques. The findings provide insights into optimizing material behavior and mechanical performance for construction-grade applications.

Keywords: Binder Jetting, Additive Manufacturing, 3D Printing in Construction, Powder Materials

1. Introduction

Additive Manufacturing (AM) is a form of layered manufacturing. It utilizes a class of machines designed to recreate a physical structure from a 3-dimensional Computer-Aided Design (CAD) model by quick and highly automated means. AM as defined by ASTM, involves building objects by joining materials layer by layer based on 3D model data. While the specific materials and methods can differ, the core approach involves slicing a CAD model into layers and producing either prototypes or final products. Initially used mainly for prototyping in product development, AM technologies are now widely applied in manufacturing fully functional end-use items. Among these techniques are Stereolithography, Binder Jetting, Material Jetting, Powder Bed Fusion, Material Extrusion, Sheet Lamination, and Directed Energy Deposition. These techniques can create solid objects in layers by using different materials and methods for bonding them together. A more detailed description of these techniques can be found in the ASTM F2792 Standard. This paper will focus on the application of binder jetting, related to construction industry.

The binder jetting process builds complex shapes layer by layer by applying a binder to powdered material with great precision. Over time, improvements in materials and post-processing techniques have widened their applications, especially in construction and materials science. Researchers have experimented with various powders and binders, such as geopolymers, cement-based materials, and silica and zirconia sands, each offering distinct mechanical and thermal properties. The following section highlights key studies that explore how material composition, processing conditions, and post-treatment methods affect the outcomes of binder jetting. These advancements showcase the technology's potential to transform construction with better mechanical strength, dimensional accuracy, and sustainability.

Submitted: June 28, 2025 Revised: August 25, 2025

2. Binder Jetting Technology

According to Gibson et al. (2015), Binder Jetting technology was first introduced at MIT in 1996 and was initially known as 3D printing (3DP). The process involves depositing a binder onto a bed of powder to create each layer of a part. After each layer is printed, a fresh layer of powder is spread evenly across the bed, smoothed with a roller, and the binder is applied again, repeating the process until the object is complete. This sequence of steps is iterated until the object is fully constructed. Depending on the material and binder employed, heat may be applied to ensure adhesion both within and between layers. Excess powder is removed using either vacuum or compressed air during post-processing stages. Generally, constructed objects undergo infiltration to enhance their mechanical properties. A schematic illustration of this process is depicted in Figure 1.

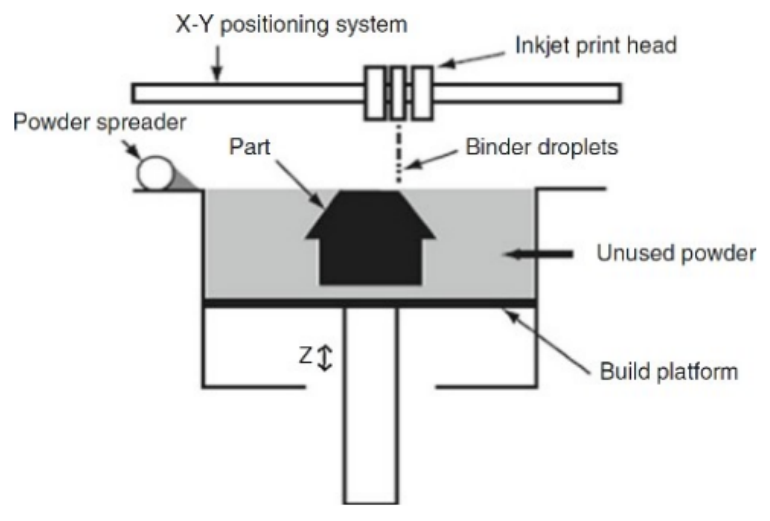


Figure 1. Schematic of the Binder Jetting Process (Source: Gibson et al. (2015))

Early applications of the binder jetting process in construction were first reported by Duxson et al. (2006), who substituted a geopolymer for the traditional ceramic powder material. This geopolymer is an alkali aluminosilicate, meaning it is similar to cement. It is made up of a mixture of fly ash and slag. Using the standard Zb 63 binder and a Z-Corp 450 3D printing (3DP) system, they carried out their experiments. According to their findings, the geopolymer material outperformed regular cement in a number of ways, including improved resistance to sulfate and acid attacks, high compressive strength, and decreased shrinkage. Furthermore, they looked at five distinct geopolymer blends and suggested a novel post-processing method. According to their research, the ideal mixture would contain 100% slag and 0% fly ash.

Xia and Sanjayan (2016), proposed a new geopolymer cement material that can be used in the ZPrinter 150 3D printer. The dimensional accuracy, apparent porosity, compressive strength, and bulk density of the 3D printed specimens were evaluated. The powder material was a mixture of fine sand, slag, and beaded anhydrous sodium metasilicate with a chemical composition of 50.7% Na2O, 47.0% SiO2, and 2.3% H2O. The original Zb63 liquid was used as binder material. Once the printing process is done, all specimens are left in the powder bed for two hours. Before the depowering process began, Then, specimens were divided into two batches; the first batch, has no

further post-processing procedures. In the second batch, specimens were immersed in a saturated anhydrous sodium metasilicate solution for 1–7 days at a temperature of 60°C. The result of the experiment shows that, without any post-processing, the compressive strength was determined to be around 1 MPa. The second batch of specimens achieved a compressive strength of around 16.5 MPa. In addition to that, the geopolymer specimens had a lower apparent porosity and a higher accuracy compared to the ZP151 specimens. Geopolymer powder exhibited lower in-process bed density and bulk density but higher powder bed porosity, compared to the ZP151 powder.

Xia et al. (2018), reported the effects of binder saturation level on linear dimensional accuracy and compressive strength of 3D printed geopolymers. For this experiment, the powder material was a slag-based geopolymer powder mixture of slag, silicate-based alkaline activator, and fine silica sand. Zb63 was used as a binder liquid. The authors used ZPrinter 150 to print samples using the binder jetting 3D printing technique. 20 mm cubic specimens were printed using a 0.00041" (0.0106 mm) layer thickness with five binder saturation levels (75%, 100%, 125%, 150%, and 170%). Before the de-powdering procedure, the cubes were placed inside the powder bed at room temperature for six hours after printing and called green samples. The post-processing of the green samples involved soaking them in a saturated anhydrous sodium metasilicate solution and heating them in an oven at 60°C for seven days. The results indicated that the increase in binder saturation level resulted in a significant increase in the compressive strengths of both green and post-processed samples in both directions. However, compared to post-processed samples, the rate at which compressive strength increased in green samples was noticeably higher. For instance, in the Xdirection, green samples with a 170% binder saturation level had compressive strength that was 3.25 times greater than the corresponding samples with a 75% binder saturation level. In addition to that, in both X- and Z-directions, the compressive strengths of post-processed samples were significantly higher than those of green samples.

Shakor et al. (2019), studied the effect of post-processing techniques on the compressive strength and flexural strength of 3D printed cement specimens. 110 specimens were printed using a binder jetting 3D printer. 54 samples were used for the compressive strength test and 56 samples for the flexural strength test. The powder material used in this experiment was fabricated by mixing calcium aluminate cement CAC (6.78 kg), ordinary Portland cement OPC (3.22 kg), fine sand (0.5 kg), and lithium carbonate (0.45 kg), which made up the total weight of the powder. The binder used was Zb63, and the layer thickness was approximately 0.1 mm (0.0039 in). Besides that, the authors studied the effect of changing the binder saturation levels of the samples on the compressive strength. In this experiment, two types of post-processing solutions were used. The first was just water, and the second was 5% calcium hydroxide (Ca (OH) 2) dissolved in the total weight of water. The specimens were cured over two periods of time (7 and 28 days), and then all specimens were dried in the oven at 104 °F for one hour. The 3D printed parts were cured for 28 days in water blended with 5% Ca (OH) 2, which resulted in low compressive strength. The 3D printed sample S170C340 (170% shell saturation and 340% core saturation) had the highest result in compressive strength at approximately 14.68 MPa (2126.25 psi) when cured for 28 days in water and then dried in the oven. It is also noted that when the size of the samples increases, the compressive strength increases. The results also indicate that, the samples S125C250 (125% shell saturation and 250% core saturation) had the highest flexural strength, at approximately 9.77 MPa (1417.02 psi).

Maravola et al. (2019), investigated the impact of powder material and infiltration process on 3D-printed samples produced by an ExOne S-Max binder jetting printer. Silica (SiO₂) and zirconia (ZrO₂) sands were used with a furan no-bake (FNB) binder system, which forms rigid parts without post-processing. After printing some samples were infiltrated with epoxy (TC-1614 A/B) at

temperatures between 66–177°C for six hours. Compression and flexural tests revealed that infiltration significantly improved mechanical properties by filling porosity gaps with epoxy. Infiltrated zirconia samples achieved the highest compressive strength (55 MPa), while non-infiltrated samples of both materials showed much lower compressive strength (~5 MPa). Similarly, infiltrated samples demonstrated higher flexural strength (45 MPa) compared to non-infiltrated ones (5 MPa). Thermal analysis showed that infiltrated samples had a higher coefficient of thermal expansion than non-infiltrated materials. The study underscores the importance of infiltration in enhancing the mechanical and thermal properties of binder jet 3D-printed parts.

Ingaglio et al. (2019), explored advancements in high-resolution binder jet printing by developing a water-based binder compatible with concrete chemistry and piezoelectric jetting. Using a Zcorp 310 3D printer, the study investigated the effects of binder saturation levels on prints made from a silica sand and cement powder mix, with sand-to-cement ratios ranging from 1.25:1 to 5.05:1. The binder consisted of water, a water-soluble polymer, and a surfactant, with saturation levels set to 150% (Mix A) and 194% (Mix B). After printing, samples were left in the powder bed for 24 hours, cleaned, and cured in water for 28 days. Results showed that cement-only samples had low densities, while adding silica sand increased density but reduced compressive strength. Cement-only specimens with a 150% saturation level achieved higher compressive strength (9 MPa) than those with a 194% saturation level (7 MPa). Lower binder saturation levels produced lower initial strength but gained strength after curing, whereas higher saturation levels resulted in higher initial strength but lower strength after 28 days of curing. The study highlights the trade-offs between binder saturation, density, and compressive strength in binder jet printing.

Shakor et al. (2020), study the effect of heat-curing and the addition of E6-glass fibers as reinforcement for 3D printed specimens using a binder jetting system. The used powder cement material contains 67.8% calcium aluminate cement, 32.2% ordinary Portland cement, and 5% fine sand as a percentage of total weight. Two groups of samples with and without E6-glass fiber were printed. Three specimens for each group were prepared for each test based on six different curing conditions. All samples were left in the powder bed for 2 hours before the depowering process began. The samples were cured in water under two different post-processing techniques. The post-processing consists of (a) curing one group of specimens for 28 days in tap water. And (b) curing another group of specimens in the oven for 3 hours, storing them in water for 28 days, and then dry them in the oven for 3 hours. This same basic post-processing sequence was used for all specimens, but at various temperatures. Specimens were cured at different temperatures. The results of this experiment reveal that the increase in curing temperature tends to increase compressive strength. Samples curing at 80 °C attained the optimum compressive strength for the printed mortar. The compressive strength of mortar with 1% glass fiber was recorded at around 37 MPa.

Rehman and Sglavo (2020), investigated how metakaolin-based geopolymer concrete's mechanical characteristics and dimensional stability were affected by inorganic binder saturation during the 3D printing process. The samples for this study were printed using a prototype powder-based 3D printer that was specially constructed. As a binder, the alkaline solution was utilized. Siliceous sand and metakaolin were combined in a range of weight ratios (from 1:1 to 8:1) and utilized as powdered material for printers. All samples were printed with the same layer thickness. The specimens were printed and kept in the powder bed for 24 hours at room temperature to gain the necessary strength. Then all parts were removed and cleaned from excessive powder. After that, flexural tests were carried out on the printed samples according to ASTM C293. The results of the test are not correlated with the alkaline solution flow rate or the proportion of the binding phase in the printed component. The printed samples were crushed after drying. The flowability of the

powder mixtures was tested. The results indicated that the high metakaolin content is considered a non-flowable material. The powder is significant in factors such as hopper geometry, wall friction, hopper wall angle, powder surface, and hopper wall angle. Furthermore, a test is conducted to compare the actual and nominal quantities in CAD. The fact that the length and width are consistently the same as the nominal values highlights the high level of in-plane accuracy achieved throughout the printing process. Finally, from this research, it can be concluded that the volume of the 3D-printed samples can increase with the activator flow rate. The length and width of it remain intact, nevertheless. With an excess of an alkaline liquid solution, the thickness of the printed specimen rises.

Odaglia et al. (2020), study the effect of changing the powder material on the compressive and flexural strengths of 3D printed parts. Three different materials have been used: gneiss sand, concrete sand, and brick sand. Potassium silicate was used as a binder. All samples were printed using a binder jetting 3D printer. Once the printing process was done, the samples were kept in the printer bed for 48 hours before the depowering process began. Three prisms' samples were printed using three different materials. After 7 days of curing at room temperature, the samples were tested in a mechanical press (Unitronic, Matest) using a 50 KN cell, applying 0.1 KN/S. The first test was to measure geometric accuracy. The dimensions of all the prisms were measured along the x, y, and z directions. After that, the flexural strength of the specimen was first evaluated through a threepoint bending test; the resulting two segments of each prism were then tested in compression, respectively parallel and perpendicular to the printing direction. As a result of these experiments, all the printed samples show a dimensional accuracy consistent with the maximum grain size of the material in use, and no remarkable difference has been observed between the samples printed with different materials. The samples were tested both parallel and perpendicular to the printing direction, and the comparison does not show notable differences. In addition to that, the compressive strength of the Gneiss Sand samples resulted in a higher compressive strength of around 5.5 MPa, and the Brick Sand, samples were lower, around 1.5 MPa. Finally, the samples printed in Gneiss had higher flexibility than the other two materials analyzed.

Shakor et al. (2020), aimed in this research to understand the difference between the Zp151 powder and the cement powder with regards to powder, wettability, powder bed porosity, and apparent porosity in 3D printed specimens. A ProJet 360 3D printer was used to print samples using the binder jetting technique. The original powder, zp151, has been replaced by cement powder. The cement powder was a mix of 67.8% calcium aluminate cement and 33.2% ordinary Portland cement. The same binder, zb63, was used in both samples printed using Zp151 and cement. The saturation level of the 3D printed samples was set at a binder/volume ratio of 0.415. All samples were printed with a saturation level of S175C340, 175% shell saturation, and 340% core saturation. The results of this research are as follows: A digital caliper was used to measure the dimensions of the 3D-printed parts, and the dimensional accuracy in all three dimensions was measured and found to be very close to the CAD model. The powder bed porosity measures the density after the powder is spread on the build chamber. The true density and bulk density of the powders were measured. The powder bed porosity in CP and ZP 151 is 73.6% and 64.9%, respectively. The apparent porosity test was used to measure the voids and porosity of the specimen. The results indicate that samples printed with cement powder have a higher apparent porosity compared with Zp151 samples. Regarding wettability, this research indicates that on the CP powder, the wetting and contact angle of the binder (water) resulted in a greater spread than on the ZP 151 powder. A higher number of particles were found on the surface of cement powder than Zp151. This indicates that the wetness of cement powder is higher than Zp151.

The impact of binder flow rate on the dimensional correctness of 3D printed items is examined by Rehman and Sglavo (2021). They investigated how hydration affected mechanical qualities over time. The binder jetting technique has been used to print samples. Commercial Portland cement mix with siliceous sand (1:3 weight mixture) was used as powder material. Pure water and water mixed with polyvinyl alcohol were used as a binder. Poly vinyl alcohol was mixed with water (water: Poly vinyl alcohol 98:2 w/w) to increase the viscosity and improve the green strength of the printed parts. All samples were left in the powder bed for 24 hours. Prior to commencing the de-powdering process, hydration was carried out by immersing the specimen in an environment with 20°C temperature and 50% humidity for specified durations, following its removal from the powder bed. Once the hydration process ended, flexural resistance, compression strength, and density tests were performed. The results of this experiment indicate that as the flow rate increased, the variation in dimensions of the printed samples increased. Width shows the largest variation. The results also indicate that the density increases with the degree of hydration. The compressive strength of samples printed using water only had a higher compressive strength (6 MPa) compared to the one mixed with polyvinyl alcohol (3 MPa). Furthermore, the author noted that the quantity of water utilized during the printing process does not affect the ultimate strength of the specimens when subsequent water hydration is performed.

Al Turk and Weheba (2021), demonstrated the feasibility of using Portland cement as a printable material in a commercial binder jetting system. Their study investigated how layer thickness, curing solution, and curing duration influence the compressive strength and dimensional accuracy of 3D printed cement parts. Using a Zprinter 450, the researchers substituted the typical ZP151 powder with Quick-Setting Cement (Quikrete 1240) and used the standard Zb63 binder. Sixteen cylindrical samples were printed with varying layer thicknesses and cured in either tap water or an alkaline solution for 14 or 28 days. A full factorial experimental design was implemented to examine all combinations of these variables. The analysis revealed that the highest compressive strength, 13.5 MPa, was achieved with a 0.0034" (0.088 mm) layer thickness and 28-day curing in the alkaline solution. Additionally, the findings showed that layer thickness significantly affects dimensional deviation when alkaline curing is applied, with the greatest height deviation also occurring at the lowest layer thickness.

Park et al. (2021), used optimization methods to improve the compressive strength of alkaliactivated material-based binder jet 3D printing (BJ3DP) outputs. The study evaluated how powder mixture, post-processing equipment, and storage solutions affect compressive strength. Printing was done using a ProJet CJP 360 with Zb63 binder and powders including GGBFS, FA, Na₂SiO₃, Ca(OH)₂, and silica sand. Twenty-one post-processing solutions were prepared with varying Na₂SiO₃/NaOH ratios, NaOH moles, and sodium silicate combinations. After printing and a 2-hour drying period in the powder bed, samples were de-powdered and immersed for 7 days at 70°C in vacuum-sealed alkaline solutions. They were then rinsed with distilled water and conditioned at 20 ± 2 °C and 60 ± 5 % humidity. Compression testing showed that increasing Ca(OH)₂ improved compressive strength without significantly reducing density. Strength was maximized by combining Na₂SiO₃ and Ca(OH)₂. Applying vacuum pressure relative to part size was also necessary. A compressive strength of 20.7 MPa was achieved after 7 days using a solution with a Na₂SiO₃/NaOH ratio of 4 and 3 mol NaOH—adequate for general construction applications.

In addition to that, Min et al. (2021), developed a method for inserting reinforcing bars into 3D-printed concrete and evaluated chloride penetration and compressive strength in binder jetting based on build orientation and powder material. Using a ProJet CJP360 printer, specimens were produced with alkali-activated materials (AAM) and rapid hardening cement as powders, and

distilled water as a binder. Post-processing included six specific steps to enhance strength, with samples dried in the printer for 2 hours and de-powdered after 24 hours. On the 28th day, AAM samples showed 22.1% lower compressive strength in the transverse direction (20.1 MPa) compared to the built direction (25.8 MPa). Rapid hardening cement samples exhibited 26.5% lower strength in the transverse direction (13.9 MPa) compared to the build direction (18.9 MPa). Chloride diffusion was significantly higher (186.1% to 407.1%) in the transverse direction due to alignment with the diffusion path, indicating reduced chloride penetration when printing in the build direction. The study underscores the impact of built orientation and material choice on strength and durability in BJ3DP components.

Salari et al. (2022), investigated the effects of six manufacturing factors on the modulus of rupture of cement-based components produced using binder jetting 3D printing. The powder mix consisted of 60.8% porous glass, 36.5% magnesium oxide (MgO), 1.5% methylcellulose, and 1.2% orthophosphoric acid (H_3PO_4), blended for three hours before printing. The liquid binder included 49.5% water, 49.5% magnesium chloride hexahydrate solution, and 1% rice starch to regulate viscosity. Rectangular specimens ($150 \text{ mm} \times 40 \text{ mm} \times 40 \text{ mm}$) were printed, hardened for 24 hours, and cured in room-temperature laboratory air for 5-7 days. Using a factorial design method, the study examined six factors: feed rate, layer thickness, binder amount, powder spread velocity, particle size, and hatch distance. Three-point bending tests were conducted according to ASTM C293 to determine the modulus of rupture. Results revealed that feed rate and powder spread velocity had negligible effects on strength, while particle size, binder quantity, and layer thickness were critical. Precise control of binder application, influenced by voxel rate and powder-bed density, was essential for improving mechanical strength.

Another research was done by Al Turk and Weheba (2024), they aimed at providing proof of the concept that polyblend calcium carbonate (grout) can be used as a material on a binder jetting 3D printer (ZPrinter 450). In achieving the project objective tile specimens were constructed using different layer thicknesses of 0.0035" and 0.005" (0.088 and 0.125 mm) and different binder saturation levels (100% and 272%). Once the printing was completed, the specimens were cured in one of two solutions (water and alkaline solution) over two periods (14 and 28 days). Both printing and curing followed a 2^4 replicated twice factorial experiment, covering all possible combinations of these four factors. In performing each run four samples were constructed making a total of 128 samples. The statistical analysis of the results indicated that the maximum breaking strength that tile specimens can reach is 2.98 KN. This was obtained when the specimens were printed using a low layer thickness of 0.0035" (0.088 mm), a high binder saturation level of %272, and cured in the alkaline solution for 28 days. The minimum deviation in the Z direction of 0.01165" (0.3 mm) was observed when specimens were cured in an alkaline solution for 28 days. A surface roughness (Ra) of 3.3 µm was obtained when the maximum binder saturation was used.

3. Summary of Binder Jetting Studies

The following table summarizes key experimental studies that explore the use of various materials and methods in binder jetting for construction applications. These studies highlight how different powder compositions, binders, and post-processing techniques influence the mechanical and dimensional outcomes of 3D-printed parts.

Table 1. Summary of Binder Jetting Studies

Study	Material	Method	Key Findings
Duxson et al. (2006)	Geopolymer (Fly ash and slag)	Z-Corp 450 3D printing system (Zb 63 binder)	Geopolymer outperforms cement in sulfate/acid resistance, compressive strength, and shrinkage. Ideal mixture: 100% slag, 0% fly ash.
Xia and Sanjayan (2016)	Geopolymer (sand, slag, sodium metasilicate)	ZPrinter 150 3D printer, Zb63 binder	Compressive strength increases from 1 MPa (no post-processing) to 16.5 MPa (with post-processing). Geopolymer has lower porosity and higher accuracy than ZP151.
Xia et al. (2018)	Slag-based geopolymer	ZPrinter 150, five binder saturation levels (75%-170%)	Increased binder saturation significantly enhances compressive strength. Post-processing improves strength in both green and cured samples.
Shakor et al. (2019)	Cement mix (CAC, OPC, fine sand, lithium carbonate)	Binder jetting 3D printing, curing with water or Ca(OH)2 solution for 7 or 28 days	Curing with 5% Ca(OH)2 yields 14.68 MPa compressive strength. Larger samples improve compressive strength; flexural strength peak at 9.77 MPa.
Maravola et al. (2019)	Silica and zirconia sands, epoxy infiltration	ExOne S-Max 3D printer, furan no-bake binder system	Infiltrated samples show higher compressive (55 MPa) and flexural (45 MPa) strength. Infiltration improves mechanical properties and thermal expansion.
Ingaglio et al. (2019)	Silica sand and cement powder mix	Zcorp 310 printer, 150%- 194% binder saturation levels	Higher binder saturation increases initial compressive strength but decreases strength after curing.
Shakor et al. (2020)	Custom-made cement mix (CAC, OPC, fine sand) with and without glass fibers	Binder jetting, curing in water or oven for 28 days	Higher curing temperature increases compressive strength. Glass fiber reduces porosity and surface roughness.
Rehman and Sglavo (2020)	Metakaolin-based geopolymer concrete	Prototype 3D printer, alkaline solution binder	High metakaolin content reduces flowability. Dimensional accuracy achieved with low flow rate of liquid.

Study	Material	Method	Key Findings
Odaglia et al. (2020)	Gneiss sand, concrete sand, brick sand	Binder jetting, curing for 7 days at room temperature	Gneiss sand samples show highest compressive strength (~5.5 MPa), brick sand lowest (~1.5 MPa).
Shakor et al. (2020)	Cement powder (67.8% calcium aluminate, 33.2% OPC)	ProJet 360 printer, Zb63 binder	Cement powder samples have higher apparent porosity and wettability compared to ZP151. Dimensional accuracy consistent with CAD models.
Rehman and Sglavo (2021)	Portland cement with siliceous sand	Binder jetting, hydration- based curing	Higher binder flow rate increases dimensional variations, but higher hydration increases density and compressive strength.
Al Turk and Weheba (2021)	Quick-Setting Cement (Quikrete 1240)	Zprinter 450 printer, alkaline curing solution	Maximum compressive strength of 13.5 MPa at low layer thickness (0.088 mm), cured in alkaline solution for 28 days.
Park et al. (2021)	Alkali-activated materials (GGBFS, FA, Na2SiO3, Ca(OH)2, silica sand)	ProJet CJP 360 printer, Zb63 binder, post-processing in Na2SiO3/NaOH solution	Increasing Ca(OH)2 content improves compressive strength. Best results (20.7 MPa) after 7 days of curing in post-processing solution.
Min et al. (2021)	Alkali-activated materials (AAM), rapid hardening cement	ProJet CJP360 printer, water binder	AAM samples show lower compressive strength in transverse direction compared to build direction; chloride penetration is higher in transverse direction.
Salari et al. (2022)	Cement-based materials (60.8% porous glass, 36.5% MgO)	Binder jetting 3D printing	Manufacturing factors significantly affect modulus of rupture in 3D-printed cement-based components.
Al Turk and Weheba (2024)	Polyblend Calcium Carbonate (Grout)	ZPrinter 450, binder jetting, saturation 100–272%, 0.088–0.125 mm layer thickness, water/alkaline cure	Max breaking strength of 2.98 KN at 272% saturation, 0.088 mm layer, 28-day alkaline cure. Min Z-deviation of 0.3 mm; surface roughness Ra = 3.3 μm.

4. Conclusion

This paper has reviewed recent advancements in binder jetting technology for construction applications, with a focus on innovative powder materials and their influence on mechanical performance, dimensional accuracy, and sustainability. The studies analyzed demonstrate that material selection, binder saturation, and post-processing conditions play critical roles in determining the quality of printed parts. Geopolymer and cement-based powders, when combined with optimized curing techniques and additives, have shown promising improvements in strength and durability. Moreover, emerging strategies, such as the use of fiber reinforcement and material infiltration, further enhance the potential of binder jetting in producing structurally sound and environmentally resilient components.

Despite the progress made, several challenges remain. Long curing times, variability in powder flowability, and dimensional stability continue to hinder large-scale adoption. Therefore, future research should prioritize the development of rapid-curing additives, standardization of material properties, and the integration of machine learning for process optimization. Binder jetting holds strong potential to reshape the construction industry, but its continued advancement will depend on multidisciplinary innovation and industrial collaboration.

Future work should focus on reducing the curing duration required to achieve high-strength 3D-printed components. One potential approach involves incorporating additive materials that accelerate strength gain without compromising final performance. For example, silica fume can be mixed with Polyblend Calcium Carbonate (Grout) to improve early compressive strength. Alternatively, additives may be integrated into the binder solution and applied layer by layer during printing.

5. Disclaimer Statements

Funding: None

Conflict of Interest: None

6. References

- Al Turk, A. A., & Weheba, G. S. (2021). 3D Printing of Portland Cement Using a Binder Jetting System. Journal of Management & Engineering Integration, 14(1), 128–136. https://doi.org/10.62704/10057/24775
- Al Turk, A. A., & Weheba, G. S. (2024). Restoring Historical Buildings Using Additive Manufacturing. *Journal of Management & Engineering Integration*, 17(1), 10–20. https://doi.org/10.62704/10057/28081
- ASTM International. (2012). ASTM F2792-12a: Standard terminology for additive manufacturing technologies. West Conshohocken, PA: ASTM International. https://doi.org/10.1520/F2792-12A
- Duxson, P., Fernández-Jiménez, A., Provis, L., Lukey, C., Palomo, A., & Deventer, S. (2006). Geopolymer technology: the current state of the art. *Journal of Material Science*, *42*, *2917–2933*. https://doi.org/10.1007/s10853-006-0637-z
- Gibson, I., Rosen, D. W., & Stucker, B. (2015). Additive Manufacturing Technologies: 3D Printing, Rapid Prototyping and Direct Digital Manufacturing (2nd ed.). *Springer, New York*. https://doi.org/10.1007/978-1-4939-2113-3
- Ingaglio, J., Fox, J., Naito, C. J., & Bocchini, P. (2019). Material characteristics of binder jet 3D printed hydrated CSA cement with the addition of fine aggregates. *Construction and Building Materials, 206, 494–503*. https://doi.org/10.1016/j.conbuildmat.2019.02.065
- Maravola, M., Conner, B., Walker, J., & Cortes, P. (2019). Epoxy infiltrated 3D printed ceramics for composite tooling applications. *Additive Manufacturing*, *25*, *59–63*. https://doi.org/10.1016/j.addma.2018.09.010

- Min, K. S., Park, K. M., Lee, B. C., & Roh, Y. S. (2021). Chloride Diffusion by Build Orientation of Cementitious Material-Based Binder Jetting 3D Printing Mortar. *Materials*, *14*(*23*), *7452*. https://doi.org/10.3390/ma14237452
- Muradyan, N. G., Arzumanyan, A. A., Kalantaryan, M. A., Vardanyan, Y. V., Yeranosyan, M., Ulewicz, M., ... & Barseghyan, M. G. (2023). The Use of Biosilica to Increase the Compressive Strength of Cement Mortar: The Effect of the Mixing Method. *Materials*, 16(16), 5516. https://doi.org/10.3390/ma16165516
- Odaglia, P., Voney, V., Dillenburger, B., & Habert, G. (2020, July). Advances in Binder-Jet 3D Printing of Non-cementitious Materials. *In RILEM International Conference on Concrete and Digital Fabrication (pp. 103–112). Springer, Cham.* https://doi.org/10.1007/978-3-030-49916-7_11
- Park, K. M., Min, K. S., Lee, B. C., & Roh, Y. S. (2021). Proposal for enhancing the compressive strength of alkali-activated materials-based binder jetting 3D printed outputs. *Construction and Building Materials*, 303, 124377. https://doi.org/10.1016/j.conbuildmat.2021.124377
- Rehman, A. U., & Sglavo, V. M. (2020). 3D printing of geopolymer-based concrete for building applications. *Rapid Prototyping Journal, 26(10), 1783–1788.* https://doi.org/10.1108/rpj-09-2019-0244
- Rehman, A. U., & Sglavo, V. M. (2021). 3D printing of Portland cement-containing bodies. *Rapid Prototyping Journal*, 28(2), 197–203. https://doi.org/10.1108/rpj-09-2020-0273
- Salari, F., Bosetti, P., & Sglavo, V. M. (2022). Binder Jetting 3D Printing of Magnesium Oxychloride Cement-Based Materials: Parametric Analysis of Manufacturing Factors. *Journal of Manufacturing and Materials Processing*, 6(4), 86. https://doi.org/10.3390/jmmp6040086
- Shakor, P., Nejadi, S., Paul, G., Sanjayan, J., & Nazari, A. (2019). Mechanical properties of cement-based materials and effect of elevated temperature on three-dimensional (3-D) printed mortar specimens in inkjet 3-D printing. *ACI Mater J*, 116(2), 55-67. https://doi.org/10.14359/51714452
- Shakor, M., Liao, D., & Zhang, Y. (2020). Heat curing and fiber reinforcement for 3D printed specimens using binder jetting technology. *Journal of Cement and Concrete Composites, 110, 103535.*https://doi.org/10.1007/978-3-030-49916-7 52
- Shakor, P., Nejadi, S., Sutjipto, S., Paul, G., & Gowripalan, N. (2020). Effects of deposition velocity in the presence/absence of E6-glass fibre on extrusion-based 3D printed mortar. *Additive Manufacturing*, 32, 101069. https://doi.org/10.1016/j.addma.2020.101069
- Xia, M., & Sanjayan, J. (2016). Method of formulating geopolymer for 3D printing for construction applications. *Materials & Design*, 110, 382–390. https://doi.org/10.1016/j.matdes.2016.07.136
- Xia, M., Nematollahi, B., & Sanjayan, J. (2018). Influence of binder saturation level on compressive strength and dimensional accuracy of powder-based 3D printed geopolymer. In *Materials Science Forum (Vol. 939, pp. 177–183)*. Trans Tech Publications Ltd. https://doi.org/10.4028/www.scientific.net/MSF.939.177

The Journal of Management and Engineering Integration (JMEI) © 2025 by AIEMS Inc., is licensed under CC BY 4.0. To view a copy of this license, visit https://creativecommons.org/licenses/by/4.0/

DOI: 10.62704/10057/31201

ELECTRIC AIRCRAFT: INFRASTRUCTURE CHALLENGES F OR AIRPORTS

Isaac M. Silver 1

Brooke E. Wheeler²

- ¹ Energy Management Aerospace
- ² Florida Institute of Technology

bwheeler@fit.edu; isaac@energymanagementaero.com

Abstract

Aviation as an industry has committed to 2050 as the target date for carbon neutrality. This requires a shift to alternative fuels, with electric aircraft being one of the options, with several examples in the certification pipeline. As technology has trended towards energy efficiency, airports have not had an impetus to focus on increasing energy distribution capacity, and therefore, they will not have the infrastructure to support electric aircraft. This will be particularly true for smaller, general aviation airports. This paper draws on experiences with an electric aircraft to provide a snapshot of what it takes to interface with the airport grid, electrical infrastructure requirements for charging, charging inefficiencies, and other limitations. The findings can be scaled up to suggest broader requirements to meet the needs of widespread deployment of electric aircraft. Airport master plans should include provisions for expanding the electrical grid capacity and ideally implementing solar projects as a sustainable solution.

Keywords: Airport Infrastructure, Electric Aircraft, Aviation Sustainability, Charging, Advanced Air Mobility (AAM), Evtol (Electric Vertical Take-Off and Landing)

1. Introduction

Aviation is an essential part of the transportation network, which increasingly focuses on sustainable options. In 2021, the Federal Aviation Administration (FAA, 2021) policy position set a goal for the aviation industry in the US to be carbon neutral by 2050; this has also been recently reaffirmed (Williams, 2024). The policy aligns with that of ICAO (international civil aviation organization) and other member states, in that the aviation industry as a whole is committing to a specific, near-term target for carbon neutrality. Meeting this goal will require actively pursuing sustainability in all areas of the aviation industry.

One of the promising technologies slated to move aircraft towards sustainability is electric aviation. In 2022, the National Academies of Sciences, Engineering, and Medicine published a review of the state of the electric aircraft industry and made recommendations for airport infrastructure planning. However, the report was completed before any significant flight test of electric aircraft and before operational considerations were field tested. Of note, the report indicates a trend towards lower electrical power demand over time, as airports adopt more efficient technologies, such as LED lighting and modernized building systems.

Even as airports decrease their overall energy usage through sustainability efforts, the vast majority of the energy consumed at an airport is still from some form of hydrocarbon fuel. Thus, for

Submitted: June 29, 2025 Revised: August 25, 2025 electric aviation, the Jet A "tank and pipeline" infrastructure analog will need to be rebuilt for powering battery electric flight, preferably via more sustainable energy sources.

This paper draws on experience gained in the field during a multiyear electric aircraft test campaign and suggests certain challenges that will need to be addressed as airports are electrified. The actual charging demand under real-world conditions (Cuhna et al., 2023; Wheeler et al., 2023) is also examined, with a recommendation that airports explore sustainable technologies and in-situ energy generation as a solution.

2. Electric Aircraft

2.1 Estimated Future Use

In the near horizon, from approximately 2025 to 2030, most electric aircraft usage in the United States is anticipated to be localized, shorter flights with support from the company or aircraft owner, not the airport. This is primarily due to the fact that no electric aircraft are certified yet. At this early stage in electric aviation, almost everything is customized; there is little to no standardization, including chargers for the aircraft currently available.

The operations are expected to be largely light general aviation and experimental. However, small commuter (e.g., small aircraft conversions from piston to electric with a drop-in electric motor) and/or cargo operations may commence during this period. The converted Beaver electric aircraft was flown in 2019 and has been used by Harbour Air (2024) in Vancouver, BC. There is also a possibility that Advanced Air Mobility (AAM), Urban Air Mobility (UAM), and other small eVTOL (electric Vertical Take-Off and Landing) aircraft will be approved and begin operations in this period, with the expectation that this part of the industry will continue to grow beyond 2030.

The far horizon of electric aircraft (beyond 2030) is more challenging to anticipate. With the improvement of batteries and thus the range of electric aircraft, medium to large electric commercial aircraft are likely to be added to the electric fleet, along with high-performance electric aircraft. Hybrid aircraft technology (e.g., hydrocarbon, hydrogen, fuel cells) may use batteries to help get off the ground and/or when there is high energy demand. However, at least some of the long-haul international operations will remain hydrocarbon fuel-based. The type of aircraft and fuel may be matched to the operation type and required range.

2.2 Language of Electric Flight

Traditionally, the power generated is measured in horsepower. However, in the language of electric flight, watts, kilowatts, and megawatts are used for motor power and charger output. The battery capacity is the stored power, which is typically referenced in watt-hours, kilowatt-hours, and megawatt-hours. Amp-hours are not used, as is the custom in constant voltage systems, because in electric aircraft there is a wide operating voltage range, while the wattage demanded from the battery is the important parameter. The power available to fly is the same as the extractable energy from the battery; on the other hand, current and voltage change during discharge. At full battery charge, it requires less current (Amps) to generate the desired power as compared to at a low battery charge. At some point in time, the current required to extract energy from the battery becomes limiting, and the power system is unable to produce the desired power. Thus, the conceptualization of stored power in the batteries of an electric aircraft is more complex than more easily quantified gallons of fuel (Jet A or avgas) in the tanks of a hydrocarbon-fueled aircraft.

2.3 Pipistrel Electric Test Program

Florida Tech Flight Test Engineering conducted 87 hours of flight testing using a Pipistrel Velis

Electro aircraft and the associated Pipistrel ground support system (see Figure 1). The Pipistrel system incorporates the same electric motor and battery technology that is expected to be deployed in the first generation of commercial electric aircraft, including AAM and eVTOL aircraft. Thus, this test aircraft is a good analog to study system performance and operational needs that can then be scaled with aircraft size.

The experimental test flights illustrated that the airport infrastructure is not quite ready for electric aviation. First, the charging system for the test aircraft required upgrades to the existing hangar electrical power systems. A 120V electrical service is not sufficient to charge the Pipistrel. Typical commercial options that would work for the system include: 3-phase, 480V service (required for full-rate charging of the batteries, and often found in commercial buildings) and single phase, 208V electrical service (the minimum for slow charging of the batteries, and what is commonly found in residential housing). An additional issue is in situ wiring, which experiences high voltage drop between the service and the electric plug, and that negatively impacts charge efficiency. A survey of hangar facilities at KMLB and X59 airports revealed that there were no existing hangar facilities that could support charging of the Pipistrel at manufacturer-specified rates. Most airport hangars had 208V service, yet only received 120V, due in part to wiring, which further limited the charging possibilities. Suitable 3-phase commercial service was not available on the general aviation ramp area at KMLB but could be connected at a commercial hangar site for testing. For flight testing, the commercial hanger had to be rewired and the power company had to improve the power supply to ensure a functional 3-phase power system at the hangar.

The experimental aircraft certificate, limited charging options, and battery range limited flights to the local area. All operations started and ended at KMLB as there were no airports in the vicinity with hookups available to power a portable charging system.



Figure 1. Pipistrel Velis Electro and components.

Left: Pipistrel Velis Electro with test pilot. Middle: Electric motor, motor controller, and front battery.

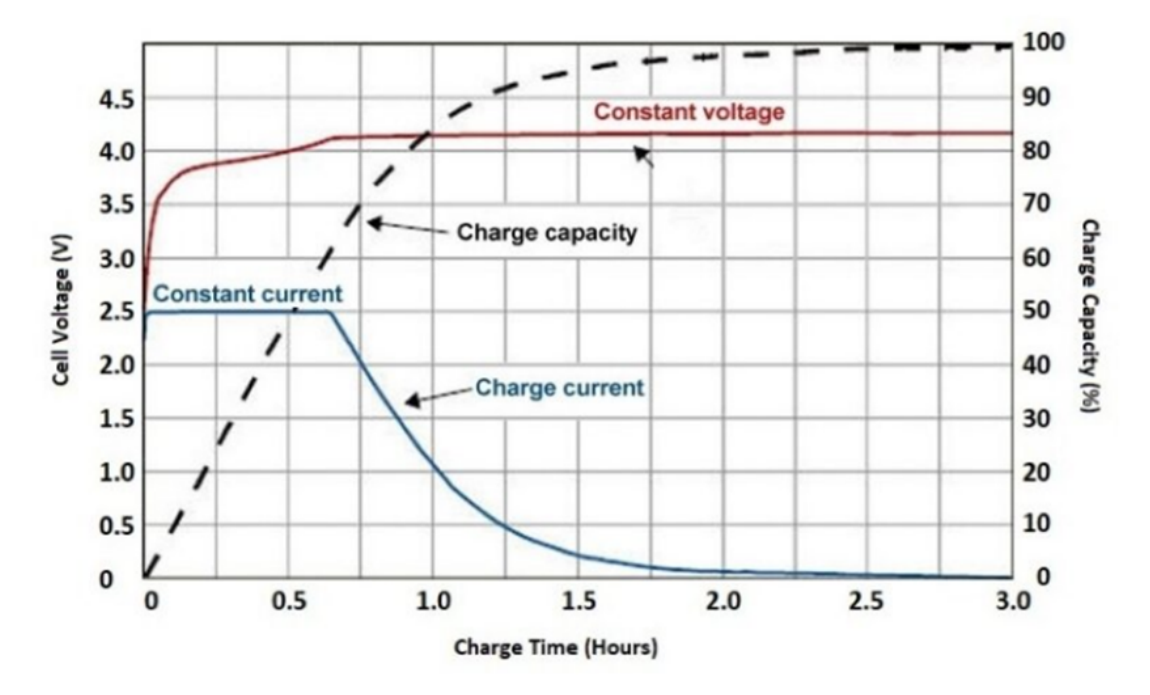
Right: Charger showing screen with source selection for charging.

3. Electric Aircraft Charging Data

The results from charging tests using different input voltage and current limits over the course of the flight testing illustrate differences by type of electric service and charging (see Figure 2) for the lithium-cobalt-manganese batteries in the test aircraft. The slow charging option on 208V service (single phase electrical service) was the worst with both the longest charging time and lowest efficiency: maximum charge rate of 10.2 kW, 152 minutes to charge, and 86% charging efficiency. The rapid charging option on 480V service (3-phase electrical service) had the highest rate of charge: maximum charge rate of 27.9 kW, 97 minutes to charge, and 91% charge efficiency. The slow charging option on 480V service (3-phase electric service) had the highest efficiency: maximum

charging rate 14.1 kW, 139 minutes to charge, and 94% charge efficiency. The slow charging option on 480V was the most efficient because the charger did not have to up-convert the voltage (i.e., 480V is already above the minimum 400V to charge the batteries), and the slower charge rate allowed time for the battery to absorb the charge with less resistance. The last ten percent of the charge is the slowest.

Currently, all available electric aircraft have both their own proprietary charge cords and plugs as well as their own charging equipment (e.g., Figure 1 Right) and software. This is in part inherent in battery design as different types of batteries will have different resistance and charging requirements. This creates another challenge in preparing the airport infrastructure for future electric fleets.



^{*}The red and blue lines represent what the charger does. The dashed line's slope is the approximate maximum charge rate.

Figure 2. Voltage and Charge Capacity vs. Charge Time

4. Charge Efficiency

The charging efficiency is determined by three primary considerations. First, the environmental conditions directly impact efficient charging; batteries are more efficient at warm temperatures than cold temperatures. Second, the highest input voltage supply will have the greatest efficiency charging. Third, the charge rate determines efficiency, with slower rates of charging being more efficient at the same charger input voltage.

Charger efficiency is measured by placing an inline energy meter before the charger to record the total power to the system, and then comparing that measurement to the power into the batteries recorded by the aircraft battery management system. The charge efficiency values incorporate both physical and program losses in the charging system. The measured differences in charging efficiency with charging program (slow/rapid charge) and electrical service (208V single phase or 480V 3-phase) ranged from 86% to 94%. This is a substantial variation in charging efficiency;

when considering required power, a difference of 8% in efficiency is quite large. Therefore, charging system design needs to be optimized to aircraft power systems, with consideration of both the physical limits of the batteries and charger, and the charging program/software.

Up-conversion of the supply voltage to higher battery charge voltages is an efficiency sink. This is why the 480V electrical service options performed better than the lower voltage; there was no delay converting up to the minimum 400V required for charging. Note that the minimum requirements will differ by aircraft and battery. For example, BETA's charging cube, which is currently the most available charging option in the US, can run on 480V electrical current. However, for a fast charge, it has to up-convert to the 1000V requirement to rapid-charge (BETA, 2025).

Power supplied to the charger will be higher than the specified charge rate for rapid charging operations due to reduced efficiency. This could significantly increase the power supply infrastructure requirements.

5. General Aviation and Advanced Air Mobility (AAM)

Airports are currently deploying manufacturer-specific charging stations at small airports to prepare their infrastructure for electric aircraft. BETA (2025) claims that it will have almost 150 stations operational by 2025. However, the availability of charging stations and options will be limited by the proprietary nature of the charging requirements of electric aircraft and also by the commercial electrical service constraints on airport. For example, BETA (2025) Technologies Cube charger requires 420 Amp, 3-phase 480-volt power to provide 320kW peak charging, which is the most you can practically achieve with standard commercial power service. However, the Cube is built to rapid charge at 1000V, although this is not a currently available commercial electric service at most airports.

Charging system standards will need to be formalized to accommodate the growing electric fleet. This is similar to what was seen with electric vehicles over time. To have a true network of available charging stations for aircraft, the plugs and software charging options will need to be standardized or available with options and conversions to accommodate multiple aircraft. Without compatible charging options, cross-country flights are not an option.

6. Challenges in Scaling to Commercial Application

The next step is to scale up to practical commercial applications. A recent study (Wolleswinkel et al., 2024) looked at the practical design requirements of a short-haul commercial aircraft with between 20 and 40 passenger seats, operating on routes less than 1000km. A minimum 4 Megawatt-hour energy requirement was predicted for this flight profile in an electric aircraft (Wolleswinkel et al., 2024). For a point of reference, the Pipistrel requires approximately 22 kW-hrs; this estimate points to requirements on the order of 200 times the power for operating the Pipistrel.

This presents several energy delivery challenges for airports based on operational limitations as we scale up from this estimate. First, targeted gate times at commercial airports are typically 60 minutes or less between flights. Assuming similar charging efficiency as the Pipistrel, charging systems on the order of 10 Megawatt per gate operating at over 1000 Volts would be required to support this type of mission. Thus, unlike fueling, which takes up a small portion of gate time, charging will likely be continuous at all occupied gates, compounding infrastructure requirements at airports supporting electric aircraft commercial operations.

To support just 10 gates, an airport will require a distribution system capable of reliably providing 100 peak Megawatts of power, or about the same as two average-sized commercial power plants.

Airports will also face other critical infrastructure challenges in electric aviation. For commercial operations, it will be necessary to develop safe operating procedures for all weather handling of high voltage, high amperage charging systems. Again, estimated charging will be for the entire time on the ground, so this will be essential. Aviation services are critical services requiring reserves on hand for both supply chain shortages and crisis situations. Airport will need to develop power redundancy to assure operations and critical aviation service levels. Currently, all airport equipment for ARFF (Airport Rescue and Fire Fighting) equipment is designed to address fires from hydrocarbon-based fuels; this includes both foams to fight fire and spill cleanup. Airports will need equipment and training in order to handle emergency scenarios involving batteries in addition to hydrocarbon fuels.

Finally, the national airspace system will need further integration of reserve-constrained electric aircraft and eVTOLs around busy terminals in order to maintain safe operations. A study that compared energy utilization for similar eVTOL and fixed-wing aircraft suggested that eVTOL-type aircraft are less energy efficient as compared to fixed wing aircraft, and thus, eVTOLs will have a significantly higher energy demand on comparable missions (Kish et al., 2022). This means a potentially larger infrastructure and planning gap for AAM.

7. Sustainable Technology and In Situ Generation as a Solution

Given the FAA's (2023) stated goal of reaching carbon-neutrality industry-wide by 2050, aviation must rapidly move towards sustainable options. The available electric aircraft technology and infrastructure point to sustainable technologies as a feasible solution for supporting electric aviation. Airports are uniquely suited to host solar power plants with large open areas to provide adequate terrain clearance for aircraft, and many airports in the US already host solar projects, although they are often third-party power projects using the airport land. Solar arrays can be mounted adjacent to aircraft operating areas on frangible assemblies to protect airborne assets and to provide energy available for charging on site and at the appropriate voltage for charging electric aircraft.

According to the National Renewable Energy Lab (NREL, 2025), KMLB receives 5.6 kWh per day per square meter on average. Considering an area equivalent to one of the runways (3040m X 46m, for a surface area of 139,840 m2), that same area covered in solar panels could recover 783 MWh of solar energy per day! This is an estimate from the NREL calculator for a particular airport using regular roof-top solar panels. There is sufficient land (and/or rooftop square footage) available for solar projects at many airports.

Sustainable energy options such as solar power plants can therefore been implemented as an immediate infrastructure solution for electric aviation. Most airports have some space, and even as little as 10% of the area in the example above would make a difference. Solar projects on the airport could be designed and built custom to match the electric aircraft needs at the given airport. This would address the higher voltage requirements for rapid charging as well as minimizing the need to transport energy.

8. Disclaimer Statements

Funding: This study was not funded; however, this is a follow-on to a Federal Aviation Administration (FAA) contract (AWD000524 Electric Aircraft Trajectory Flight Test Data).

Conflict of Interest: None

9. References

- BETA. 2025. Charging. BETA Technologies. https://beta.team/charge.
- Cuhna, D., Wheeler, B., Silver, I., & Andre, G. (2023). Electric aircraft battery performance: examining full discharge under two conditions. *International Journal of Aviation Science and Technology.* 4(1), 5-13. https://doi.org/10.23890/IJAST.vm04is01.0101.
- de Vries, R., Wolleswinkel, R. E., Hoogreef, M. F. M., & Vos, R. (2024). A New Perspective on Battery-Electric Aviation, Part II: Conceptual Design of a 90-Seater. In *Proceedings of the AIAA SCITECH 2024 Forum Article AIAA 2024-1490* (AIAA SciTech Forum and Exposition, 2024). https://doi.org/10.2514/6.2024-1490.
- FAA. 2021. United States 2021 Aviation Climate Action Plan. Federal Aviation Administration. https://www.faa.gov/sites/faa.gov/files/2021-11/Aviation Climate Action Plan.pdf.
- Harbour Air. 2024. Going Electric. Harbour Air. Accessed 26 June 2025 at https://harbourair.com/going-electric/?tab=Specification.
- Kish, B. A., Wilde, M., Silver, I., Wheeler, B., Cleveland, A., & Reppen, K. (2022, March). Flight test comparison of three air vehicles flying urban air mobility mission trajectories. In *2022 IEEE Aerospace Conference (AERO)* (pp. 1-9). IEEE. https://doi.org/10.1109/AERO53065.2022.9843555
- National Academies of Sciences, Engineering, and Medicine. 2022. *Preparing Your Airport for Electric Aircraft and Hydrogen Technologies.* Washington, DC: The National Academies Press. https://doi.org/10.17226/26512
- National Renewable Energy Lab. 2025. *PVWatts Calculator*. API version 8.0. US Department of Energy. PVWatts Calculator accessed at https://pvwatts.nrel.gov/.
- Wheeler, B.E., Silver, I.M., Kish, B.A., Wilde, M., & Andre, G. (2023). Assessing battery characteristics during a full discharge in an electric aircraft. In Emerging Trends in *Electric Aviation: International Symposium on Electric Aircraft and Autonomous Systems 2022*. p. 79-84. Springer. https://doi.org/10.1007/978-3-031-37299-5_11.
- Williams, D. (2024, July 25). Update on ICAO and U.S. Aviation Climate Action Plan. FAA Office of Environment and Energy (AEE). https://www.faa.gov/media/82136.
- Wolleswinkel, R. E., de Vries, R., Hoogreef, M., & Vos, R. (2024). A New Perspective on Battery-Electric Aviation, Part I: Reassessment of Achievable Range. In *AIAA Scitech 2024 Forum* (p. 1489). https://doi.org/10.2514/6.2024-1489

The Journal of Management and Engineering Integration (JMEI) © 2025 by AIEMS Inc., is licensed under CC BY 4.0. To view a copy of this license, visit https://creativecommons.org/licenses/by/4.0/

WINTER 2025



AIEMS

AIEMS is committed to furthering the integration between business management, engineering, & industry. Our objective is to promote research, collaboration, & practice in these multidisciplinary areas. AIEMS seeks to encourage local, national, & international communication & networking via conferences & publications open to those in both academia & industry. We strive to advance professional interaction & lifelong learning via human & technological resources, and to influence and promote the recruitment and retention of young faculty and industralists.

AIEMS
VOL18
NO 2